ANGULAR STRUCTURES OF EXTRAGALACTIC RADIO SOURCES AND COSMOLOGY

BY
VIJAY K. KAPAHI

A Thesis submitted for the
Ph. D. degree of the
University of Bombay

TATA INSTITUTE OF FUNDAMENTAL RESEARCH, BOMBAY
1975

ANGULAR STRUCTURES OF EXTRAGALACTIC RADIO SOURCES AND COSMOLOGY

by

VIJAY K. KAPAHI

Tata Institute of Fundamental Research
Homi Bhabha Road, Bombay 400 005
India

A Thesis

submitted for the

Ph.D. degree

of the

University of Bombay

June 1975

TO

MY PARENTS

ANGULAR STRUCTURES OF EXTRAGALACTIC RADIO SOURCES AND COSMOLOGY

SYNOPSIS

In this thesis we investigate the cosmological implications of the observed angular sizes of extragalactic radio sources. Angular sizes appear to provide a very useful statistical measure of the distances of radio sources. Also, since the angle subtended by a source depends on the cosmological world model, angular sizes can in principle be used as a test of world models. Due to the difficulty of measuring redshifts for a majority of radio sources the angular sizes have to be determined over a wide range of observed flux density. Systematic mapping of source structures with high angular resolutions has hitherto been limited to the relatively strong sources, such as those in the 3C catalogue. The first part of this thesis describes the measurement at 327 MHz, of the brightness distribution of a large sample of weaker radio sources by the method of lunar occultation, using the Ooty radio telescope. From the data on weak sources and the available structural information on the stronger sources, several important cosmological results are obtained in the second part of the thesis.

The observations of lunar occultations with the Ooty radio telescope, and the method of analysis of records are briefly described. Accurate radio positions and brightness distributions with angular resolutions varying between about 1" to 10" arc have been derived for over 250 radio

sources, most of them in the flux range of 0.3 to 5 Jy (1 Jy = 10^{-26} Watt m^{-2} Hz^{-1}) at 327 MHz. It is for the first time that the method of lunar occultation has been exploited to obtain angular size information on such a large sample of weak radio sources. For the purposes of a statistical study, we use an unbiased sample of 164 sources for which the derived angular structure, the observed flux density and the optical identification are tabulated.

The correlation between the angular size (θ) and flux density (S) of radio sources in the Ooty occultation sample and in the 3CR sample of 199 sources is investigated. It is found that the median value of angular size, θ_m , is well correlated with flux density, in the sense that weaker radio sources have smaller angular sizes. The observed $\theta_m(S)$ relation provides strong evidence that the weaker sources lie at statistically greater distances. The relation also suggests that the lack of any Hubble type correlation between redshift and flux density of radio galaxies, noted earlier by other authors, results from the limited number of redshift measurements, which suffer from observational selection effects; at any flux density, redshifts have preferentially been measured for the optically brighter and hence nearer radio galaxies.

The method of angular size counts or the log N-log θ relation, where N is the number of sources with an angular size greater than a value θ in a radio survey complete to a certain flux density, is investigated to study cosmology. The $N(\theta)$ relation depends on the world model, the radio luminosity function (RLF) and the distribution of physical sizes of radio sources (radio size function). The method of calculating the

expected log N-log θ relations for a uniform distribution of sources in space is outlined for the case of power law luminosity functions, i.e. $\rho(P) \propto P^{-\gamma}\, dP$, and an empirically derived size function.

The log N-log θ relation is constructed for the complete sample of 3CR sources, down to values of $\theta = 10''$ arc, and compared with the predictions of Einstein-de Sitter and Steady State cosmologies. Since values of $\theta \gtrsim 100''$ arc arise only from sources of small z, the slope of the $N(\theta)$ relation for larger values of θ is practically independent of the world model, the size function, and any evolutionary effects in source properties. It depends strongly on the form of the RLF and can be used to determine the luminosity function for radio galaxies. The local luminosity function is derived to be of the form $\rho(P) \propto P^{-2.1}\, dP$ in the luminosity range of about $10^{23} < P_{178} < 10^{26}$ W Hz^{-1} ster^{-1}. This is in good agreement with the RLFs determined from measured redshifts or from the optical magnitudes of identified galaxies. It is also shown that the RLF in the above luminosity range cannot be as steep as $\gamma \gtrsim 2.5$, even if possible evolutionary effects are taken into account.

We find that the observed $\theta_m(S)$ relation and the log N-log θ relation for the 3CR sample are not compatible with the predictions of simple cosmological models in which the comoving density of sources remains constant with epoch. It is difficult to explain the observations in the simple Steady State cosmology even if (a) QSOs are excluded from the source samples and (b) the possible local deficiency of strong sources (which has been suggested to explain the log N-log S data) is taken into account: the number of missing sources has to be rather large and the physical sizes of the missing sources have to be small.

Evolutionary effects in source properties with epoch are necessary to explain the angular size data. The simplest evolutionary scheme that gives a fairly good fit to the observed $N(\theta)$ and $\theta_m(S)$ relations implies

(a) that the slope of the local RLF steepens considerably ($\gamma \sim 2.7$ to 2.8) for $P_{178} \gtrsim 10^{26}$ W Hz^{-1} ster^{-1};

(b) that the RLF changes with epoch as $\rho(P, z) = \rho(P, z = 0)\ (1 + z)^{5.5}$ for $P_{178} \gtrsim 10^{26}$ W Hz^{-1} ster^{-1}, and

(c) that the maximum linear sizes of radio sources vary approximately as $(1 + z)^{-1}$.

Angular size counts of radio sources thus provide new evidence of evolutionary effects in source properties.. The steepening of the local RLF and the increase in the co-moving density of high luminosity sources implied by the angular size data are infact similar to what has been inferred from flux density counts of radio sources and from the Luminosity-Volume tests for quasars. Angular size counts show in addition that similar evolutionary effects in numbers and physical sizes exist for quasars as well as radio galaxies.

ACKNOWLEDGEMENTS

I should like to express my gratefulness to GOVIND SWARUP for his guidance and encouragement. Working with him - whether on astronomical problems or on the telescope - has always been a rich and rewarding experience. I was indeed fortunate to have started my research career with him and to have seen at first hand the growth of radio astronomy in India, for which he is largely responsible.

The successful running of the large Ooty telescope owes a great deal to the untiring efforts of a dedicated staff of the Radio Astronomy Centre, Ooty.

The computer program to analyse the occultation records was written mainly by GOPAL-KRISHNA with later contributions from JEWEL CHOWDHARY and C.R. SUBRAHMANYA. MOHAN JOSHI and C.R. SUBRAHMANYA did much of the painstaking work of optical identifications.

T.R. KRISHNAMURTHY provided invaluable help in Bombay in running the many computer programs on the CDC 3600 computing facility at TIFR.

I should also like to thank V.V. KARAPPAN for the fine job of typing the manuscript and the staff of the Drawing, the Photography and the Duplicating facilities of the TIFR for their help in bringing out this thesis.

Finally, it is a pleasure to thank my friends MRIDULA and ASOKA RATNAM for their interest and constant hospitality in Bombay.

TABLE OF CONTENTS

List of Figures

List of Tables

Chapter 1

INTRODUCTION

1.1 Radio Galaxies and Quasars

The tremendous excitement witnessed in the field of extragalactic radio astronomy during the last two decades followed from two important implications of the identification by Baade and Minkowski (1954), of the strong radio source Cyg-A with a galaxy of redshift $z = 0.056$. The first was the realization of the high intrinsic luminosities of radio galaxies. It is now well known that most of the galaxies identified with radio sources are in fact strong 'radio galaxies' with power outputs in the radio region, of about 10^{33} to 10^{37} Watt, a few orders of magnitude greater than those for our own or other 'normal galaxies' such as M 31. The source of these enormous energies has been a challenging problem in astrophysics.

Secondly, the strong apparent intensity of Cyg-A implied that similar radio galaxies should be observable to far greater redshifts, so that it should be possible to use radio sources to investigate the large scale structure of the universe. Much effort has, therefore, been devoted in the last two decades to making systematic surveys of the sky, going down to lower apparent intensities. With steady improvements in receiving techniques and the construction of more powerful radio telescopes, radio sources a million times fainter than Cyg-A can now be detected, and tens of thousands of sources have already been catalogued by radio astronomers.

The largest redshift known for a radio galaxy today is $z = 0.46$ (for 3C 295; Minkowski 1960). However, most galaxies with measured redshifts still have $z < 0.3$. The measurement of larger redshifts is limited by observational difficulties due to the faintness of galaxy images, even when seen with the largest optical telescopes.

With the identification of the radio source 3C 273 with a 13th magnitude stellar object by Hazard et al. (1963), and the measurement of its redshift ($z = 0.158$) by Schmidt (1963), a new class of radio sources of large redshifts was discovered. Hundreds of such 'quasi stellar objects' (QSOs or 'quasars') have since been identified, and redshifts measured for some 250 of them. The measured redshifts for most QSOs lie in the range of $z = 1$ to 2, much larger than those for radio galaxies. The largest now known is $z = 3.53$ (Wampler et al. 1973) for the radio source OQ 172. Ever since the discovery of quasars there has been much lively discussion in the literature on the nature of their redshifts. Although no suitable alternative has been forthcoming, the cosmological nature of the redshifts is still not entirely beyond question (e.g. Burbidge 1973). If their redshifts are of cosmological origin, QSOs differ from radio galaxies mainly in their larger optical outputs. In many of their radio properties they do not appear to be very different from strong radio galaxies. Their radio power output ranges from about 10^{34} to 10^{38} Watt.

1.2 Source Counts and Cosmology

The most widely used method of studying cosmology with radio source surveys has been to count the number of radio sources, N, above successively decreasing flux densities, S. The log N–log S relation has

been extensively studied using radio surveys made with different telescopes at different observing frequencies now going up to 5000 MHz (Kellermann, Davis and Pauliny-Toth 1971). The most extensive work on the subject has been carried out at 408 MHz, by Ryle and his group at Cambridge (Pooley and Ryle 1968), from source surveys going down to flux levels of 0.01 Jy (Jy = Jansky = 10^{-26} W m^{-2} Hz^{-1}). On the observational side there appears to be a broad agreement in the shapes of the log N-log S relations derived from surveys at different observing frequencies, if the spread in the radio spectral indices of sources is taken into account (Kellermann 1972). The same cannot be said of the interpretation of the observed counts, for this has been a subject of much controversy. The principal conclusions of the most widely held interpretation (e.g. reviews by Longair 1971; Rees 1972) may be summarized as follows:

(a) The steep slope of the log N-log S curve at high flux densities does not agree with the predictions of uniform relativistic world models.

(b) Evolution in the mean properties of sources with cosmic epoch is necessary in the sense that there have to be many more high-luminosity sources at earlier epochs than now. The evolution has to be quite strong, something like a $(1 + z)^{5 \text{ to } 6}$ dependence of the comoving space density of sources with epoch. Differences in the predictions of various world models are small in comparison, so that the counts cannot be used to select the correct cosmological model. The evolutionary scheme cannot also be uniquely determined since to do so one needs to know the world model and the local luminosity function of radio sources, i.e. the

number of radio sources per unit volume of space (at small z) with different intrinsic luminosities. There is considerable uncertainty in our knowledge of the local luminosity function, specially at its high luminosity end. This is so because the intrinsically luminous sources are seen at large redshifts and their volume density in the local space cannot be determined without knowledge of the world model and without correcting for evolutionary effects, which one is trying to determine! A variety of evolutionary schemes can therefore be worked out within the uncertainties of the world model and the luminosity function, to fit the observed counts satisfactorily (e.g. van Hoerner 1973).

(c) A cut-off or a drastic reduction in the density of sources is required beyond epochs corresponding to about $z = 2$ to 4, in order to obtain the rapid convergence in the counts observed at very low flux densities.

(d) The Steady State theory of the universe is unlikely to be true, as it does not permit a change in the mean properties of radio sources with cosmic epoch.

The above interpretation of source counts has often been questioned (e.g. Hoyle 1968 ; Brecher et al. 1971; Kellermann 1972). It is sometimes argued that the steep slope of the log N-log S relation at high flux densities can equally well be interpreted as a deficiency of nearby sources rather than as an excess of distant sources.

The controversy arises mainly because the distances of most radio sources are not known. The slope of the log N-log S relation at a given flux level depends on the cosmological world model and on the

average distance where such sources are located. There is no way of estimating the distance of a radio source from radio observations alone; it has to be obtained by identifying the source with an optical object and measuring its redshift. Although the problem of optical identification has become considerably simpler with the continuous improvement in the accuracy with which radio source positions can be measured, it became clear in the sixties that even at relatively high flux levels, many sources could not be identified as no optical object was seen at their locations on the photographs of the Palomar Sky Survey. The percentage of such unidentified sources in radio surveys made at low frequencies ($\lesssim$ 400 MHz), where much of the work on source counts has been carried out, appears to increase with decreasing flux-density, from $\sim$ 30 per cent in the 3CR catalogue which has a limiting flux density of 9 Jy at 178 MHz, to $\sim$ 90 per cent in the 5C catalogues (e.g. Parkes and Penston 1973) that go down to $\sim$ 0.01 Jy at 408 MHz.

The measurement of the redshifts of identified sources presents another problem. Since many of the identified galaxies are faint, the measurement of the optical spectrum is difficult. As a result, redshifts have been measured only for a very small fraction of the identified galaxies, mainly confined to the strongest radio sources.

Thus, in the range of flux densities where a large excess of weak sources is indicated by source counts, there is no direct evidence that the sources are located at cosmologically significant distances. While the QSOs could be much nearer than indicated by their redshifts, the radio galaxies (the cosmological origin of their redshifts has not

generally been questioned) have mostly been found to have $z < 0.1$. How then can the source counts give us information about the properties of radio sources at early epochs?

Although the observed counts do not appear to have been convincingly explained in the Steady State theory (see e.g. Longair and Rees 1972; Schmidt 1972) or in Friedman cosmologies without recourse to evolutionary effects, cosmological tests other than source counts are highly desirable.

1.3 Angular Structures and Cosmology

Apart from flux density, the angular structure of a radio source is another important parameter that can be measured by radio telescopes. From interferometric measurements, Jennison and Das Gupta (1953) were the first to show that unlike in normal galaxies, the radio emission from Cyg-A originated in two separate regions about 1.'5 arc apart, located on either side of and well away from the optical galaxy. Later observations with better resolving power have shown the 'double structure' to be the most common structural type exhibited by radio galaxies and quasars (e.g. Fomalont 1969; Mackay 1971). The two radio components are typically of equal intensity and have separations of the order of 100 to 200 kpc, while the components themselves are typically 10 to 50 kpc in extent. Many sources have been found with more complex structure, such as having three or four components, or with 'tails' and 'bridges' between the components. It is remarkable, however, that 95 per cent of the resolved sources in a complete sample of the 3CR catalogue have their radio emission concentrated along a narrow band on the sky which, in the case of identified sources, passes through the associated galaxy or QSO (Mackay 1971).

It is generally agreed that the origin of the extended radio sources lies in energetic events in the nuclei of galaxies or QSOs, in which vast amounts of energy in the form of particles and magnetic fields or in the form of low frequency electromagnetic radiation from pulsar-like objects (Rees 1971) is released. The details of how and in what form the energy is transported from the nucleus to form the compact radio emitting blobs at large distances, and how it is confined to the components over periods of 10^6 to 10^9 years, are far from understood. None of the theoretical models that have been proposed can explain the observations satisfactorily (the difficulties have been discussed in De Young and Burbidge 1973; Longair, Ryle and Scheuer 1973).

Apart from the question of generation and confinement of radio sources that a detailed study of their angular structure can help find an answer to, angular sizes of radio sources also provide a useful statistical measure of their distances, and are of considerable importance to observational cosmology. It is with these latter aspects of the angular size information that the present thesis is mainly concerned.

The angular size subtended by a source of fixed physical size (a 'rigid rod') seen at various epochs depends on the cosmological world model. It was pointed out by Hoyle (1959) that in relativistic cosmologies with $q_o > 0$ (where q_o is the deceleration parameter), the angular size first decreases with increasing z, reaches a minimum in the region of about $z = 1$ to 2 and increases thereafter for larger redshifts. In the Steady State theory on the other hand, the angular size should reduce continuously, approaching a constant value asymptotically as z increases to ∞. It was hoped that by using the separation between components of double sources as a 'rigid rod' it may be possible to choose the correct cosmological model, by measuring the angular sizes of radio sources to large redshifts.

The practical application of the redshift-angular size test is made difficult by the dispersion in physical sizes of radio sources and the problem of measuring redshifts for a large number of sources. As large redshifts have been measured only for quasars, the test was first applied to quasars with known double structure by Legg (1970). It appeared to indicate that intrinsic sizes of quasars were smaller at earlier epochs. Later studies using larger samples of quasars have provided further support to this conclusion.

A purely radio test that does not require the measurement of redshifts and can therefore be used with large unbiased samples of sources is to study the angular size-flux density relation. A meaningful statistical application of this test requires only that the angular structures of radio sources be measured over a large range of observed flux density. Most of the observations to obtain the detailed structures of radio sources have been carried out using interferometers and aperture synthesis techniques. The mapping of source structures by aperture synthesis is time consuming and has generally been limited to relatively strong radio sources. Furthermore, the resolution obtainable with such interferometers was till recently limited to tens of seconds of arc at cm λ . It was demonstrated in the early sixties by Hazard (1961, 1962) that the method of Lunar Occultation is another powerful means of deriving the structure of extragalactic radio sources. It was soon realized that the method could be used to derive radio positions accurate to about a second of arc and one dimensional brightness profiles across sources with resolutions of the order of a second of arc. However, the method was not fully exploited, due mainly to the lack of a suitable large radio telescope.

1.4 The Present Work

The Ooty radio telescope (Swarup et al. 1971a), designed specifically to observe Lunar occultations of a large number of weak radio sources, came into operation in 1970, and occultations of over 400 radio sources, going down to a flux density of about 0.2 Jy at 327 MHz, were observed upto the end of 1971. We have used the observations to derive accurate radio positions and brightness scans across the sources with angular resolutions of about 1" to 10" arc.

For the purposes of the work reported here we have used the angular size information derived from occultations of about 280 radio sources. We use an unbiased sample of 164 sources, most of them in the flux density range of about 0.3 to 5 Jy. It is for the first time that high resolution angular size information on a decently large sample of sources extending to such low flux levels has been obtained.

In Chapter 2 we describe briefly the method of observation of lunar occultations with the Ooty radio telescope and the analysis of occultation records.

The observed flux densities, the derived structural information and the results of a parallel program of optical identifications, are given in Chapter 3. A brief discussion of the angular structures is also given in this chapter.

In Chapter 4, we consider the angular size-flux density relation for extragalactic radio sources. In order to cover a large range of flux densities we have combined the occultation data for weak radio sources with the available structural information for the stronger sources in the revised 3C catalogue (Bennett 1962) and in the recent

All-sky catalogue (Robertson 1973). We find the median values of the angular size, θ_m, for sources in different ranges of flux density and show that a clear correlation exists between θ_m and S, in the sense that weaker sources have smaller values of θ_m. This correlation, which is largely free of observational selection effects, can be looked upon as a sort of 'Hubble relation', and is of immense cosmological importance.

The cosmological implications of the angular size information are examined in Chapter 5. We first consider the use of 'angular-size counts' or the log N-log θ relation in which for a radio survey complete above a flux density S, the number of sources N, with angular size $> \theta$ is plotted against θ. Such a relation depends on the cosmological model and on the distribution of radio sources in depth. The angular size counts are constructed for a complete sample of 3CR radio sources down to values of $\theta = 10''$ arc. We show that the slope of the observed $N(\theta)$ relation for $\theta \gtrsim 100''$ arc, the range of sizes which arise from sources at small redshifts, can be used to derive rather stringent limits to the form of the luminosity function for radio sources. The luminosity function is well determined in the range of about 10^{23} to 10^{26} W Hz^{-1} $ster^{-1}$ at 178 MHz, without the explicit use of redshift information, and is in good agreement with other determinations based on optical identifications of radio sources.

A comparison with observations, of the predicted log N-log θ relation and the θ_m -S relation in the Einstein-de Sitter and Steady State cosmologies shows that the observations are incompatible with a uniform distribution of radio sources in space and in particular, do not agree with the predictions of the Steady State cosmology.

The observations provide independent evidence of strong evolutionary effects in radio source properties with epoch. The extent of evolutionary effects required is investigated for the Einstein-de Sitter world model. It is found that evolution is required both in the space density and in physical sizes of radio sources. The amounts of evolution determined independently from angular size data are in broad agreement with those implied by the log N-log S data, the Volume-Luminosity tests, and the Q - z relation for QSOs. Similar evolutionary effects are indicated even if the identified QSOs are excluded from source samples.

The conclusions are summarized in Chapter 6.

Chapter 2

LUNAR OCCULTATIONS OF RADIO SOURCES WITH THE OOTY RADIO TELESCOPE

2.1. The Ooty Radio Telescope

The observation of lunar occultations of a large number of weak radio sources requires a telescope of large collecting area capable of tracking the Moon continuously. The Ooty radio telescope has been specially designed to meet these requirements (Swarup et al. 1971a). It has a parabolic cylindrical surface, 30 m wide and 529 m long, which is formed of 1100 thin stainless steel wires supported by 24 parabolic frames. The cylinder is equatorially mounted by making its long north-south axis parallel to Earth's rotation axis. This has been done by locating the cylinder on a hill of slope equal to the local latitude ($+ 11^{\circ}23'$). Hour angle tracking is thus achieved by a simple mechanical rotation of the parabolic frames around the long axis. The hour angle coverage extends from $-4^{h}\ 05^{m}$ to $+5^{h}\ 29$ m.

In declination the telescope beam is steered electrically by means of phase shifters and delay lines. The feed system at the local line of the parabolic cylinder has been described by Kapahi et al. (1975). Briefly, it consists of an array of 968 half-wave dipoles spaced 0.57 λ apart and mounted collinearly inside a 90° corner reflector. The array is divided into 22 modules of 44 dipoles each. The dipoles in each module are connected in series (as shown in Fig. 2.1) through radio frequency (RF) phase shifters and quarter-wave directional couplers whose couplings have been suitably graded (Kapahi et al. 1975) in order to obtain a uniform illumination of the

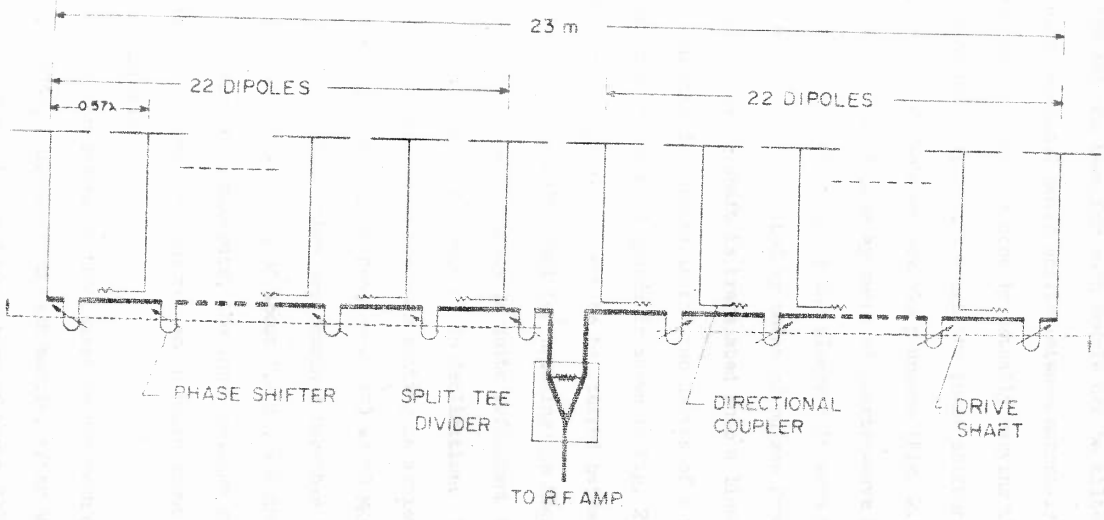

FIG. 2.1 A schematic of the series feed arrangement for the 44 dipoles in each module.

dipoles. The antenna beam for each module can be tilted in declination by introducing identical phase shifts between successive dipoles in each half of the module. This is done by actually varying the length of transmission line between dipoles, through the phase shifters. The phase shifters consist basically of U-shaped movable plungers (Fig. 2.2) connected to the main rectangular coaxial line by means of quarter-wave RF choke joints. A wire and pulley arrangement links the plungers in each module to a common drive shaft which can be rotated by means of pulses from the control desk. A rotation of the drive shaft is translated into a linear movement of the plungers in opposite directions in the two halves of a module. A perspective view of a section of the feed system is shown in Fig. 2.2.

The system allows the beam to be steered between $+36^{\circ}$ and -36° in declination (a range sufficient for tracking the Moon) in steps of about 1 min of arc. This accuracy is quite sufficient as the half-power beam width of each module is about 2° in declination. The final accuracy of about $\pm$ 0.25 min of arc in the beam setting is achieved by introducing phase shifts at an intermediate frequency (IF) of 30 MHz in the signal paths from the 22 modules, before they are combined together (Sarma et al. 1975).

Each module has a loss of about 1.2 db, and due to the careful matching of the various components, the input voltage standing wave ratio at each module is generally found to remain below about 1.3 as the beam is steered in declination.

The receiver system of the telescope has been described by Sarma et al. (1975). Signals from each module, after amplification by low noise RF amplifiers (noise temperature of about 220 K) and conversion to an IF of 30 MHz, are brought to the central control room through low-loss underground cables. The signals from the 22 modules are then amplified

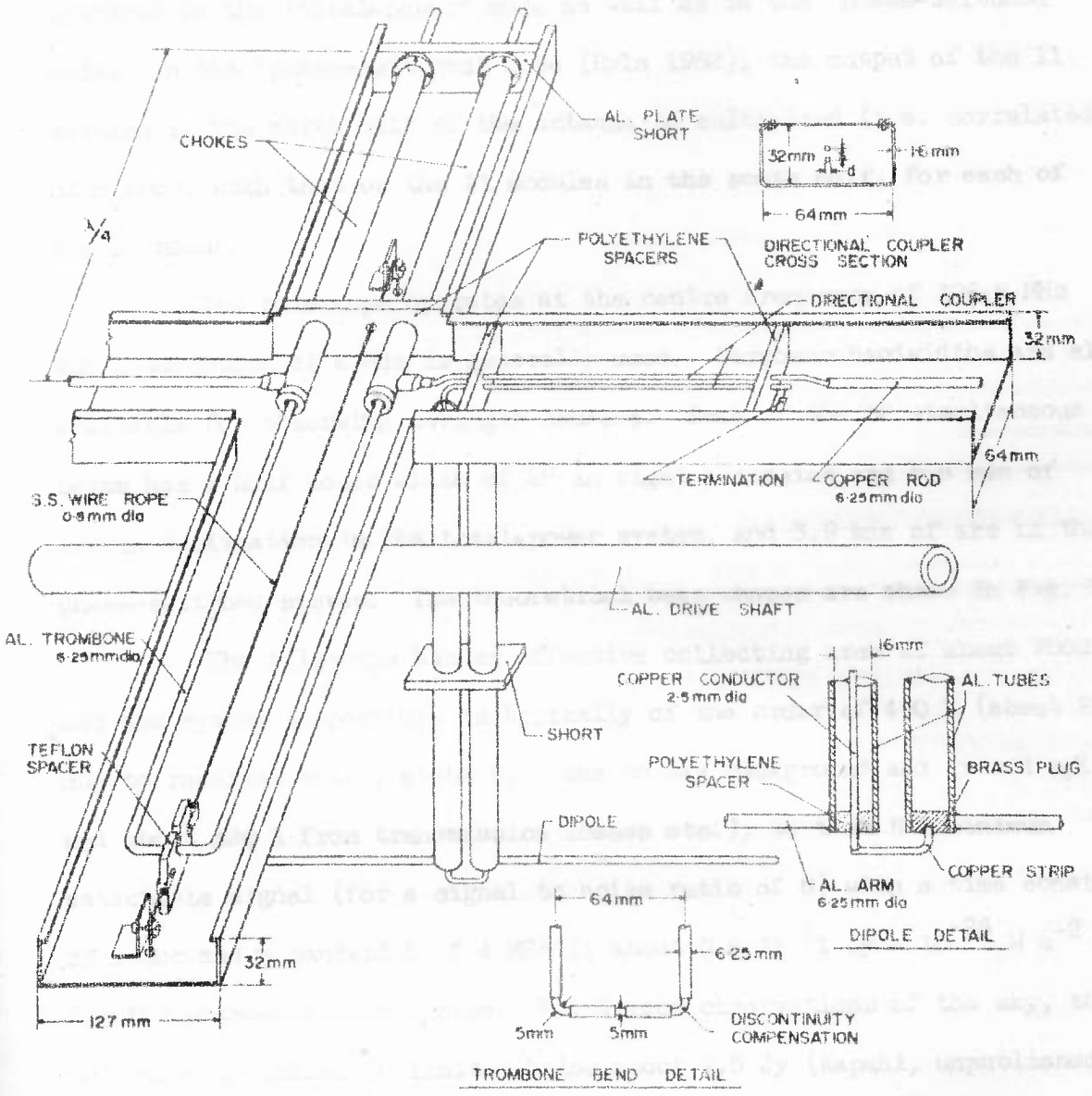

FIG. 2.2 A perspective view of a dipole, a directional coupler and an RF phase shifter.

and appropriately combined together in order to form 12 simultaneous beams, separated by 3 sec δ min of arc in declination. The 12 beams can be operated in the 'total-power' mode as well as in the 'phase-switched' mode. In the 'phase-switched' mode (Ryle 1952), the output of the 11 modules in the north half of the antenna is multiplied (i.e. correlated, Blum 1959) with that of the 11 modules in the south half, for each of the 12 beams.

The telescope operates at the centre frequency of 326.5 MHz and a bandwidth of 4 MHz is generally used. Narrower bandwidths are also available for observing stronger sources. Each of the 12 simultaneous beams has a half power width of 2^{o} in right ascension and 5.6 min of arc in declination in the total-power system, and 3.9 min of arc in the phase-switched system. The theoretical beam shapes are shown in Fig. 2.3.

The telescope has an effective collecting area of about 7000 m^2 and the system temperature is typically of the order of 400 K (about 220 K due to receiver noise, about 60 K due to sky background and ground spillover, and about 120 K from transmission losses etc.), so that the minimum detectable signal (for a signal to noise ratio of 5) with a time constant of 1 sec and a bandwidth of 4 MHz is about 0.6 Jy (1 Jy = 10^{-26} W m^{-2} Hz^{-1}) for the phase-switched system. For direct observations of the sky, the telescope is confusion limited below about 1.5 Jy (Kapahi, unpublished work).

2.2 Observations of Lunar Occultations

Since the telescope can detect occultations of sources much weaker than those already catalogued in the Moon's path (e.g. the 4C catalogue has a sensitivity limit corresponding to about 1.3 Jy at 327 MHz)

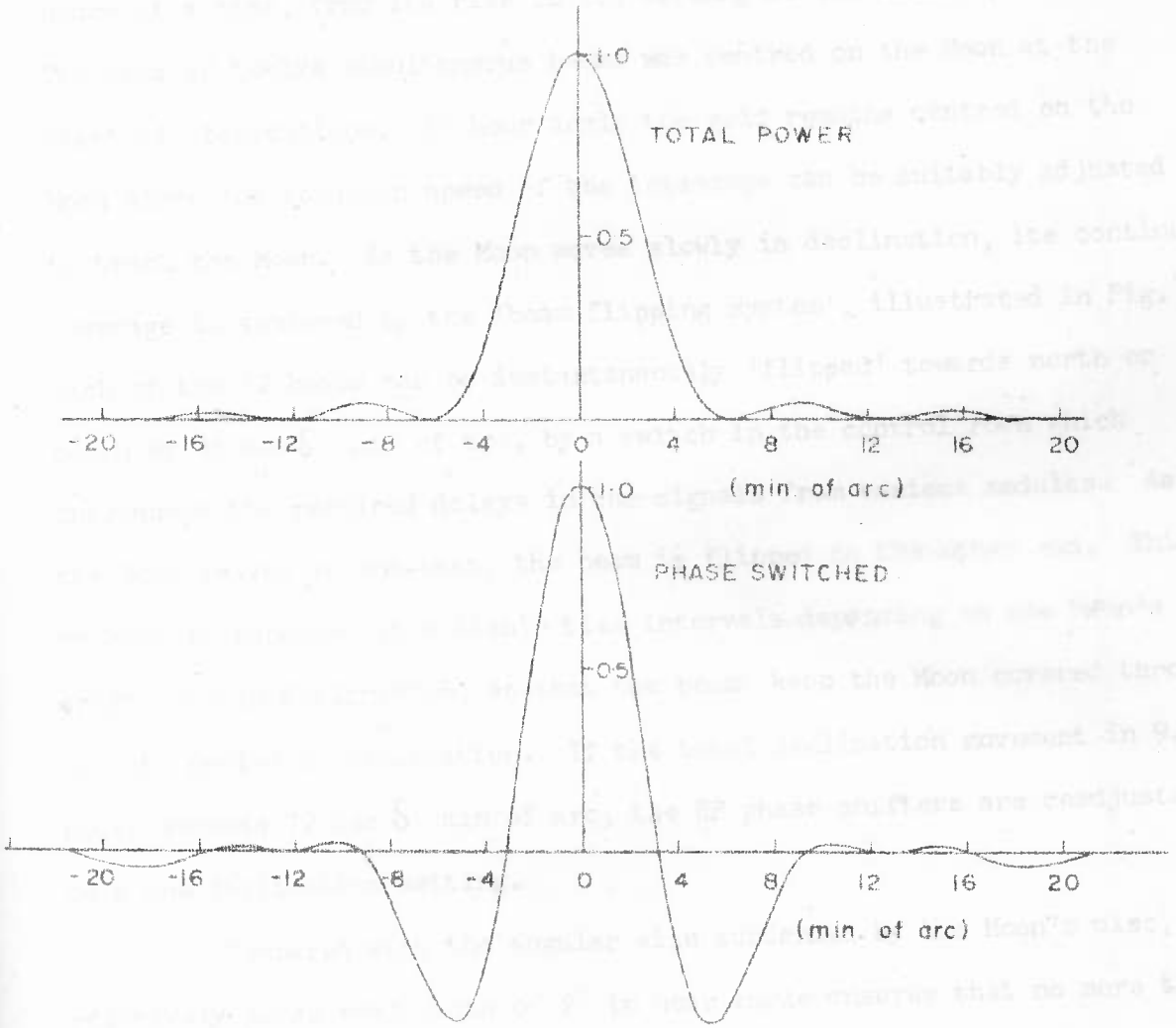

FIG. 2.3 Theoretical power patterns of the Ooty radio telescope in declination for the 'total power' and 'phase switched' systems.

the telescope was generally used to make a survey of sources by the occultation technique, rather than to observe the predicted occultations of catalogued sources. The Moon was tracked continuously for about 9.5 hours at a time, from its rise to its setting at the telescope horizons. The grid of twelve simultaneous beams was centred on the Moon at the start of observations. In hour angle the grid remains centred on the Moon since the rotation speed of the telescope can be suitably adjusted to track the Moon. As the Moon moves slowly in declination, its continuous coverage is achieved by the 'beam flipping system', illustrated in Fig. 2.4. Each of the 12 beams can be instantaneously 'flipped' towards north or south by 36 sec δ min of arc, by a switch in the control room which introduces the required delays in the signals from various modules. As the Moon leaves an end-beam, the beam is flipped to the other end. This process is repeated at suitable time intervals depending on the Moon's drift rate in declination, so that the beams keep the Moon covered throughout the period of observation. If the total declination movement in 9.5 hours exceeds 72 sec δ min of arc, the RF phase shifters are readjusted to a new declination setting.

Compared with the angular size subtended by the Moon's disc, the relatively large beam width of 2° in hour angle ensures that no more than about 5 per cent of the maximum sensitivity is lost due to the displacement of the beam centres from the lunar edge where occultations take plase. The loss in sensitivity due to the displacement of the beams in declination with respect to the peak of the antenna pattern due to each module (beam width in declination $\sim 2^{\circ}$) can be considerably larger. The average loss for the flipped beams amounts to about 20 per cent.

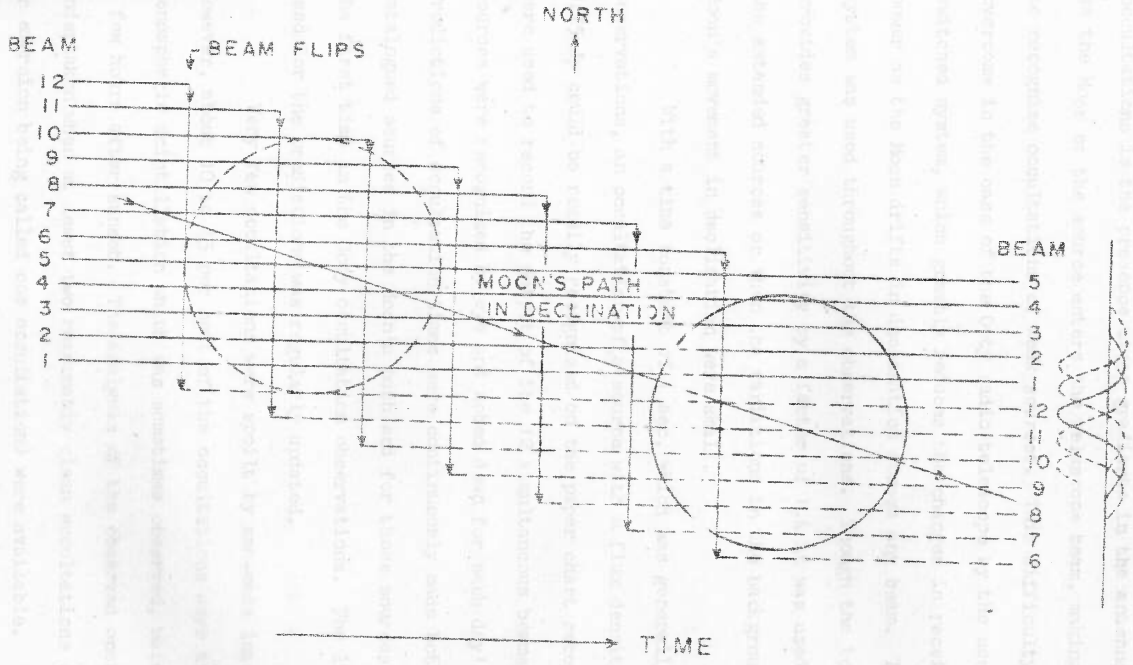

FIG. 2. The 'beam flipping' system for tracking the moon in declination.

A problem often encountered in the observation of lunar occultations is the presence steep gradients in the antenna temperature as the Moon or the source enters the telescope beam, making it difficult to recognize occultations of weak sources. This difficulty is largely overcome in the case of the Ooty radio telescope by the use of the phase-switched system, which greatly reduces the changes in receiver output power as the Moon drifts in declination across any beam. The phase switched system was used throughout the observations. Though the total power system provides greater sensitivity by a factor of 1.4 it was used mainly for the extended sources or when the variations in the background and the Moon's movement in declination were small.

With a time constant of 1 sec, which was generally used for the observations, an occultation of a source with a flux density of about 0.25 Jy could be readily recognized on the paper chart recorders that were used to record the output of the 12 simultaneous beams. All such sources were recognized by eye and noted down for each day's observations. Predictions of occultation times were continuously made both for the catalogued sources in the Moon's path and for those sources observed for the first time in the Ooty occultation observations. The list of sources used for the predictions was regularly updated.

Very few occultations were spoilt by man-made interference. However, about 10 to 15 per cent of the occultations were affected by ionospheric scintillation which was sometimes observed, mainly during a few hours after sunset. The analysis of the observed occultations was undertaken when at least two reasonably clean occultations (each immersion or emersion being called one occultation) were available.

2.3 Analysis of Occultation Records

The theory of lunar occultations (e.g. Cohen 1969) and the method of analysis to obtain the radio position and the brightness distribution across a source are now well known, and will not be described in detail. The position is obtained from the points of intersection of the apparent limbs of the Moon at the times of occultations. In general there is an ambiguity in the source position as there are two points where the lunar limbs intersect. This ambiguity is, however, easily resolved in the case of the Ooty telescope since the lunar limb is covered by 12 beams, each of which is quite narrow in declination. The ambiguity was encountered only in a very few cases in which the two possible positions differed by less than about 0.5 min of arc in declination.

The method of deriving the strip brightness distribution across a source has been worked out in a now famous paper by Scheuer (1962), who first showed that the brightness distribution, as would be observed with a narrow fan beam, can be recovered from the observed diffraction pattern by convolution with a suitable restoring function, i.e.

$$B(\theta) = I(\theta) * R(\theta)$$

where $I(\theta)$ is the observed occultation curve, $R(\theta)$ the restoring function and $B(\theta)$ is the restored strip scan of the brightness distribution. The restoring function $R(\theta)$ is given by

$$R(\theta) = S(\theta) * I''_p(-\theta)$$

where $I''_p(\theta)$ is the second derivative of the diffraction pattern for a point source, and $S(\theta)$ is a smoothing function, which is generally taken to be a Gaussian, say of half power width β . The restored brightness

strip scan $B(\theta)$, is thus the true distribution as it would be observed with a Gaussian fan beam of width β, in a position angle perpendicular to the Moon's limb at the point of occultation. Scheuer (1962) has also shown that the attainable angular resolution does not depend on the size of the first Fresnel zone but is limited only by the signal to noise ratio of the observation.

Scheuer's method of restoration has been investigated in detail by von Hoerner (1964), who has also calculated the restoring functions for several Gaussian widths and developed a computer program to do the restorations. von Hoerner has also investigated the accuracy of restoration as a function of noise and receiver bandwidth. Most of the problems and complications encountered in the actual analysis of occultation records have been discussed by Sutton (1966).

The restoration procedure used by us was very similar to that described by von Hoerner (1964). Since a stable digital recording system became available only in late 1971 the observed occultation data were manually digitized from paper chart records at uniform time intervals, varying generally from about 0.5 to 2 sec, depending on the chart speed and the signal to noise ratio. Visual estimates of the times of occultation from the chart records were first used to calculate the positions of the lunar limbs and their points of intersection and other occultation parameters, such as the position angle of occultation and the Moon's limb velocity in the sky. The same computor program then used these parameters to perform the restorations with specified Gaussian resolutions (half power widths), β. A coarse resolution ($\sim$ 15" or 30" arc) was first used to obtain more accurate estimates of occultation times and the restorations then performed

with increasing resolutions till the signal to noise ratio on the restored outputs became less than 5. The observed offsets in the component positions with respect to the adopted origin (corresponding to the occultation times) were combined graphically to obtain the final radio positions, after applying corrections (generally $< 2''$ arc) for irregularities of the lunar limb at the points of occultation, as determined from the limb maps of Watts (1963).

Source sizes were determined from the observed broadening of the strip scans with the Gaussian beam shapes of the restorations. The effective resolution of each scan, β_e, was first estimated by allowing for the effects of time constant, manual digitization and the receiver bandwidth (all these had negligible effect on the resolution for $\beta \gtrsim 5''$). The broadening was estimated generally from the scans with the highest resolutions that permitted a meaningful measurement of sizes in the presence of noise in the restored outputs (i.e. signal to noise ratio $\gtrsim 5$). For double sources the separation and orientation of the components were determined graphically by combining the positions from two or more occultations. It should be noted that if the two components are of identical size and flux density there is an ambiguity in pairing them from only two occultations. This was, however, rarely found to be the case.

A typical occultation record of a source (OTL 1123+012; $S_{327} \sim 1.2$ Jy) is shown in Fig. 2.5 and the restored strip scans in Fig. 2.6. With $\beta_e = 1''.3$ arc the source appears resolved in both the position angles. Angular sizes in the two PAs are estimated to be about $2''$ and $3.5''$ arc respectively. The source may be double in PA $11^{\circ}.7$.

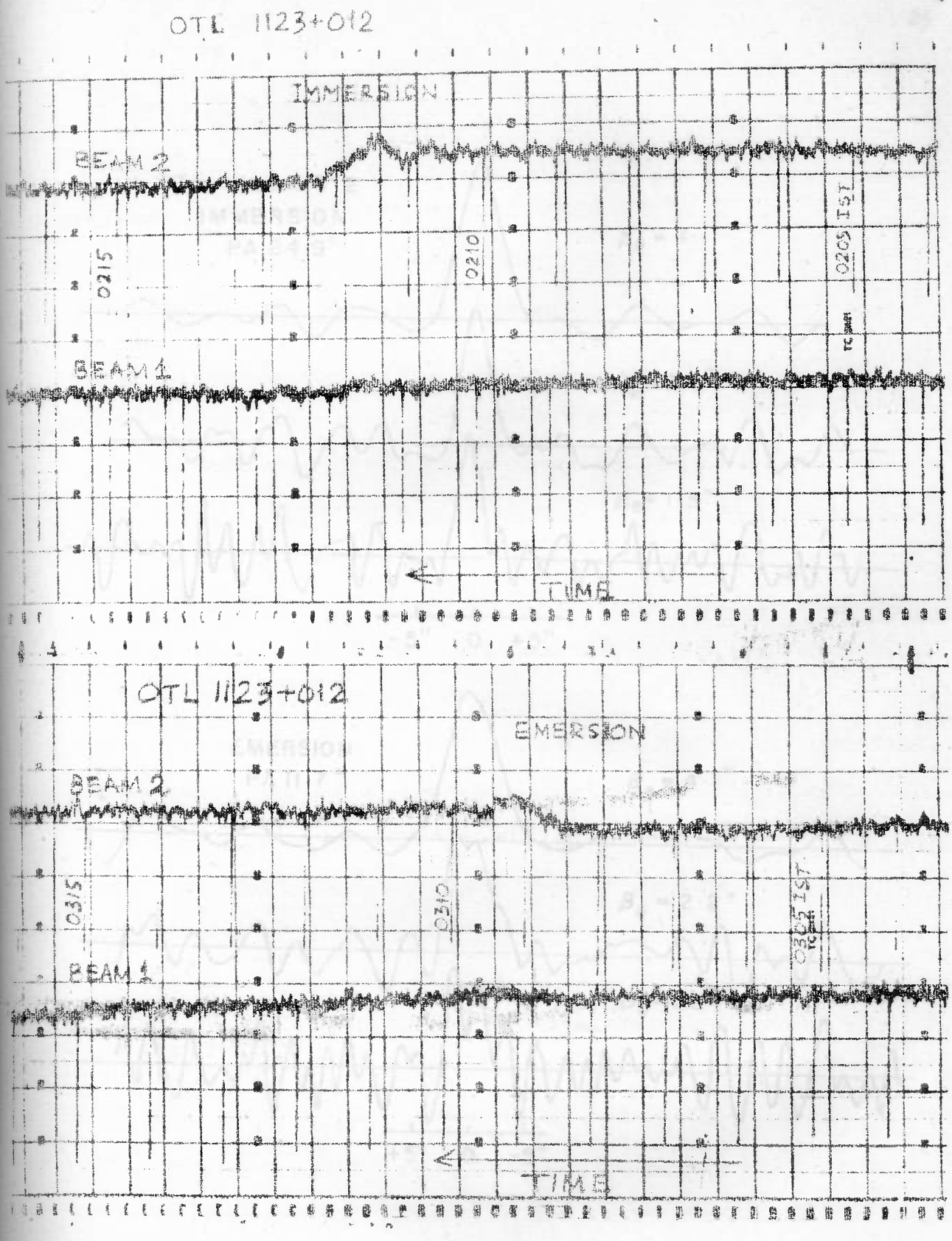

FIG. 2.5 Typical occultation record of a radio source; OTL 1123+012. Time marks are one minute apart.

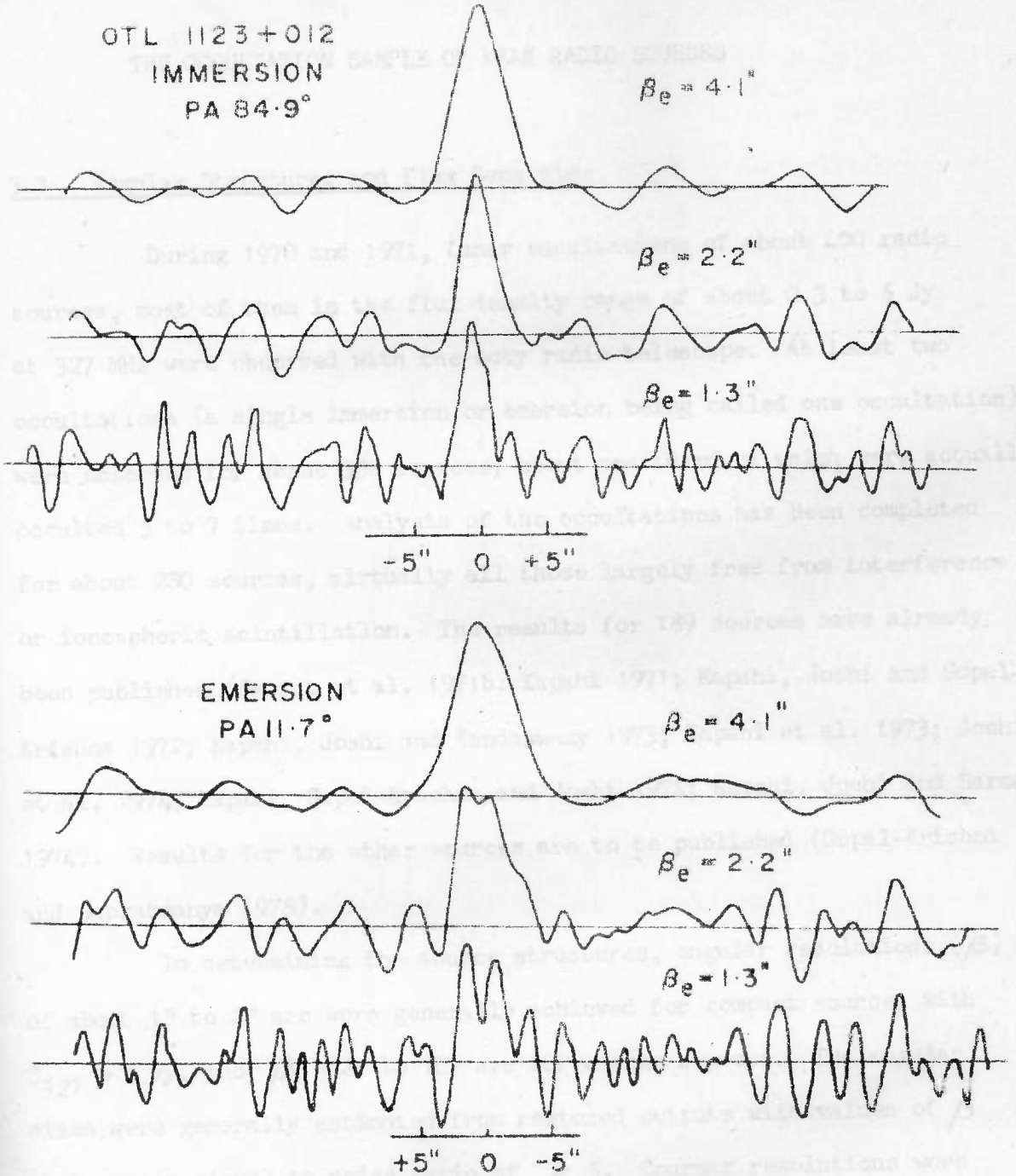

FIG. 2.6 Restored strip scans across the radio source OTL 1123+012 with different effective resolutions, β_e.

Chapter 3

THE OCCULTATION SAMPLE OF WEAK RADIO SOURCES

3.1 Angular Structures and Flux Densities

During 1970 and 1971, Lunar occultations of about 400 radio sources, most of them in the flux density range of about 0.3 to 5 Jy at 327 MHz were observed with the Ooty radio telescope. At least two occultations (a single immersion or emersion being called one occultation) were observed for about 330 sources, about one third of which were actually occulted 3 to 7 times. Analysis of the occultations has been completed for about 280 sources, virtually all those largely free from interference or ionospheric scintillation. The results for 189 sources have already been published (Swarup et al. 1971b; Kapahi 1971; Kapahi, Joshi and Gopal-Krishna 1972; Kapahi, Joshi and Kandaswamy 1973; Kapahi et al. 1973; Joshi et al. 1974; Kapahi, Gopal-Krishna and Joshi 1974; Kapahi, Joshi and Sarma 1974). Results for the other sources are to be published (Gopal-Krishna and Subrahmanya 1975).

In determining the source structures, angular resolutions (β) of about 1" to 2" arc were generally achieved for compact sources with $S_{327} > 1$ Jy, and β = 2" to 10" arc for weaker sources. The angular sizes were generally estimated from restored outputs with values of β that gave a signal to noise ratio of $\gtrsim 5$. Coarser resolutions were also used in all cases to look for any weak and/or extended components in the brightness distributions. A source was considered unresolved if the restored distribution with an optimum β (signal/noise ~ 5) was broadened by less than about 1.3 or 1.4 times β .

To calculate the total flux density of an occulted source, the peak deflection was first estimated by fitting the amplitudes of the occultation steps in 3 or 4 neighbouring beams with the known beam pattern of the phase-switched system in declination. The flux was then determined by comparison with the peak deflections produced by calibration sources (generally chosen from the 3C and Parkes catalogues) observed before or after a day's observing session. The measured flux densities, in general, had rms errors of $\pm 20\%$ for sources with $S_{327} > 1$ Jy and $\sim 30\%$ for the weaker sources.

In order to obtain more accurate flux density information, most of the occultation sources south of $\delta = 20^{\circ}$ were observed by G. Swarup and J. Sutton (to be published) at 408 MHz with the Molonglo Cross telescope during August-September 1973. These measurements have estimated rms errors of $\sim 8\%$ and are referred to the absolute flux scale of Wyllie (1969).

3.2 Optical Identifications

Optical identifications were attempted for the occultation sources from the prints of the Palomar Sky Survey, and the results are given in the papers mentioned above. Most of the identification work was done by Dr. M.N. Joshi and Mr. C.R. Subrahmanya. Details of the identification procedure and the measurement of accurate (better than 1" arc) optical positions have been described by Kapahi et al. (1973). Because of the accurate radio positions and structures provided by the occultation data, the suggested identifications should be highly reliable. It should also be noted that the good agreement in radio and optical positions implies that the Blue Stellar Objects (BSOs) identified with Ooty sources are almost certainly QSOs, since the probability of chance coincidence within a few

arc sec is negligible. Only about 30% sources could be identified; ~17% with galaxies and 13% with BSOs (Joshi 1975).

3.3 The Sample of 164 Ooty Sources

For the purpose of investigating the cosmological implications of the observed angular sizes, to be described in Chapters 4 and 5, we have selected an unbiased sample of 164 sources from the Ooty occultation lists, on the basis of the following two criteria.

(i) We exclude sources which have a galactic latitude of $|b| < 10^{\circ}$. This ensures that the sample consists almost entirely of extragalactic sources. Although most of the excluded sources are also likely to be extragalactic (sources suspected to be galactic from their very large angular sizes are not included in the lists of 280 sources) it is difficult to make reliable optical identifications at low galactic latitudes.

(ii) We also exclude those sources for which the extreme position angles of occultations differed by $< 30^{\circ}$ or $> 150^{\circ}$ (considering the position angles to lie between 0° and 180°). The angular size of a source estimated from strip scans along a limited number of position angles is, in general, smaller than the true size, since none of the directions of scan need coincide with the direction of elongation of the brightness distribution. Statistically, the uncertainty in the largest angular size of a source due to the limited number of scans is greatly reduced if the directions of scan are well separated in angle.

The final list of 164 retained sources does not form a 'complete sample' in the usual sense of containing all sources above a certain flux density in a given solid angle on the sky. Nevertheless, the sample should

be 'representative' and unbiased with regard to angular sizes, since sources have been analysed and chosen irrespective of their angular structures. We have not made a detailed analysis of the total surface area of the sky covered in the Ooty survey. An approximate analysis shows that the area increases with flux density from about 0.014 ster for sources in the range 0.25 to 0.5 Jy to $\sim$ 0.1 ster for those in the range of about 2 to 5 Jy. The larger area for stronger sources arises because on many occasions observations were limited to predicted occultations of catalogued sources.

Data for the 164 sources is listed in Table 3.1, which is arranged as follows:

Column 1. Source number. The last digit refers to the tenths of degree in declination. Sources from List 1 (Swarup et al. 1971b), in which only two digits were used for the declination, have now been given 3 digits, as in all the subsequent lists.

Column 2. The corresponding source number from another catalogue whenever available. Only one catalogue is mentioned although some of the stronger sources may occur in several catalogues. References to other catalogues are given in Dixon (1970), except for the following.

Source Designation	Catalogue	Reference
ON - OZ	Ohio Survey; Southern part	Ehman, Dixon & Kraus (1970)
B2	Bologna Survey	Colla et al. (1972)
PKS $\pm 4^{\circ}$	Parkes 2.7 GHz Survey	Wall, Shimmins & Merkelijn (1971)

TABLE 3.1

Lunar Occultation Sample of 164 Radio Sources

(1) Source No. OTL	(2) Other Name	(3) S_{327} (J_y)	(4) S_{408} (J_y)	(5) Structure	(6) θ (arc sec)	(7) Flux ratio	(8) Opt. Id.	(9) Ref.
0004+040		0.4	0.28		≤ 8			6
0006+046	0B+013	1.0	1.01		~ 16		G	6
0011+054	4C 05.03	4.2	3.95	D	3.5	3		3
0023+058		0.6	0.53		< 4		Q?	5
0038+086	4C 08.05	3.5	3.47	D	91	1	G	3
0042+082		0.3	0.30		~ 18			4
0057+105	4C 10.04	1.0	0.95*		~ 1.7			6
0116+128		0.7	0.75		~ 29		G	6
0117+138		0.3	0.30		~ 22			6
0133+146		0.8	0.53		≤ 3			1
0134+142	4C 14.07	1.2	1.06	C	~ 30			5
0139+155		0.8	0.90		≤ 2		Q	1
0142+153		0.6	0.85		~ 12		G	1
0208+183	4C 18.08	0.8	0.79		≤ 2		Q	3
0209+184		0.8	0.65		< 2			3
0210+190		0.8	0.48		~ 3.5			5
0216+190		0.5	0.41		≤ 5			4
0240+208		0.4	0.34*		≤ 5			4
0240+210		0.4	0.34*		~ 4		G	4
0325+238		0.5	0.42*		~ 23			6
0327+241	4C 24.07	1.8	1.63*	C	~ 36		G	3
0327+246		1.2	1.25**	C	~ 50		G	3

Table 3.1 (Continued)

(1)	(2)	(3)	(4)	(5)	(6)	(7)	(8)	(9)
0328+248	4C 24.08	1.4	1.45**	D	6".5	1		3
0341+251	4C 25.13	1.5	1.37**	D	17	1.4		3
0358+251	B2	0.4	0.84**		~42			6
0400+258	OF 200	1.0	1.46**		< 1.2		Q	2
0405+258	B2	1.0	1.11**		~ 2			4
0410+266	4C 26.15	2.1	2.07**	D	3	1.7		1
0416+270	4C 27.13	2.8	2.20**	D	72	2.4		4
0433+262	B2	1.7	0.83**	D	16	1.4		6
0434+269		0.4	0.34*		~ 2.7			6
0435+270		0.6	0.53*	D	10	1.5		4
0437+273	B2 0437+27A	0.4	0.34*		~12		G	4
0450+270	B2	0.5	0.53**		≤ 15			6
0638+273	OH 264	1.0	0.95*		< 2			5
0642+266	4C 26.24	1.4	1.11**	C	~18			3
0648+263	4C 26.25	2.3	1.91**	D	16.5	1.1	G	3
0710+257	4C 25.20	1.4	1.29**	D	17	2.2		3
0710+241	4C 24.14	0.5	0.42*		~ 3.7			6
0719+248	B2	0.4	0.36**		< 8		G	6
0725+248	B2 0725+24B	0.7	0.63*		<10			5
0802+212	PKS	0.4	0.34*		~ 18			6
0803+214		0.7	0.63*	D	13	1.4		6
0805+225	4C 22.19	1.5	1.43*	D	15	1		3
0806+210		0.5	0.42*		~20			6
0814+201	H 0814+20	0.5	0.40		≤15			6

Table 3.1 (Continued)

(1)	(2)	(3)	(4)	(5)	(6)	(7)	(8)	(9)
0811+227	4C 22.20	2.5	2.5*	D	22"	1.4	Q	3
0815+238	4C 23.19	1.5	1.43*		< 2		Q	1
0815+229		0.6	0.54*		~13		S	4
0817+212		0.3	0.25*	D	11	1.5		5
0818+214	OJ 230	0.6	0.54*		~12			5
0820+225	4C 22.21	3.5	3.5*		< 2.5		Q	1
0823+207		0.7	0.63*		~ 3			5
0840+184	4C 18.25	1.05	1.00*		~ 6.5			6
0848+181	4C 18.26	1.0	0.87	D	16	1	Q	3
0854+191		0.25	0.22*		≤ 3			5
0856+178		0.5	0.36		≤ 6			5
0857+171	4C 17.47	2.3	1.58	D	13	1.5		3
0907+185	PKS	2.0	2.22		~ 5.5			5
0911+174	4C 17.48	5.0	4.88	D	46	3	Q	3
0914+175	VRO 17.09.02	1.2	1.23		~10			4
0939+140	3C 225A	4.1	4.1*	D	7.5	2.3	G?	8
0943+123	4C 12.35	1.4	1.34*	D	12	2.8	Q	6
0951+131		0.5	0.42		~14			6
0954+125		0.5	0.42		≤ 4			5
0954+126		0.4	0.45		≤10			5
0958+113	4C 11.33	1.4	1.37	D	6	1		3
1003+130		1.0	1.04		< 3.5			1
1020+104		0.7	0.68		~ 4			4
1023+078	4C 07.31	1.9	1.50	D	10.2	1		3

Table 3.1 (Continued)

(1)	(2)	(3)	(4)	(5)	(6)	(7)	(8)	(9)
1025+076		0.35	0.30*		~ 8"			6
1037+067	4C 06.41	2.0	1.68		< 3			5
1038+064		1.7	1.49		< 4		Q	5
1040+062		1.5	1.47	D	15	1.3		6
1041+058	4C 05.45	1.8	2.19		~ 8			3
1104+058	4C 05.48	2.0	2.04		≤ 10		G	3
1108+034	4C 03.21	4.2	3.85	D	8	2		1
1123+012	PKS ± 4°	1.2	1.17		~ 3.5		G	5
1127+012	4C 01.30	2.1	1.64	C	~ 52		G	4
1129+014		0.5	0.52		~ 5			4
1130+009	PKS ± 4°	0.5	0.42	D	12	2.3	Q	2
1132-000	4C-00.45	3.0	2.93		< 1.4		S	2
1140-021		1.1	0.48		< 2			6
1142-002	4C-00.46	3.0	3.20	D	29	3.3		4
1155-029	PKS ± 4°	0.9	0.90		≤ 6		G	5
1159-023	4C-02.50	2.4	2.44		< 1.5			1
1215-052		0.4	0.32		≤ 5			6
1216-069	PKS	3.5	3.50	D	49	2		6
1225-083	ON-043	2.2	1.85		~ 10		G	6
1241-089		0.3	0.25*		< 8			5
1257-113		1.3	0.83	D	150	1.5		6
1302-112		1.1	0.66		~ 20			4
1304-101	OP-107	1.4	1.60		~ 4			4
1311-122	PKS	2.2	1.4		≤ 2			4

Table 3.1 (Continued)

(1)	(2)	(3)	(4)	(5)	(6)	(7)	(8)	(9)
1350-154		1.0	0.38		$\sim 3''$			1
1354-174	PKS	1.5	0.84		≤ 1.2		Q	2
1354-176	PKS	2.4	2.62	D	10.5	1.8	Q	4
1402-177		0.4	0.34		~ 16			4
1411-191		0.9	1.08		< 2			1
1417-192	PKS	5.5	4.56	C	~ 60			5
1426-195		0.7	0.83		≤ 2			4
1514-241	PKS	1.5	1.70		< 0.8		G	7
1527-242		0.8	0.75	D	21	1.3	G	1
1529-246		0.5	0.20		~ 23		G	6
1547-254		0.9	0.74		~ 5			5
1556-260		0.6	0.92		~ 14			1
1556-262		0.8	0.82		~ 10			6
1557-263		0.9	1.02		~ 21			1
1559-265		0.4	0.64		~ 5			1
1627-272		0.8	1.22	D	24	3		1
1628-278		0.5	0.77		~ 5			4
1628-268	MSH 16-205	8.0	5.48	C	~ 105			5
1854-261		0.5	0.42		~ 11.5			6
1859-274		0.4	0.34*	C	~ 30			4
1905-253		0.4	0.32		~ 16			6
1906-272		0.4	0.34		≤ 3			4
1907-256		0.3	0.25		< 8			6
1912-269	MSH 19-203	6.3	5.89	C	~ 125			4

Table 3.1 (Continued)

(1)	(2)	(3)	(4)	(5)	(6)	(7)	(8)	(9)
1928-237		0.6	0.36		~23"			6
1945-250		0.8	0.61		~ 4			4
1950-249		1.0	0.52		< 12			4
1951-232	OV-286	0.6	0.54*		< 8			6
1952-234		0.3	0.25*		~ 9			6
1952-236		0.5	0.33		≤ 4		G	4
2006-238		0.7	0.66	D	17	2		4
2010-231		0.9	0.82	D	13	3	Q?	5
2019-202	OW-232	0.9	1.02		~ 2		Q	6
2020-211	OW-233	2.1	1.42	D	86	1.4	G	5
2023-200	OW-248	0.4	0.68		≤ 7			6
2034-198	OW-257	0.8	0.72		≤ 2.1		G	5
2040-219		1.3	0.98	C	~ 20		G	4
2042-212	OW-271	0.6	0.5		~ 10		G	4
2050-188	PKS	2.1	1.91	D	2.6	1.2		5
2053-201	PKS	5.6	6.56	D	27	1	G	4
2054-198		0.6	0.62		~15			4
2057-179	PKS	2.2	2.72	D	10	2.6		5
2058-179	PKS	3.5	2.99		~ 4		Q	5
2103-195	OX-105	0.6	0.44		~ 2			4
2109-188		0.6	0.54	D	9½	1.1		1
2110-160	PKS	2.1	2.31	D	10	1.1	Q	6
2111-185	OX-119	3.0	2.14	D	16	1	Q?	1
2113-163		0.3	0.46	D	15	1		5

Table 3.1 (Continued)

(1)	(2)	(3)	(4)	(5)	(6)	(7)	(8)	(9)
2120-166	PKS	6.0	5.71	D	16"	2.7		5
2125-153.1		0.4	0.41		≤ 8			5
2125-153.2	OX-143	0.5	0.48		< 3		G	5
2127-157	PKS 2126-15	0.7	0.73		< 7			5
2150-142	OX-183	0.6	0.55		≤ 2.2			1
2151-140	OX-185	1.7	1.23		~ 16			4
2153-119		0.5	0.42*		~ 3.3			6
2154-117	PKS	3.0	3.93	D	21	1.6		5
2154-129		1.0	1.23	C	~ 29		G	5
2200-130		0.7	0.63	D	27	1.7	G	4
2204-115		0.8	1.18		~ 6			4
2232-062	4C-06.73	1.6	0.67		~ 15			6
2232-068		1.6	1.57*	D	16	1.3		6
2254-039	OY-092	1.2	1.14*	C	~ 19			6
2255-065		0.5	0.61		≤ 7		G	4
2256-054	OY-094	0.9	1.02	D	19	3.3		4
2257-048	4C-04.86	1.5	1.64		~ 2.2			3
2301-043	OZ-003	0.3	0.38		≤ 4			4
2302-025	4C-02.87	3.0	2.62	D	36	1.4		6
2310-033		0.5	0.58		≤ 7			5
2321-012		0.4	0.42		≤ 25			5
2333-002	OZ-056	0.6	0.62		≤ 20			5

Columns 3 and 4. Flux densities at 327 and 408 MHz respectively. Flux densities at 408 MHz are based on measurements at Molonglo (Swarup and Sutton 1975). Values of S_{408} marked by one asterisk (*) have been taken from the Bologna Catalogue (Colla et al. 1972), and multiplied by 1.08 to conform to Wyllie's (1969) scale. Values marked with two asterisks have been converted from S_{327} measured at Ooty by multiplication with appropriate factors determined from observations of other occultation sources at Molonglo.

Column 5, 6 and 7. Structural information. The overall angular size θ, is given in column 6. The value of θ depends on the structure type. The following criteria have been used.

If a source is clearly double (marked 'D' in column 5), θ refers to the separation between the two components. In such cases, the ratio of the intensities in the two components (stronger/weaker) is given in column 7. For sources with complex structure ('C' in column 5), θ refers to the largest angular size associated with the structure. For single and partially resolved sources, θ gives the half power width of a gaussian fit to the distribution along the position angle in which the size was found to be the largest. Upper limits to θ are given for the unresolved or marginally resolved sources.

Column 8. Optical identification. The symbols used are G = Galaxy, C = Blue Stellar Object; S = Stellar Object. Question marks are used if classification is uncertain.

Column 9. Reference to the occultation list where the structural and identification information has been given. For a few sources additional

occultations observed subsequently have been used to improve upon the information given in the original lists. The references are,

(1) Swarup et al. (1971b)

(2) Kapahi, Joshi & Kandaswamy (1973)

(3) Kapahi et al. (1973)

(4) Joshi et al. (1974)

(5) Kapahi, Joshi & Sarma (1974)

(6) Gopal-Krishna and Subrahmanya (1975)

(7) Kapahi (1971)

(8) Kapahi, Joshi & Gopal-Krishna (1972)

Some revisions to List 1 (Swarup et al. 1971b) are given in the Appendix (p.46).

3.4 Discussion of Source Structures

In general, the types of source structures revealed by the occultation observations at Ooty have been found to be similar to those known for stronger sources from aperture synthesis observations (e.g. Mackay 1971). As the distances of radio sources in the Ooty sample are not known the intrinsic sizes associated with source structures cannot be estimated. We therefore discuss briefly, some aspects of the observed structures that do not depend on distance.

The angular resolution achieved in determining the source structure from a lunar occultation depends on flux density and angular extent of a source. In the Ooty sample of 164 sources the resolution varies generally between about 1" to 10" arc. It is interesting that nearly 70 per cent of the sources in the entire sample have been resolved. The numbers and percentages of resolved and resolved sources in four flux density ranges of the sample are listed in Table 3.2. The partially resolved sources

TABLE 3.2

Statistics of resolved and unresolved sources in the Ooty sample

Flux Range (408 MHz)	Number of sources	Number resolved	Number unresolved or partially resolved
≥ 1.5 Jy	40	34 (85%)	6 (15%)
1.0 to 1.49 Jy	30	24 (80%)	6 (20%)
0.50 to 0.99 Jy	50	30 (60%)	20 (40%)
< 0.5 Jy	44	25 (57%)	19 (43%)
Total	164	113 (69%)	51 (31%)

(which appeared broadened by less than 1.3 or 1.4 times the effective resolution, β_e) have been grouped along with the unresolved (no noticeable broadening) sources. The fraction of resolved sources is seen to decrease appreciably with flux density. This is explained partly by the generally poorer angular resolution at lower flux levels and partly by the decreasing overall angular extents of radio sources with decreasing flux density (the relation between angular size and flux density is investigated in detail in the next Chapter). The best data, from the point of view of sensitivity as well as angular resolution, are those for the 40 sources with $S_{408} \geq 1.5$ Jy (with a median value of $S_{408} \sim 2.2$ Jy, which is about 3.5 times smaller than for the 3CR sources that have been well studied by the Cambridge group at high frequencies). In the subsequent discussion we shall confine outselves mainly to this smaller sample of Ooty sources.

3.4.1 Sources with $S_{408} \geq 1.5$ Jy

(a) Overall structure

Of the 40 sources with $S_{408} \geq 1.5$ Jy, 34 ($\sim$ 85 per cent) are found to be resolved. Of these 34 resolved sources, as many as 23 ($\sim$ 60%) show a basic double structure, while 5 have more complex distribution of brightness and 6 appear to consist of a single component. None of the 6 single sources is highly resolved, (with resolutions of about 2" to 10" arc) and it is possible that most of these may also exhibit double or complex structure when observed with higher angular resolution. It appears then, that almost all the resolved sources show a double or more complex distribution of brightness. Sources with complex structure have either 3 or more components (so that it is difficult to make a two dimensional model of the brightness distribution from scans along 2 or 3 position angles) or have a 'head and tail' type structure (e.g. OTL 1417-192 or OTL 1628-268; Kapahi, Joshi and Sarma 1974). None of the sources has a clear 'core-halo' type of structure.

Flux densities for all the 40 sources are known at 1.4 GHz and in most cases also at 2.7 GHz from measurements made by Dr. T.K. Menon with the NRAO 300 ft. telescope, or from measurements reported in the literature. It is interesting to note that of the six sources that are unresolved (5 with angular resolutions in the range of 1" to 3" arc and 1 with β_e = 10" arc; the angular resolution on this source, 1104 + 508, is limited by ionospheric scintillation in the records, but there is some evidence of partial resolution) two, viz. 0820 + 225 and 1514-241 have a flat spectrum (spectral index $\alpha < 0.5$) between 408 MHz and 2.7 GHz. On

the other hand, none of the 34 resolved sources has a spectral index < 0.5, in the above range of frequencies. Of over 200 Ooty sources down to ~ 0.5 Jy at 327 MHz for which flux densities are available at 1.4 GHz (T.K. Menon and V.K. Kulkarni, private communication) only 10 appear to have a spectral index $\alpha < 0.5$. These observations confirm the following general conclusions that have been reached by several investigators in the last few years.

(i) Sources with flat spectra are almost always associated with compact components, and

(ii) the fraction of sources with flat spectra is quite small ($\lesssim 5$ per cent) in surveys made at low frequencies ($\lesssim 400$ MHz).

(b) Flux ratios for double sources

The distribution of the ratio of flux density in the stronger component to flux density in the weaker component for the 23 double sources is shown in Fig. 3.1. It is clear from the distribution that the components of double sources tend to have similar intensities, as is well known for the 3CR sources (Mackay 1971). The rare occurrence of sources with flux ratios exceeding ~ 3 is unlikely to have been caused by observational difficulties since the sensitivity of the observations should have enabled flux ratios as large as ~ 6 to be detected if the components were well separated. If the components are close together (within $\sim 2''$ or $3''$ arc), however, it is possible that the weaker component is not detected in the occultations; but the number of such sources cannot be appreciable since most of the sources have, in fact, been resolved into two or more components.

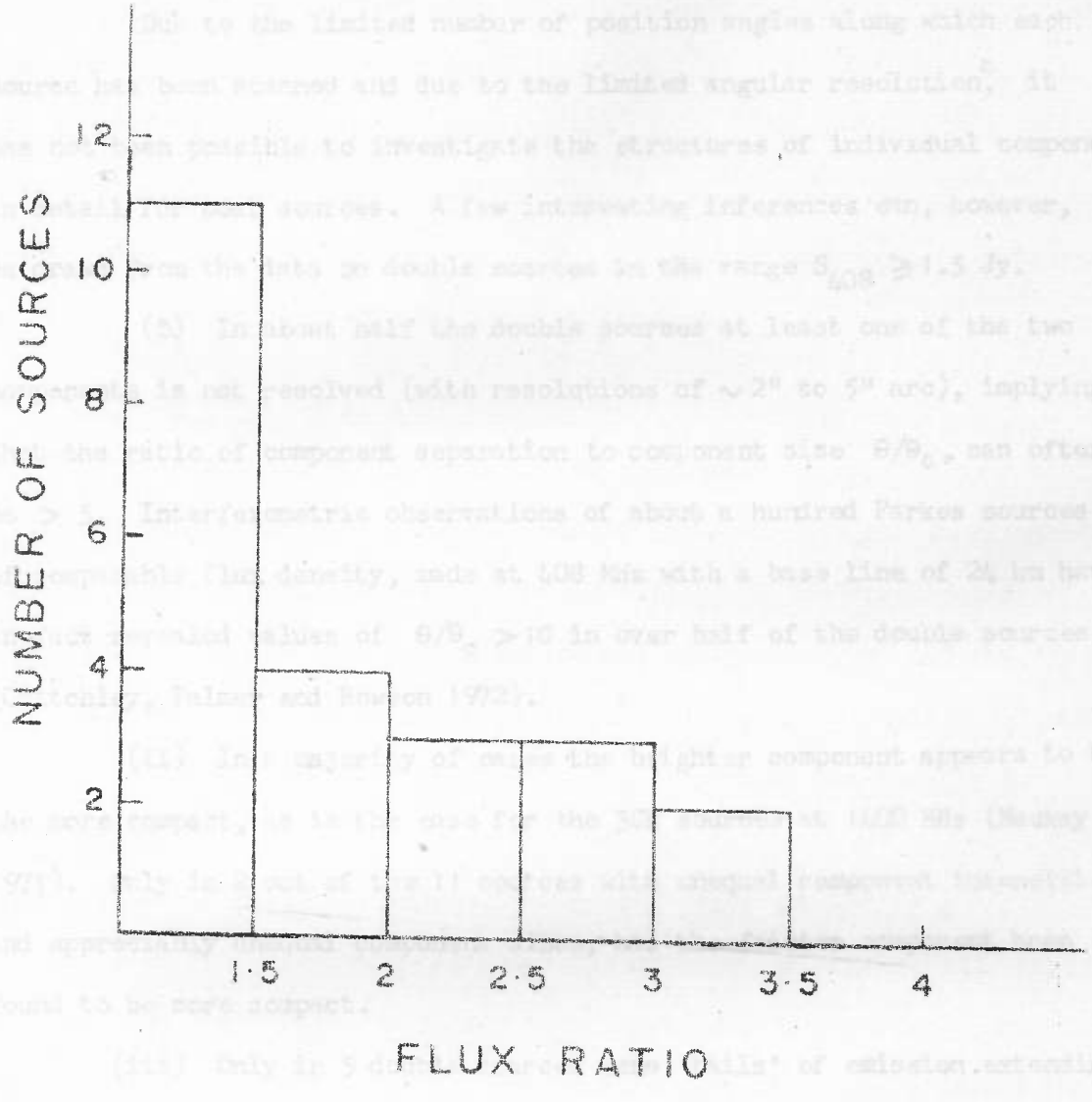

FIG. 3.1 Distribution of flux ratios for 23 double sources with $S_{408} \geq 1.5$ Jy.

(c) Structure of individual components

Due to the limited number of position angles along which each source has been scanned and due to the limited angular resolution,* it has not been possible to investigate the structures of individual components in detail for most sources. A few interesting inferences can, however, be drawn from the data on double sources in the range $S_{408} \geq 1.5$ Jy.

(i) In about half the double sources at least one of the two components is not resolved (with resolutions of $\sim 2''$ to $5''$ arc), implying that the ratio of component separation to component size θ/θ_c, can often be > 5. Interferometric observations of about a hundred Parkes sources of comparable flux density, made at 408 MHz with a base line of 24 km have in fact revealed values of $\theta/\theta_c > 10$ in over half of the double sources (Critchley, Palmer and Rowson 1972).

(ii) In a majority of cases the brighter component appears to be the more compact, as is the case for the 3CR sources at 1400 MHz (Mackay 1971). Only in 2 out of the 11 sources with unequal component intensities and appreciably unequal component sizes, has the fainter component been found to be more compact.

(iii) Only in 5 double sources were 'tails' of emission extending inwards from one or both components detected. Although weak 'tail' or 'bridges' might have gone undetected in some cases due to observational difficulties, it seems unlikely that such diffuse components accounting for a sizeable fraction of the total flux are very common at 327 MHz.

---

* It may be pointed out that higher angular resolutions are expected to be achieved for the occultations observed at Ooty since 1973 due to (a) digital recording of data on magnetic tapes and (b) the use of an optimum deconvolution technique for data analysis developed by Subrahmanya (1975), which gives a marked improvement in resolution over Scheuer's restoration technique.

(iv) In none of the 23 double sources (except for one possible exception in OTL 0416+270), has a compact central component, (associated with the optical object or lying between the two components in the case of unidentified sources) contributing more than about 10% per cent of the source flux density, been detected. Such components are often seen at high frequencies. Their absence in the occultation sources is consistent with the central components having flat spectra.

(d) Location of scintillating components

Information on the presence of components of angular extent $\lesssim$ 1" arc can be obtained also from observations of interplanetary scintillation (IPS) of radio sources. The IPS surveys at low frequencies ($\lesssim$ 430 MHz), and at flux levels corresponding to $\sim$ 2 Jy at 408 MHz, indicate that about 50 to 60 per cent of all sources have such scintillating components (Harris and Hardebeck 1969; Bhandari, Ananthakrishnan and Pramesh Rao 1974; Readhead and Hewish 1974). These observations do not, however, give information on the location of scintillating components within the overall structure of radio sources. Although the occultation observations have not provided sufficient resolution to resolve such compact components in many sources, statistically the observations provide strong evidence that in a large fraction of sources ($\gtrsim$ 25 per cent) the scintillating components are likely to be located within the pair of components of double sources. This conslusion follows from the fact that about 70 per cent of the Ooty sources with $S_{408} \geq 1.5$ Jy are found to be double or complex with no evidence of compact central components. Recent observations of Cyg-A

(Hargrave and Ryle 1974) with the Cambridge 5 km telescope indicate the presence of compact components with sizes of 2 to 3 kpc at the outer edges of the two main components. Similar compact 'heads' have also been observed in a recent occultation of 3C 33 at Ooty (Gopal-Krishna, Joshi and Ananthakrishnan 1975). From the above discussion it appears likely that compact components at the leading edges of double sources as in Cyg-A and 3C 33 are fairly common.

Chapter 3A

APPENDIX

Revisions to List 1

A reanalysis of the occultations of 25 radio sources in the first published list of Ooty occultations (Swarup et al. 1971b) shows that the positional and structural information for a few sources in this list needs some revision. The reanalysis was undertaken in the light of experience gained in the interpretation of occultation records and in view of additional occultations observed subsequently for some sources. It should also be noted that the radio positions quoted in List 1 were based on Newcomb's equinox, whereas those in the subsequent lists have been referred to the FK4 equinox. However, the differences in the two equinoxes amount generally to $< 0''.5$ arc, which is smaller than the standard errors for most sources.

The revised structural information differs appreciably from the published information only for 3 sources and is given in Table 3A-1. The revised positions for 5 sources are given in Table 3A-2. The optical identifications for the above sources are not affected by the revisions in position.

In the case of OTL 0556+28, we should like to thank Dr. C.M. Wade of the NRAO for communicating to us a difference of $\sim 5''$ arc in the occultation position and the radio position measured by him with the NRAO interferometer, which led to the detection of an error in the sign of the limb correction applied in the Ooty occultation analysis. The revised position for this source is in good agreement with Dr. Wade's measurement.

TABLE 3A-1

Revised Structural Information for 3 sources in List 1

Source OTL	Flux 327 MHz	No. of Scans	Observed data: β_e	Observed data: PA of Scan	Observed data: Ang. Size of components A	Observed data: Ang. Size of components B	Derived Structure: PA A to B	Derived Structure: Comp. Sepn.	Derived Structure: Flux Ratio
0018+05*	2.0 Jy	3	2".3	13°	≤ 3"	~5"	16°	7".5	1
			3.2	198	≤ 3	~5			
1627-27	0.8	6	2.2	59	≤1.7	~5.5	108	24	3
			2.2	306	≤1.7	~5.5			
2109-18	0.6	2	8	103	≤ 8	≤15	92	92	1.1
			8	189	≤ 8	≤15			

* Not in the sample of 164 sources as all three PAs lie within 30° of each other.

TABLE 3A-2

Revised Positions for 5 sources in List 1

Source OTL	No. of occultations		Radio Position (1950.0) Right Ascension				Declination			
0139+15	7		01^h	39^m	$00^s.54 \pm 0^s.04$		+15°	32'	12".3 ± 0".5	
0556+28*	2		05	56	30.98	0.07	+28	18	10.1	1
1556-26	4		15	56	23.39	0.07	-26	05	17.8	1
1627-27	6	A	16	27	55.77	0.05	-27	16	43.6	0.7
		B	16	27	57.35	0.1	-27	16	50.9	1
2109-18	2	A	21	09	29.00	0.1	-18	52	45.4	2
		B	21	09	35.50	0.2	-18	52	48.0	3

* Not in the sample of 164 sources, as its galactic latitude is < 10°.

Chapter 4

THE ANGULAR SIZE - FLUX DENSITY RELATION

4.1 Introduction

A correlation between the observed angular sizes and flux densities of extragalactic radio sources is of considerable cosmological interest, since both θ and S depend on the world model. In the absence of redshift information for most of the known radio sources, the measured angular sizes can also provide important statistical information on the location of fainter and unidentified sources. It has not so far been possible to study the θ - S correlation, mainly because of the limited range of S over which source structures have been determined with adequate angular resolution. Moreover, it is important that unbiased samples of sources, free of observational selection effects be used for such a statistical study. By combining the data for the weak occultation sources (Chapter 3) with the available structural information on complete samples of stronger sources, Swarup (1975) has recently shown that a clear correlation exists between the median values of angular size θ_m, and flux density S, in the sense that the fainter sources have smaller angular sizes. In view of the importance of the $\theta_m(S)$ relation as a cosmological test, to be discussed in the next Chapter, we shall review and reexamine the derivation of the $\theta_m(S)$ relation by Swarup in this Chapter, paying particular attention to the effects of observational and instrumental selection effects in the data.

The structural data for the Ooty sources has already been described in Chapter 3. Data for the stronger sources from the complete samples of the 3CR and All-sky surveys is considered in Section 4.2. These data will be used also in the next Chapter to study the angular size counts of radio sources. The relation between the median values of θ and S is derived in Section 4.3 and the possible selection effects in the data investigated. A discussion of the observed $\theta_m(S)$ relation is given in Section 4.4.

4.2 The Data for Strong Sources

4.2.1 The 3CR sample

The 200 sources in the 3CR catalogue (Bennett 1962), in 4.25 steradian of the sky defined by $\delta > 10^\circ$ and $|b| > 10^\circ$, form a complete sample with $S_{178} \geq 9$ Jy. Excluding 3C 326, which is perhaps a galactic source (Mackay 1971) the structures of 199 sources have been determined by aperture synthesis with the Cambridge One-mile telescope (Macdonald, Kenderdine and Neville 1968; Mackay 1969; Elsmore and Mackay 1969) at the principal frequency of 1407 MHz, with an angular resolution of 23" arc in right ascension and 23" x cosec δ arc in declination. In most cases the observations allowed sources with angular sizes as small as about 10" in RA and 10" x cosec δ in declination to be partially resolved. But for a total of 59 sources in the complete sample it has been possible only to place an upper limit to θ (mostly in the range of 8" to 30" arc). However, observations with higher angular resolutions, made with other interferometers

at different frequencies, or data from lunar occultations, are available for 40 of these 59 sources. For these 40 sources we use the best available value of θ from the references listed in Swarup (1975). For the other 19 sources definite values of θ are not known and we use only the upper limits given in the Cambridge observations. For the resolved sources we use the values of θ measured with the Cambridge One-mile telescope at 1407 MHz, although for several sources observations at higher frequencies and resolutions are now available. The differences in the estimates of θ in most such cases are not significant. We take θ to be the largest angular size of a source (the same as LAS of Miley 1971) as defined in the last Chapter (difficulties in defining θ for some structural types are considered in Section 4.3.1). Comments on some individual sources are given below.

(i) The sources 3C 83.1B and 3C 84A in the Perseus cluster are considered as independent sources and the angular sizes taken to be the half power widths of the 'tail' and 'halo' components respectively, at 408 MHz (Ryle and Windram 1968). The origin of the extended low surface brightness component enveloping the two sources (Ryle and Windram 1968) is not clear; it could possibly arise from the interaction of relativistic electrons that have diffused out from several active galaxies with an intracluster magnetic field (Miley et al. 1972). Similarly, the size of 3C 274 (Virgo-A) has been taken to be that of the halo component at 408 MHz (Macdonald et al. 1968).

(ii) In the case of 3C 66 and 3C 442 we assume the compact components about 6' and 30' arc away respectively from the extended components in the two sources to be physically unrelated to the extended

components, as suggested by Mackay (1971) from statistical and structural arguments. The compact component in 3C 66 has recently been identified with a possible QSO (Wills and Wills 1974). We have also regarded the two main components of 3C 225 to be physically unrelated (Kapahi, Joshi and Gopal-Krishna 1972). In each of the above three sources, only the component with $S_{178} > 9$ Jy has been included in the complete sample.

(iii) We take $\theta = 2340''$ arc for 3C 236, as observed recently by Willis, Strom and Wilson (1974).

(iv) It is not clear if the components of 3C 435.1 and 3C 437.1 ($\theta = 3348''$ and $3800''$ arc respectively) represent genuine structure or result from chance coincidence of unrelated sources. We have assumed the components in both cases to be physically related.

In deriving a $\theta - S$ relation we use the flux density information for the 3CR sample both at 178 MHz as well as at 408 MHz. The use of 178 MHz appears preferable as the 3C survey was made at this frequency.* Although the sample is likely to be less complete at 408 MHz, there is the advantage that flux densities for the 3CR as well as most of the Ooty sources are available at this frequency. At 178 MHz we use the flux densities tabulated by Kellermann, Pauliny-Toth and Williams (1969) and at 408 MHz those measured by the Cambridge group with the One-mile radio

---

* Improved flux densities tabulated by Kellermann et al. (1969) show that 18 sources have $S_{178} < 9$ Jy, so that the sample is not strictly complete even at 178 MHz. Also the source 3C 133 with a galactic latitude of $b = -9^{\circ}.92$, should not strictly be included in the sample of 199 sources, as appears to have been done by the Cambridge group. These minor uncertainties in the 3CR sample are unlikely, however, to change the $\theta - S$ statistics appreciably.

telescope. In a few cases flux values at 408 MHz had to be interpolated from those at neighbouring frequencies given by Kellermann et al. (1969). Flux densities at both the frequencies are based more or less on the CK. scale (Conway, Kellermann and Long 1963), which appears now to be too low by about 10 per cent (Wyllie 1969; Braude et al. 1970; Conway and Munro 1972; Roger, Bridle and Costain 1973). We have therefore multiplied the flux densities at both frequencies by a factor of 1.10 in order to conform approximately to the Wyllie (1969) scale which has also been used for the Ooty sources measured at Molonglo (Swarup and Sutton 1975).

4.2.2 The All-Sky catalogue

The All-sky catalogue of Robertson (1973), which is complete for $S_{408} \geq 10$ Jy (on the Wyllie scale) consists of 160 sources in 10.2 ster, the area of the entire sky excluding the galactic plane, $|b| < 10^{\circ}$, and the region of the Magellanic clouds. Unfortunately, systematic observations of angular sizes, particularly at the lower flux levels, are not available for the entire sample. A search of the literature shows that while no angular size information is available for 10 sources, only one dimensional structures are known for a large number of the remaining sources. Reasonably complete data are available only for sources with $S_{408} \gtrsim 16.5$ Jy. We therefore restrict the use of the All-sky catalogue only to the 62 sources with $S_{408} \geq 16.5$ Jy, in order to improve the statistics for the strong sources in the 3CR sample. Of the 62 sources, 26 are common to the 3CR sample. Angular size information for the other 36 sources has been taken from Cooper, Price and Cole (1965); Fomalont (1968); Ekers (1969); Fomalont and Moffet (1971); Bridle et al. (1972); Schwarz, Cole and Morris (1973); and Wall and Cole (1973). Most of these observations have been made between 1400 and 5000 MHz.

4.3 Correlation in θ and S

Figure 4.1 shows a plot of θ against S_{408} for the 164 Ooty sources*, 199 3CR sources and 36 All-sky sources. Different symbols have been used to distinguish between QSOs, identified radio galaxies and the unidentified sources. The optical identification data for the stronger sources have been taken from the compilation of Veron and Veron (1974). Identifications from the recent deep optical surveys of Kristian, Sandage and Katem (1974) and of Longair and Gunn (1975) have been included. Sources with doubtful identifications have been treated as unidentified.

Although there is a fairly large spread in angular sizes at any flux density, it is clear from Fig. 4.1 that the fainter radio sources tend to have smaller sizes. This is also evident from the histograms of angular sizes in different ranges of flux density which are shown in Fig. 4.2. Before considering a quantitative relation between θ and S, it is important to investigate the effect of possible observational or instrumental selection effects in the data.

4.3.1 Instrumental and observational selection effects

(i) While the 3CR sample is selected on the basis of flux density at 178 MHz, the angular sizes have been determined generally at 1400 MHz. It has thus been assumed that the overall angular extents of sources are independent of the observing frequency. Angular structures with comparable resolutions at frequencies $\gtrsim$ 400 MHz have been determined for many sources, mostly from the 3C catalogue. Although the flux ratios of components of

---

* The source OTL 2053-201 which has the highest flux density ($S_{408} \sim 6.56$ Jy) in the Ooty sample, has not been included by Swarup (1975) in his analysis.

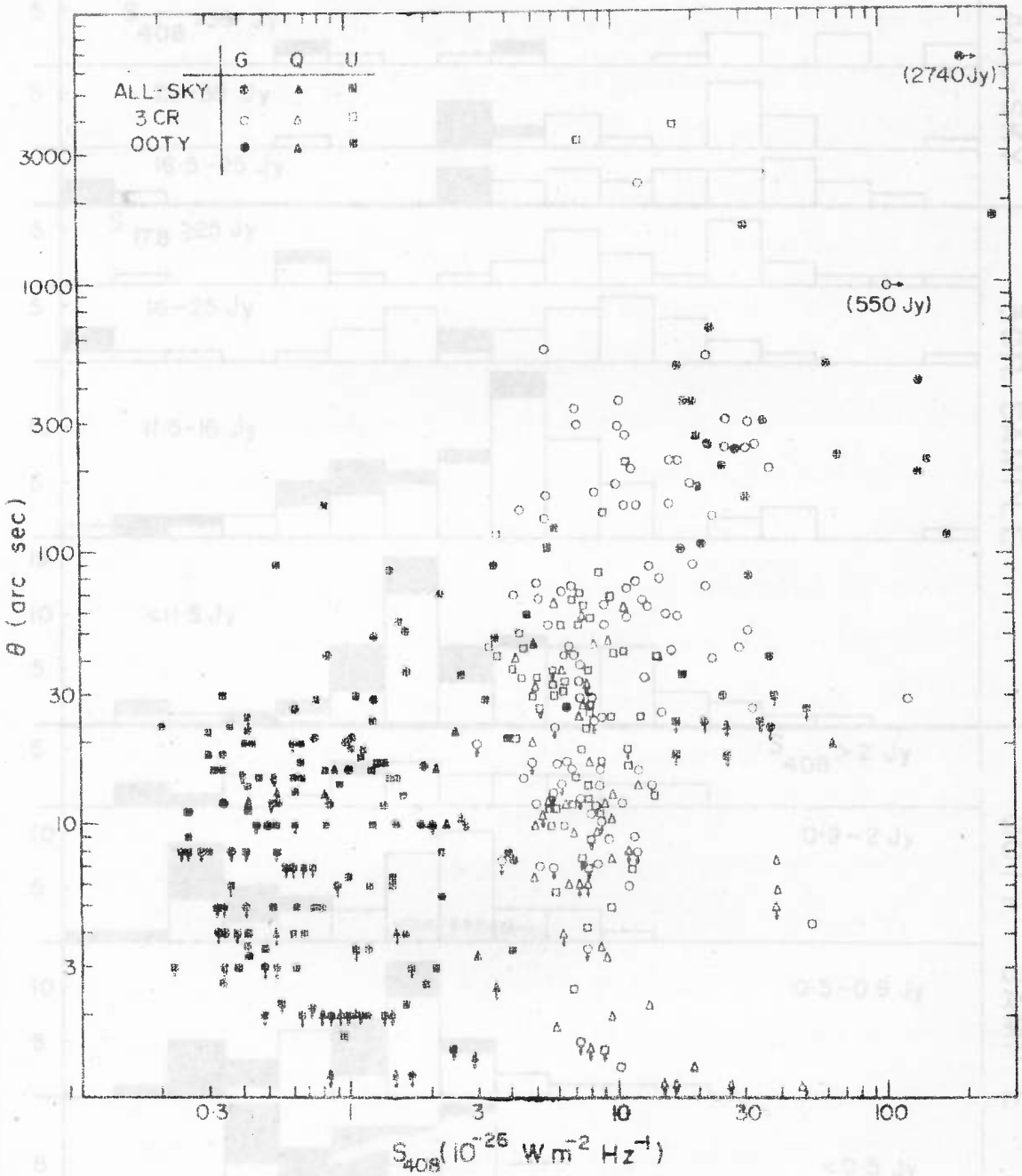

FIG. 4.1 The angular size θ, plotted against flux density at 408 MHz for sources from the All-sky, 3CR and Ooty occultation samples. Different symbols have been used to denote galaxies (G), QSOs (Q) and unidentified sources (U). Upper limits to θ are shown by arrows.

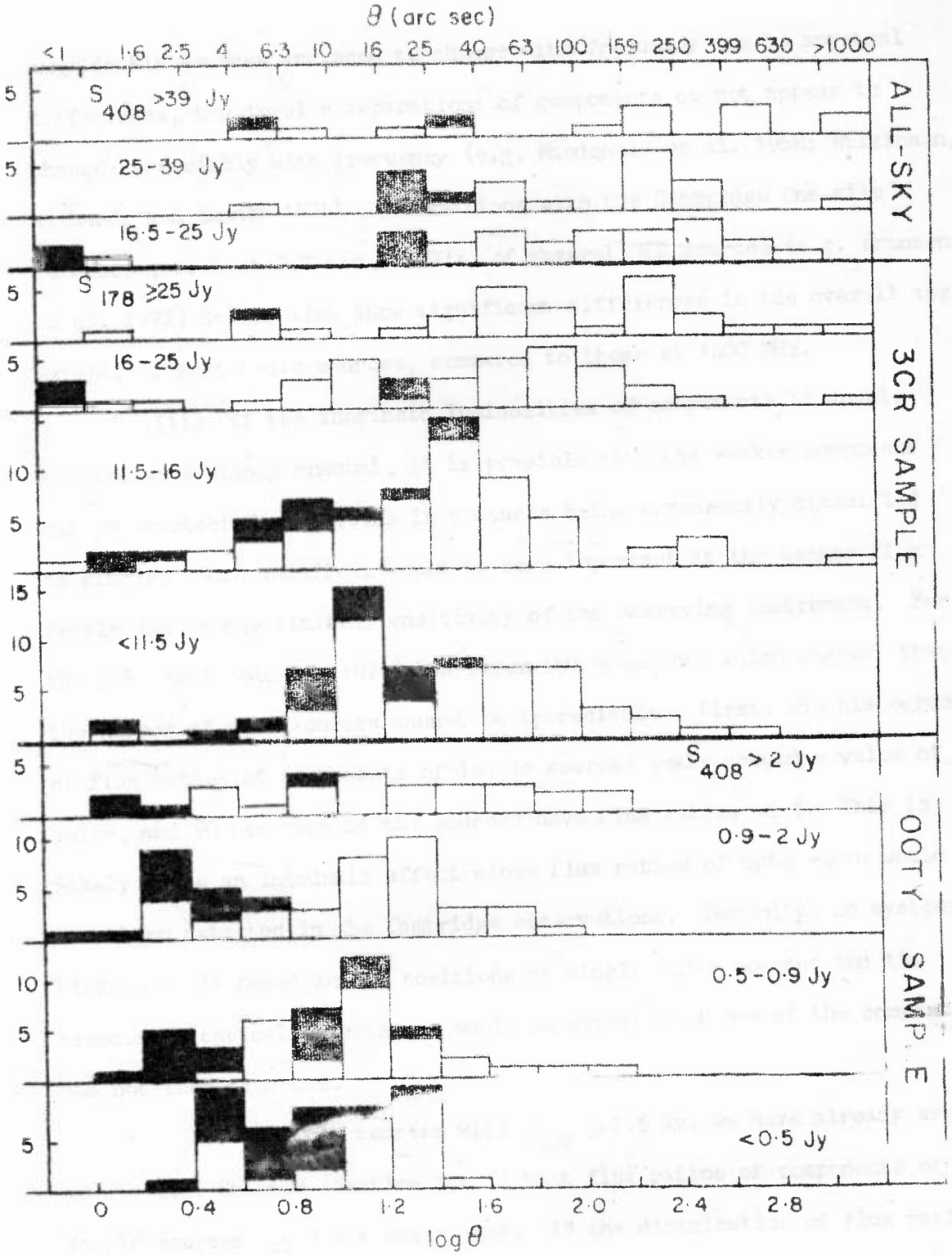

FIG. 4.2 Distribution of observed angular sizes in different flux density ranges of the three source samples. Filled parts of the histogram refer to sources for which only upper limits to θ are known.

many double sources are seen to change with frequency due to spectral differences, the angular separations of components do not appear to change appreciably with frequency (e.g. Macdonald et al. 1968; Wilkinson, Richards and Bowden 1974). Observations with the Cambridge One-mile telescope, even at 2.7 and 5.0 GHz, of several 3CR sources (e.g. Branson et al. 1972) do not also show significant differences in the overall angular extents of most radio sources, compared to those at 1400 MHz.

(ii) If the intrinsic luminosities of components of double sources were highly unequal, it is possible that the weaker component can go undetected, resulting in a source being erroneously classified as single. Such an effect would be more important at the weaker flux levels due to the limited sensitivity of the observing instrument. For the 3CR sample Mackay (1971) has given two arguments which suggest that the number of such sources cannot be appreciable. First, the histogram of flux ratios of components of double sources peaks around a value of unity, and 90 per cent of the sources have flux ratios < 5. This is likely to be an intrinsic effect since flux ratios of upto ~ 10 would have been detected in the Cambridge observations. Secondly, no systematic difference is found in the positions of single radio sources and the associated optical objects, as would be expected if one of the components had not been detected.

For the Ooty sources with $S_{408} \geq 1.5$ Jy, we have already argued in the last Chapter (Section 3.4.1) that flux ratios of components of double sources $\gtrsim 3$ are quite rare. If the distribution of flux ratios is similar for the weaker sources as well, the possibility of having missed the weaker component in an appreciable number of sources is likely

to be important only at flux levels of $\lesssim 0.5$ Jy. It is possible that the angular sizes of upto 25 per cent of the weakest sources in the Ooty sample have been underestimated due to this observational difficulty.

(iii) Unlike the case of double or multicomponent sources where the definition of θ is generally straight-forward and has a clear meaning, the definition of θ for 'core-halo' or 'head-tail' sources is not always clear-cut. In such sources the value of θ can be quite sensitive to the relative intensities of the compact vs. extended components and to the angular resolution of the observations. The sizes of extended components in some sources appear also to depend on the observing frequency due perhaps to the different limiting sensitivities in surface brightness for telescopes at different frequencies.

However, the number of sources with 'core-halo' or 'head-tail' structures appears to be quite small (only 4 or 5 in the 3CR sample and a similar number in the Ooty sample).

(iv) Another possible selection effect concerns the observational bias against sources of very large angular extent. Although the 3CR catalogue is known to be somewhat incomplete for sources of $\theta \gtrsim 5'$ arc (Bennett 1962), it is unlikely that an appreciable number of such sources have been missed (Mackay 1971). The differential angular size counts for the 3CR sample, considered in the next Chapter, do not also show any noticeable deficit of very large diameter sources.

Large diameter sources can be missed in the Ooty occultation observations if their surface brightness is so low that the occultations cannot be distinguished from the slow gradients in the received power due mainly to the Moon's drift in declination. At flux levels of $\gtrsim 1$ Jy, this

problem is not expected to be important for sources with an extended distribution of brightness over angular extents of $\lesssim 3'$ arc. At the weakest flux levels of the Ooty data (0.3 to 0.5 Jy) sources of $\theta \lesssim 1'$ arc should have generally been recognized. The observed decrease in the number of Ooty sources at angular sizes considerably smaller than the above limits (see Fig. 4.2), suggests that only a small number of extended sources, particularly at the lowest flux densities, are likely to have been missed.

To summarize, it is possible that a few sources of large angular extent have not been recognized both in the 3CR and Ooty samples and that the angular sizes of a few sources have been under-estimated due to the observational difficulty of detecting very weak or extended components in their brightness distributions. Nevertheless, these and other selection effects in the data are unlikely to have altered the observed θ - S correlation seriously.

4.3.2 The $\theta_{med}(S)$ relation

Due to the large spread in angular sizes, and the fact that only upper limits to θ are available for many sources, the use of median value of θ appears to be the most practical for deriving a quantitative relation between θ and S. We have estimated the median values θ_m, in several ranges of S as listed in Tables 4.1 to 4.3 and shown in the histograms of Fig. 4.2. The flux ranges have been chosen as a compromise between having a large number of ranges and at the same time having enough sources in each range in order to obtain reasonable statistics. The results are not highly sensitive to the choice of flux range. Values of θ_m were

TABLE 4.1

Median Values of θ and S_{408} for the All-Sky Sample

Flux Range (Jy)	Number of Sources	S_m (Jy)	θ_m (arc sec)
> 39	15	103	160^{+105}_{-63}
25 to 39	21	31.5	100^{+70}_{-41}
16.5 to 24.9	26	19.5	100^{+58}_{-37}

TABLE 4.2

Median Values of θ and S_{408} for the Ooty Occultation Sample

Flux Range (Jy)	Number of Sources	S_m (Jy)	θ_m (arc sec)	Correction Factor, η^{-1}	θ_m (Corrected) (arc sec)
≥ 2.0	28	3.1	13.0	1.05	$13.7^{+6.9}_{-4.5}$
0.90 to 1.99	48	1.3	10.0	1.09	$10.9^{+3.3}_{-2.5}$
0.50 to 0.89	44	0.66	9.0	1.12	$10.1^{+2.5}_{-1.9}$
0.20 to 0.49	44	0.36	7.5	1.14	$8.6^{+2.7}_{-2.1}$

TABLE 4.3

Median Values of θ, S_{178} and S_{408} for the 3CR Sample

Frequency	Flux Range (Jy)	Number of Sources	S_m (Jy)	S_m (Wyllie Scale) (Jy)	θ_m (arc sec)
178 MHz	$S_{178} \geq 25$	28	46.6	50.6	90^{+45}_{-30}
	16.0 to 24.9	39	19.5	21.5	$33^{+20}_{-12.5}$
	11.5 to 15.9	68	13.0	14.3	$24^{+5.4}_{-4.4}$
	< 11.5	64	10.1	11.1	$20^{+6.9}_{-5.1}$
408 MHz	$S_{408} \geq 15$	28	25.5	28.0	85^{+43}_{-29}
	9.6 to 14.9	38	11.0	12.1	$41^{+13.5}_{-10}$
	6.5 to 9.5	67	7.5	8.25	$20^{+5.4}_{-4.2}$
	< 6.5	66	5.2	5.7	$26^{+6.0}_{-4.9}$

estimated by making cumulative plots of number against θ in each flux range and by fitting a smooth curve near the value of θ_m. The cumulative plots for the three source samples considered are shown in Figures 4.3 to 4.6. The median values of S in each flux range were estimated similarly. Only for a very few sources, particularly in the lowest flux density ranges of the 3CR and Ooty samples, do the upper limits to angular sizes of unresolved sources exceed the median values of θ, and do not therefore affect the values of θ_m appreciably.

In the $N(>\theta)$ plots of Figs. 4.3 to 4.6, the dots present the $N(>\theta)$ curves if the upper limits of θ for the unresolved sources are taken to be definite values, while the crosses indicate the shapes of the $N(>\theta)$ curves if the actual values of θ for the unresolved sources are much smaller than the upper limits. The true $N(>\theta)$ curves should lie in between the above two extremes. It is clear from the $N(>\theta)$ plots that the uncertainty in the actual θ values of the unresolved sources does not have an appreciable effect on the determination of θ_m, except perhaps for the lowest two flux ranges of the Ooty and 3CR samples. The uncertainty in the estimation of θ_m even for these flux ranges is, in any case, expected to be of the same order or smaller than the standard errors in θ_m.

Standard errors in the median values, estimated from the grouped frequency distributions, are given by (Yule & Kendall 1950)

$$\sigma(\theta_m) = \sqrt{n}/(2f_p)$$

in units of the class interval of log θ, where n is the total number of sources, and f_p the smoothed ordinate value of the frequency distribution

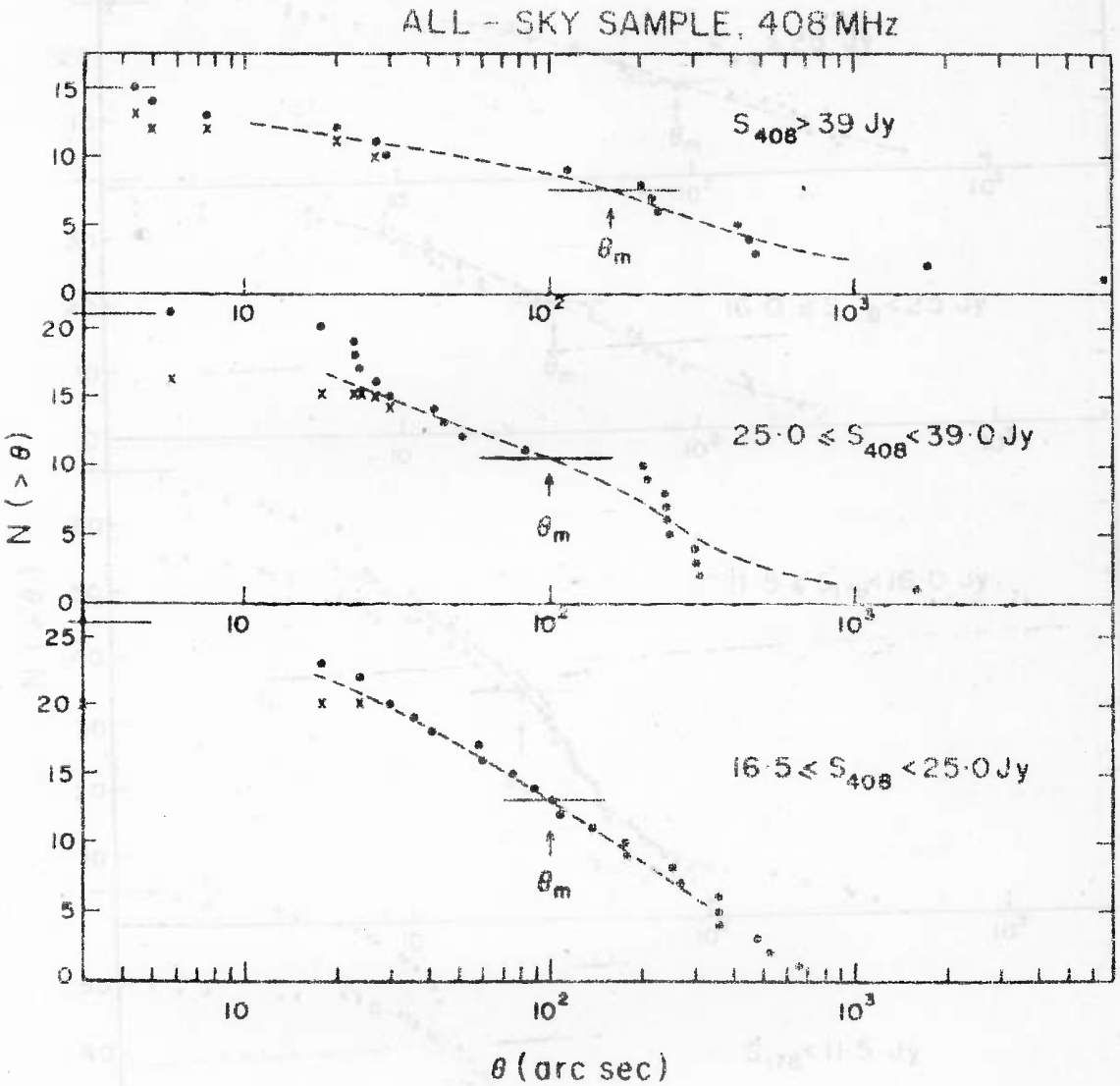

FIG. 4.3 Cumulative plots $N(>\theta)$, in three flux ranges of the All-sky sample. Where only upper limits are known to θ, the dots represent the total number if upper limits are taken to be definite values while the crosses indicate the total number if such sources are assumed to be point sources. Median values of θ are indicated by arrows.

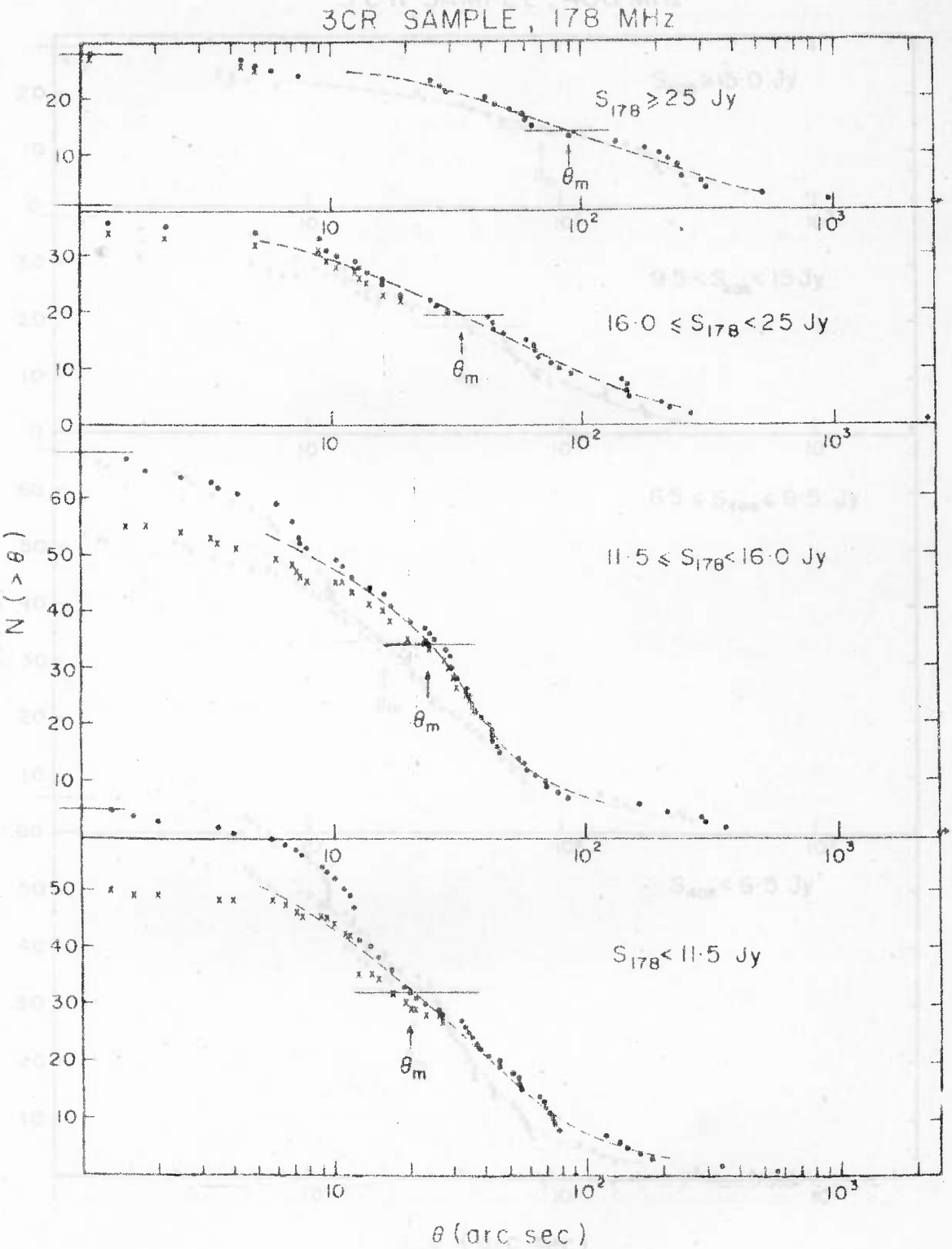

FIG. 4.4 Cumulative plots $N(>\theta)$, in four flux ranges of the 3CR sample at 178 MHz. Dots and crosses as in FIG. 4.3.

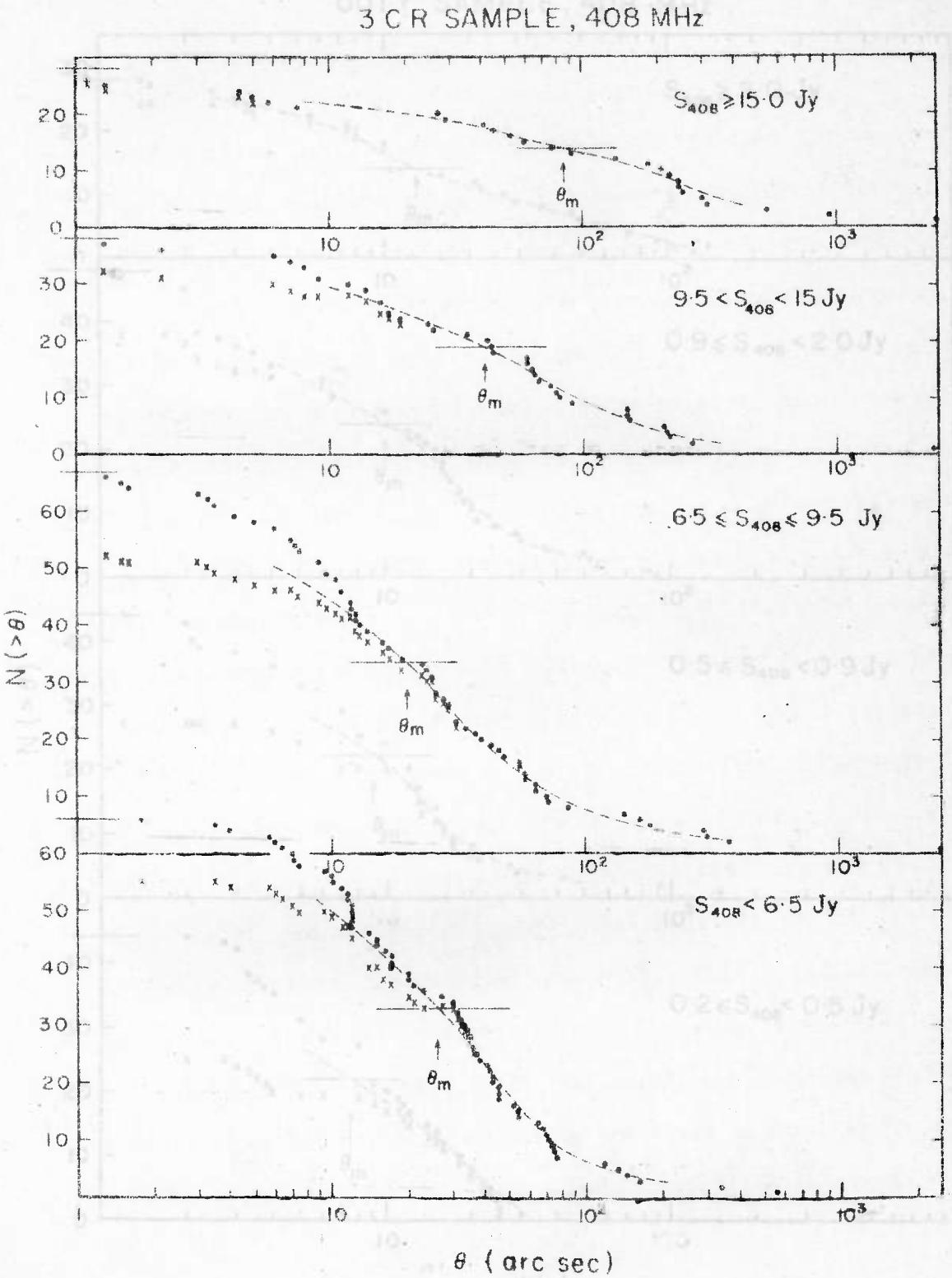

FIG. 4.5 N(> θ) plots for the 3CR sample, with flux densities at 408 MHz. Dots and crosses as in FIG. 4.3.

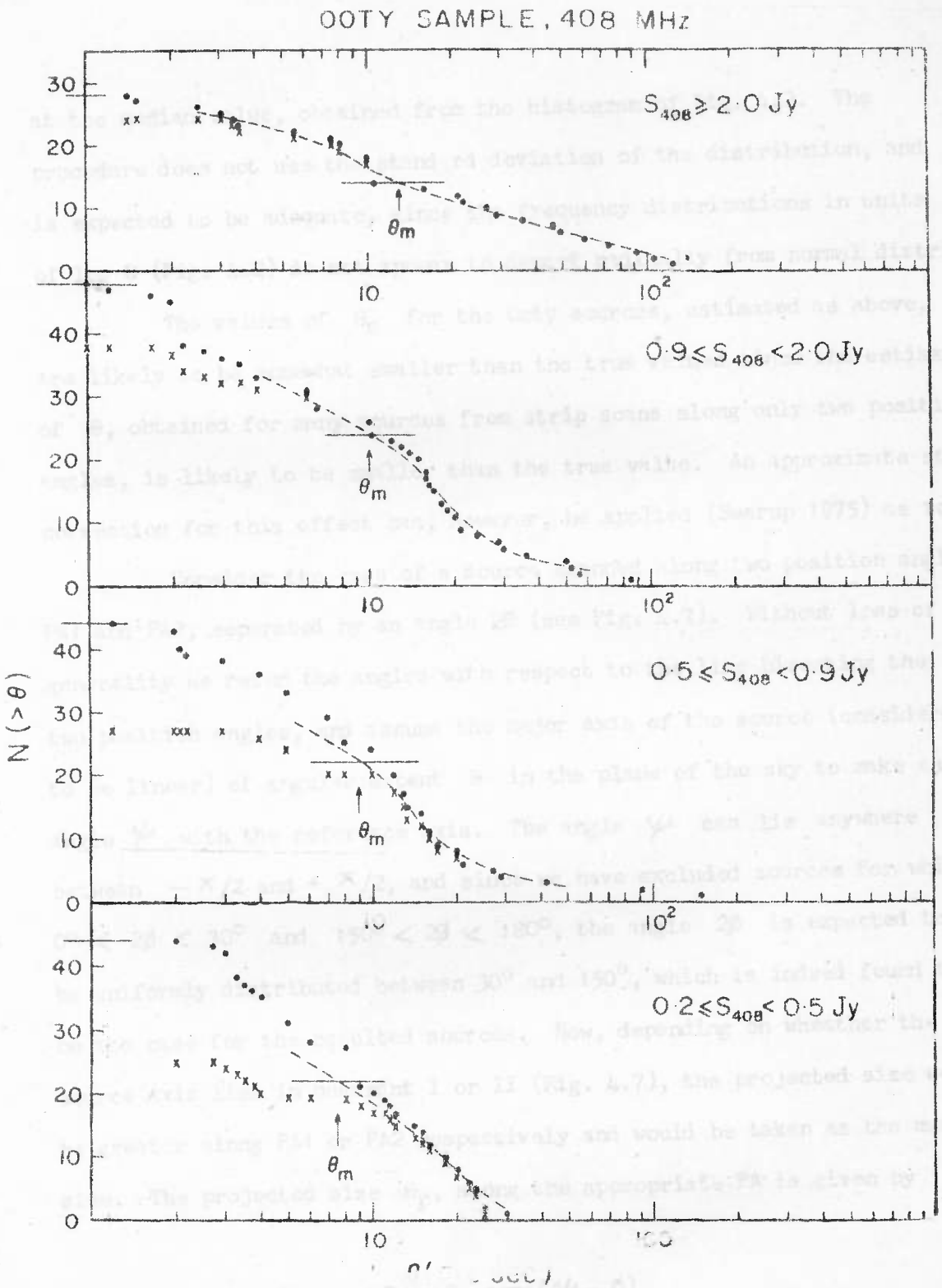

FIG. 4.6 N(> θ) plots in four flux ranges of the Ooty sample. Dots and crosses as in FIG. 4.3.

at the median value, obtained from the histogram of Fig. 4.2. The procedure does not use the standard deviation of the distribution, and is expected to be adequate, since the frequency distributions in units of log θ (Fig. 4.2) do not appear to depart radically from normal distributions.

The values of θ_m for the Ooty sources, estimated as above, are likely to be somewhat smaller than the true values since the estimate of θ, obtained for many sources from strip scans along only two position angles, is likely to be smaller than the true value. An approximate statistical correction for this effect can, however, be applied (Swarup 1975) as follows.

Consider the case of a source scanned along two position angles, PA1 and PA2, separated by an angle 2ϕ (see Fig. 4.7). Without loss of generality we refer the angles with respect to the line bisecting the two position angles, and assume the major axis of the source (considered to be linear) of angular extent θ in the plane of the sky to make an angle ψ with the reference axis. The angle ψ can lie anywhere between $-\pi/2$ and $+\pi/2$, and since we have excluded sources for which $0^\circ < 2\phi < 30^\circ$ and $150^\circ < 2\phi < 180^\circ$, the angle 2ϕ is expected to be uniformly distributed between 30° and 150°, which is indeed found to be the case for the occulted sources. Now, depending on wheather the source axis lies in quadrant I or II (Fig. 4.7), the projected size would be greater along PA1 or PA2 respectively and would be taken as the measured size. The projected size θ_p, along the appropriate PA is given by

$$\theta_p = \theta . \cos (\psi - \phi)$$

The ratio of the average value of the measured projected size to the

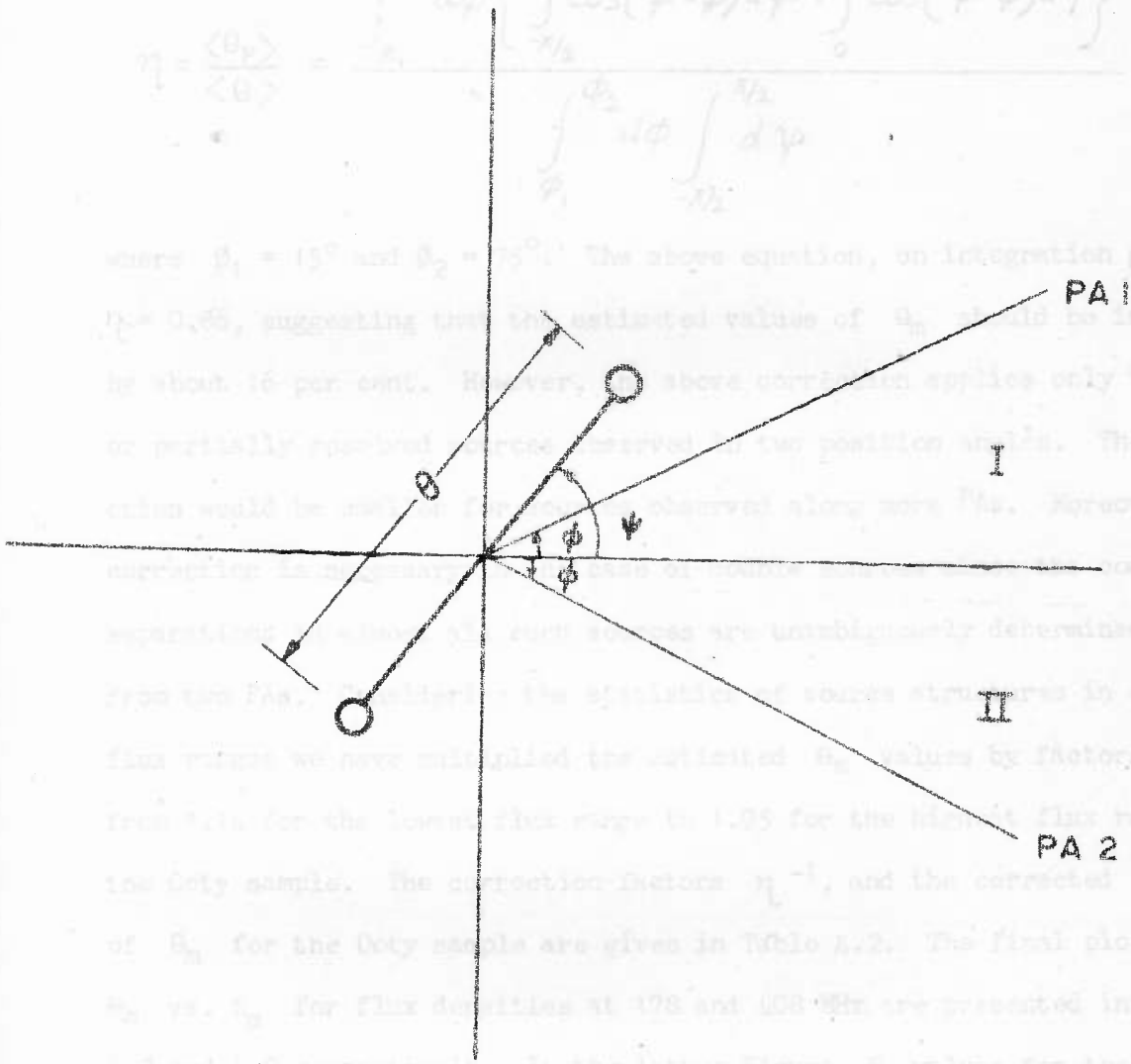

FIG. 4.7 A source scanned along two position angles, PA1 & PA2.

true projected size is, therefore, given by

$$\eta = \frac{\langle \theta_p \rangle}{\langle \theta \rangle} = \frac{\int_{\phi_1}^{\phi_2} d\phi \left\{ \int_{-\pi/2}^{0} \cos(\psi - \phi)\, d\psi + \int_{0}^{\pi/2} \cos(\psi - \phi)\, d\psi \right\}}{\int_{\phi_1}^{\phi_2} d\phi \int_{-\pi/2}^{\pi/2} d\psi}$$

where $\phi_1 = 15^\circ$ and $\phi_2 = 75^\circ$. The above equation, on integration gives $\eta = 0.86$, suggesting that the estimated values of θ_m should be increased by about 16 per cent. However, the above correction applies only to single or partially resolved sources observed in two position angles. The correction would be smaller for sources observed along more PAs. Moreover, no correction is necessary in the case of double sources since the component separations in almost all such sources are unambiguously determined even from two PAs. Considering the statistics of source structures in different flux ranges we have multiplied the estimated θ_m values by factors ranging from 1.14 for the lowest flux range to 1.05 for the highest flux range of the Ooty sample. The correction factors η^{-1}, and the corrected values of θ_m for the Ooty sample are given in Table 4.2. The final plots of θ_m vs. S_m for flux densities at 178 and 408 MHz are presented in Figs. 4.8 and 4.9 respectively. In the latter Figure, S_m values for the All-sky and Ooty samples have been converted to 178 MHz using a constant spectral index of $\alpha = 0.75$. Standard errors in S_m are negligible in comparison with those for θ_m.

In the lowest flux density ranges of both the 3CR and the Ooty samples, the values of θ_m lie only slightly above the observational angular resolutions for many sources. If a source is only partially resolved its

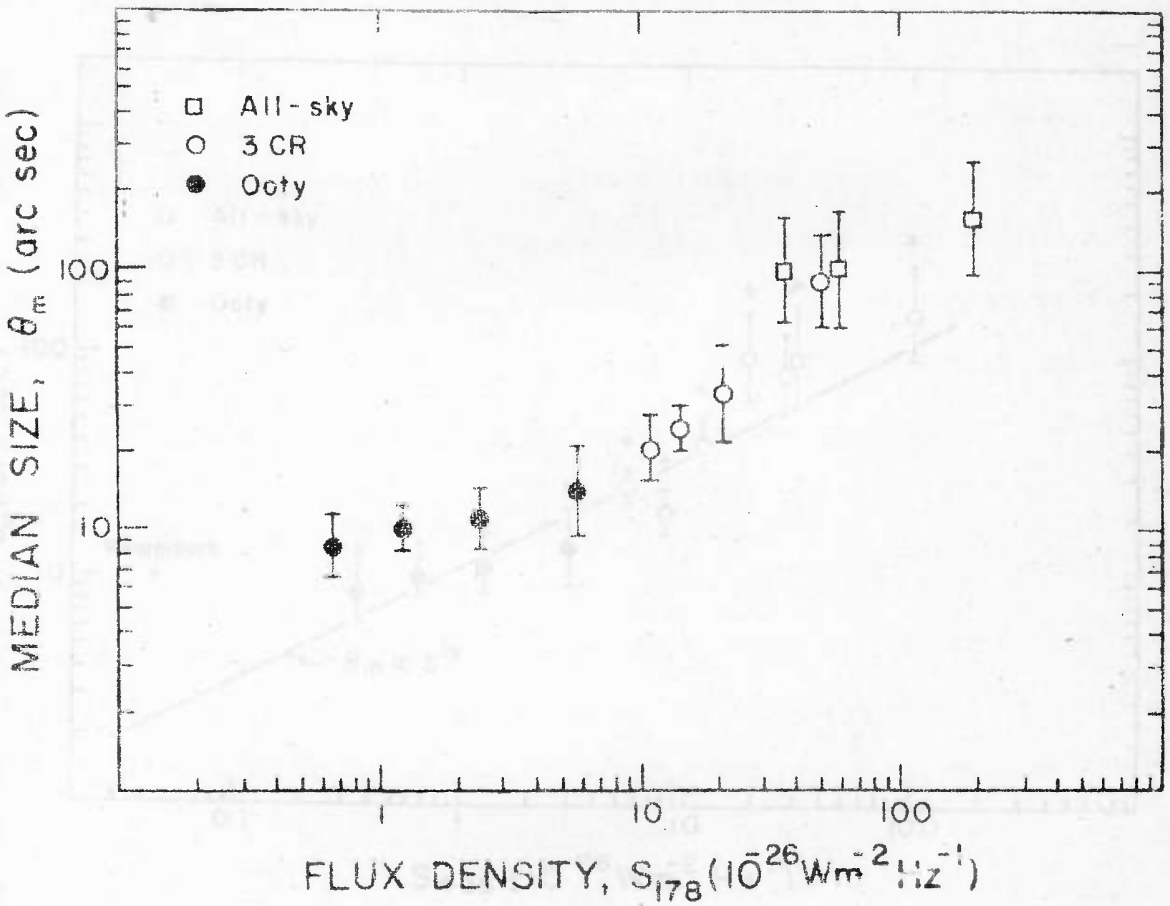

FIG. 4.8 The observed $\theta_m(S)$ relation at 178 MHz. Values of θ_m for the All-sky and Ooty samples estimated at 408 MHz have been translated to 178 MHz using a constant spectral index $\alpha = 0.75$.

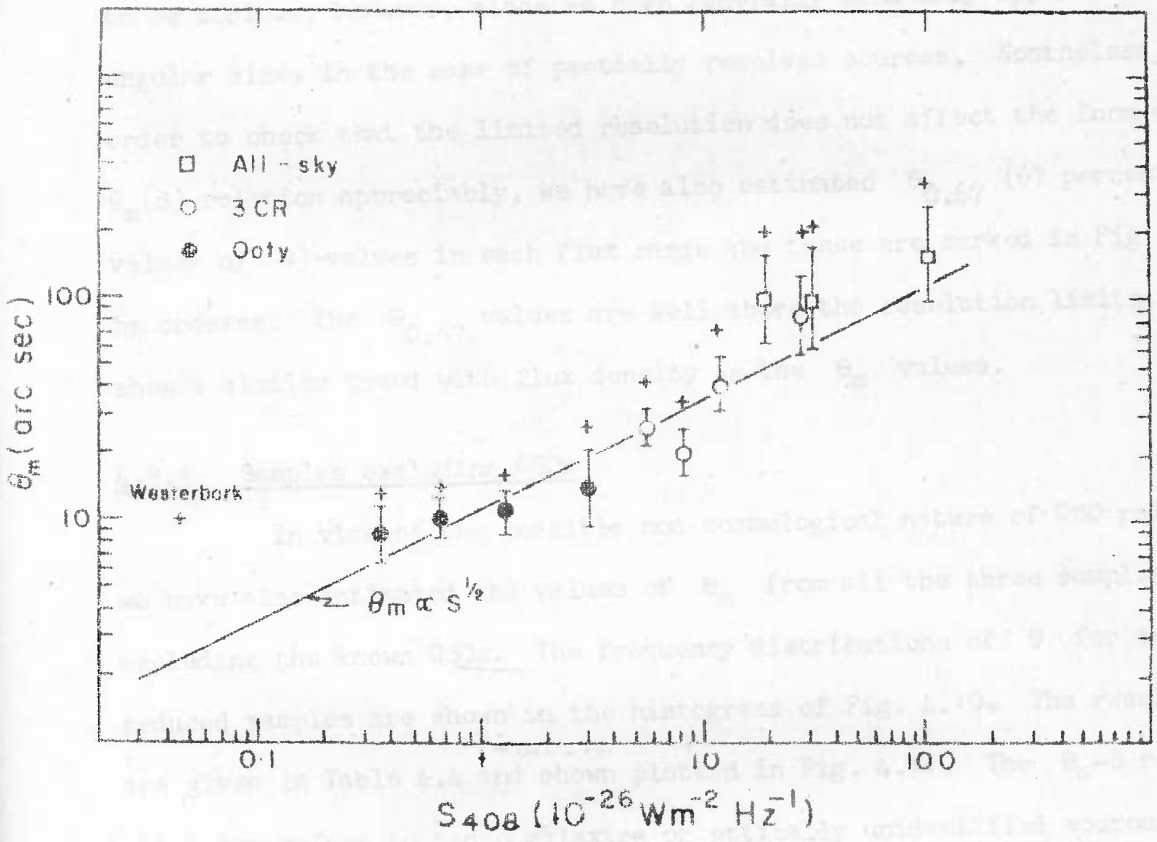

FIG. 4.9 The observed $\theta_m(S)$ relation at 408 MHz. The 67 percentile values of θ are shown by crosses. The cross marked 'Westerbork' is from the deep survey of Katgert & Soinrad (1974).

angular extent estimated by fitting a single Gaussian component is somewhat higher than the component separation of a double source model. The extent of overestimation of angular size depends on the amount of resolution and can be as high as $\sim 40\%$ for some Ooty sources. The effect is not likely to be serious, however, since we have generally used only upper limits to angular sizes in the case of partially resolved sources. Nontheless, in order to check that the limited resolution does not affect the form of the $\theta_m(S)$ relation appreciably, we have also estimated $\theta_{0.67}$ (67 percentile values of θ) values in each flux range and these are marked in Fig. 4.9 by crosses. The $\theta_{0.67}$ values are well above the resolution limits and show a similar trend with flux density as the θ_m values.

4.3.3 Samples excluding QSOs

In view of the possible non cosmological nature of QSO redshifts, we have also estimated the values of θ_m from all the three samples by excluding the known QSOs. The frequency distributions of θ for these reduced samples are shown in the histograms of Fig. 4.10. The results are given in Table 4.4 and shown plotted in Fig. 4.11. The θ_m-S relation, which now refers to radio galaxies or optically unidentified sources, shows a similar behaviour as the total sample, except that the θ_m values, particularly at the higher flux levels, are somewhat larger due to the exclusion of a few compact sources associated with QSOs.

As in the case of the complete 3CR sample, the use of flux densities at 178 MHz or at 408 MHz does not have a significant effect on the form of the $\theta_m(S)$ relation.

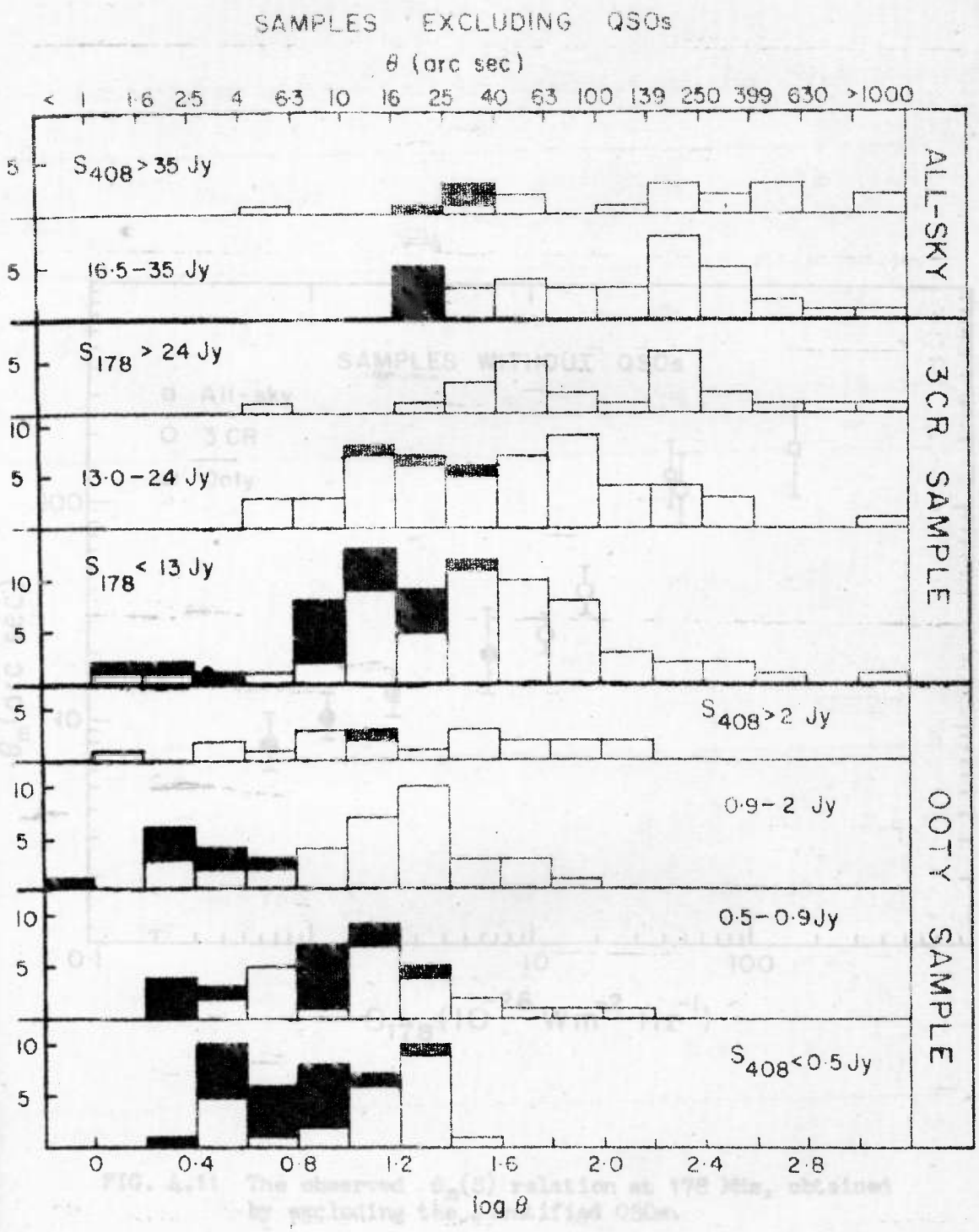

FIG. 4.10 Distribution of angular sizes in different flux density ranges of the three sources samples, without QSOs. Filled portions refer to sources with upper limits on θ.

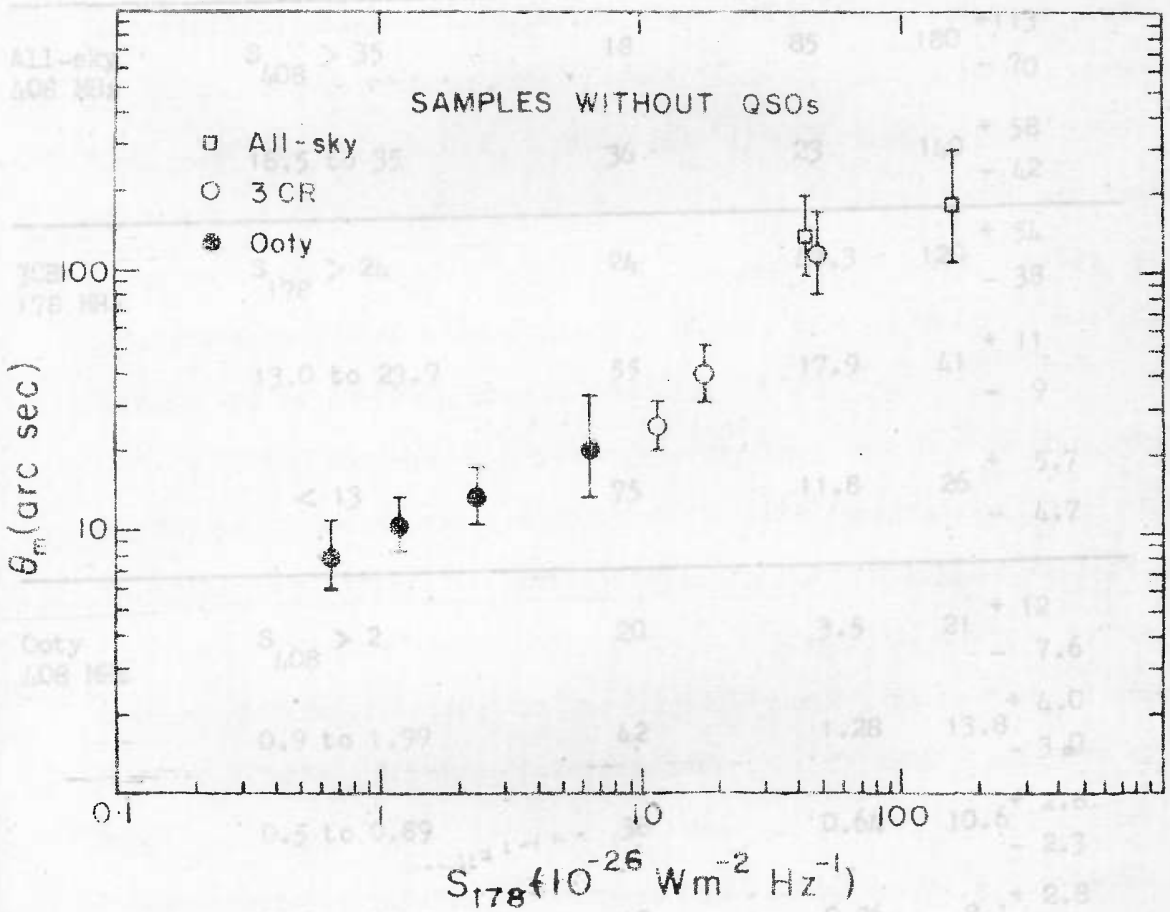

FIG. 4.11 The observed $\theta_m(S)$ relation at 178 MHz, obtained by excluding the identified QSOs.

TABLE 4.4

Median Values of θ and S for source samples excluding QSOs

Source Sample	Flux Range (Jy)	No. of Sources	S_m (Jy)	θ_m arc sec
All-sky 408 MHz	$S_{408} > 35$	18	85	180^{+113}_{-70}
	16.5 to 35	36	23	140^{+58}_{-42}
3CR 178 MHz	$S_{178} > 24$	24	47.3	120^{+54}_{-38}
	13.0 to 23.9	55	17.9	41^{+11}_{-9}
	< 13	75	11.8	$26^{+5.7}_{-4.7}$
Ooty 408 MHz	$S_{408} > 2$	20	3.5	$21^{+12}_{-7.6}$
	0.9 to 1.99	42	1.28	$13.8^{+4.0}_{-3.0}$
	0.5 to 0.89	38	0.64	$10.6^{+2.8}_{-2.3}$
	0.2 to 0.49	43	0.36	$8.1^{+2.8}_{-2.1}$

The nature of the unidentified sources is of vital importance in interpreting the statistics of source samples obtained by excluding the known QSOs. Bolton (1969) has presented four arguments to suggest

that most of the unidentified sources in the low frequency catalogues at moderately strong flux levels (corresponding to the 3CR and Parkes surveys), are likely to be radio galaxies, presumably too distant to be seen on the plates of the Palomar Sky Survey. The arguments are based on the observed distributions among radio galaxies, QSOs and unidentified sources of a) optical magnitudes b) percentage of sources showing interplanetary scintillation, c) spectral indices and d) polarization parameters. Furthermore, recent optical surveys in the positions of selected 3C sources and going to fainter limiting magnitudes than the Palomar Sky Survey, appear to provide some direct observational support to this conclusion (Kristian, Sandage and Katem 1974; Longair and Gunn 1975).

Even for the weaker Ooty sources the distribution of optical magnitudes of the identified QSOs, unlike that for galaxies, peaks considerably above the plate limits of the Sky Survey, suggesting that identifications with QSOs are largely complete (Joshi 1975). The scintillation characteristics of sources in the Ooty IPS survey, going down to about 2 Jy at 327 MHz (Bhandari, Ananthakrishnan and Pramesh Rao 1974), also support the hypothesis that most unidentified sources are likely to be distant radio galaxies. The samples obtained by excluding the QSOs are therefore likely to consist mainly of radio galaxies.

4.4 Discussion

4.4.1 Are the fainter sources farther away?

Figs. 4.8, 4.9 and 4.11 show that the value of θ_m decreases continuously from nearly 200" arc at the highest flux densities ($\sim$ 100 Jy at 408 MHz) to only $\sim$ 10" arc in the lowest flux range of the Ooty data (0.2 to 0.5 Jy). The simplest explanation for this correlation, which is substantially free from observational selection effects, is that statistically the weaker sources are located at greater distances. If this explanation is correct, there should be a correlation between flux density and redshifts of radio sources. But it is known that in the 3CR catalogue, for which the best redshift data are available, flux densities are not correlated with z, both for QSOs (e.g. Longair and Scheuer 1967) as well as for radio galaxies (e.g. Hoyle and Burbidge 1970). It must be noted, however, that the redshift data for radio galaxies (their redshifts have generally been accepted to be cosmological), which constitute the majority of 3C sources, are incomplete and also likely to be seriously biased in favour of the brighter and therefore nearer galaxies at any flux density, due to the difficulty of measuring redshifts of faint galaxies. The following arguments based on the observed statistics with regard to flux densities, angular sizes and optical magnitudes can be given to demonstrate this bias.

(a) In the 3CR sample of 199 sources, 94 sources are reliably identified with radio galaxies but redshifts are known for only 51 galaxies (redshift data from Burbidge 1970; Lynds 1971; Burbidge and Strittmatter 1972; Tritton 1972; Spinrad and Smith 1973; Kristian et al. 1974; Longair

and Gunn 1975). In Table 4.5 we give the statistics of radio galaxy identifications and of measured redshifts for the sample, divided into four ranges of flux density (the same ranges as used for the θ_m-S relation) at 178 MHz. The marked observational bias with regard to redshift measurements of radio galaxies is evident from Table 4.5. While z is known for 81 per cent of the identified galaxies in the highest flux density range, only about 31 per cent of the galaxies in the lowest flux range have had their redshifts measured. It is in the lower ranges of S that the identified galaxies would be expected to have the largest redshifts if S and z were correlated. Furthermore, the fraction of unidentified sources in the lower flux ranges is seen to be considerably more than in the higher flux ranges, suggesting that fainter sources are likely to be farther away.

TABLE 4.5

Statistics of redshift measurements for galaxies in the 3CR sample

Flux Range (Jy)	Number of Sources	No. identified with galaxies	No. with measured z	Percentage* of gals. with measured z
$S_{178} > 25$ Jy	28	21	17	81% (100%, 62%)
16.0 to 24.9	39	20	14	70% (90%, 50%)
11.5 to 15.9	68	24	11	46% (58%, 33%)
$S_{178} < 11.5$	64	29	9	31% (48%, 14%)
Total	199	94	51	54% (79%, 30%)

* Values in brackets refer to the identified galaxies arranged according to decreasing θ.

(b) If the identified galaxies in each flux range of Table 4.5 are arranged in order to decreasing angular size θ, and divided into two equal classes according to θ, the percentage of galaxies with measured redshifts in the upper and lower θ classes are listed in the last column of Table 4.5. It is seen clearly that redshifts are known for a larger fraction of the galaxies of higher θ than for those with lower θ, showing the bias against smaller θ galaxies which are expected to be more distant.

(c) While the 51 galaxies of known z have a median optical magnitude of $\sim 15.5^{m}$, that for the other 43 galaxies in the 3CR sample is $\gtrsim 19^{m}$, indicating a distance effect. This in fact is the most likely cause for the observational bias since redshifts are difficult to measure for faint galaxies.

The lack of any Hubble-type correlation betwen S and z for the 3CR galaxies can thus be explained to some extent by selection effects in the redshift data (a fairly large scatter in the correlation would in any case be expected due to the spread in the intrinsic luminosities of ragio galaxies). From the above considerations and the fact that no new class of optical objects have been identified or radio structures seen amongst the weaker Ooty sources, it seems quite reasonable to conclude that statistically the fainter radio sources (at least those identified with galaxies and the unidentified sources) are located farther away, rather than being nearby objects of low luminosity. On the assumption that the fainter sources, as a class, have similar physical sizes as the stronger sources, an approximate estimate of the location of fainter sources can be obtained from the angular size data as follows.

In the 3CR sample the median values of z and θ for the 51 galaxies of known redshift are $z_m \sim 0.075$ and $\theta_m \sim 125"$ respectively. For the remaining 103 sources that are either unidentified or are galaxies of unknown z, we find $\theta_m \sim 25"$ arc. Assuming θ_m to decrease linearly with z_m (the Euclidean case), the median z for the 103 sources is given, to a first approximation, by $z_m = 0.075\ (125/25) = 0.375$. At the flux levels of the Ooty samples, z_m is likely to be even higher since θ_m decreases further to $\sim 10"$ arc. It would appear then, that a large fraction of the Ooty sources (excluding QSOs) are likely to be located at redshifts $\gtrsim 0.5$.

Due to the small number of QSOs in the source samples it is not practical to study the θ - S relation for them separately. It is interesting to note, however, that the values of θ_m for all the QSOs in the 3CR and Ooty samples are $\sim 9"$ and $\sim 5"$ arc respectively, which might indicate a distance effect; the number of QSOs (18) in the Ooty sample is, however, too small for this conclusion to be statistically significant.

4.4.2 The form of the $\theta_m(S)$ relation

It is of considerable interest to examine the form of the θ_m - S relation in more detail. In a static Euclidean universe, for a given class of sources of luminosity P and physical size ℓ, we have

$$\theta = \ell\, r^{-1} \quad \text{and} \quad S = P\, r^{-2}$$

so that

$$\theta = (\ell\ P^{-1/2})\ S^{1/2}$$

For any other class of sources of different P and ℓ, one would find $\theta \propto S^{1/2}$. One would thus expect $\theta_m \propto S^{1/2}$ for any distribution of P and ℓ, provided the distributions are independent of distance r.

A least square fit of the log θ_m - log S_m data with a straight line of slope 0.5 is shown in Fig. 4.9. Although the data do not show statistically significant departures from the expected relation in an Euclidean universe, there appears to be a suggestion that the slope of the log θ_m - log S_m relation becomes considerably smaller than 0.5 at the lowest flux densities. It must be remembered also that the possible bias against sources of large angular size at the lowest flux values of the Ooty data may have resulted in under-estimating the values of θ_m somewhat. The Ooty data thus suggest that the value of θ_m at lower flux levels may be asymptotically approaching a constant value in the region of about 6 to 8" arc. It is of course possible that θ_m may start increasing again at very low flux levels. Angular size measurements with resolutions considerably better than 10" arc are necessary to extend the $\theta_m(S)$ relation to fainter flux levels than the Ooty data.

The limited angular size information in a recent deep survey with the Westerbork synthesis telescope at 1415 MHz (Katgert and Spinrad 1974) appears to provide some evidence that the value of θ_m does not continue to decrease as $S^{1/2}$. In the Westerbork survey complete down to $\sim$ 0.01 Jy at 1415 MHz (S_m = 0.024 Jy), there are a total of 53 sources, of which 36 have an angular size $\gtrsim$ 10" arc, the limit of resolution of the survey. The approximate 67 percentile value of θ ($\sim$ 10" arc) for this survey is shown in Fig. 4.9, plotted at the median S_{408} (0.046 Jy)

obtained by assuming a constant spectral index of $\alpha = 0.52$, the average value found by Katgert and Spinrad (1974) between 1415 and 610 MHz. Considering the ratios of $\theta_{0.67}$ and θ_m for the Ooty sources, the value of θ_m for the Westerbork survey is estimated to lie between 5" and 8" arc, which is well above the value of about 2.5" arc expected from the Euclidean fit of a straight line shown in Fig. 4.9. It should be noted also that the Westerbork survey has been made at a frequency much higher than that of the 3CR or Ooty surveys and would, therefore, contain a larger proportion of flat spectrum sources which generally have compact unresolved angular structures. A low frequency survey to comparable flux densities would be expected to have somewhat higher value of θ_m.

There is thus some evidence that at flux densities below $\sim$1 Jy at 408 MHz, the $\theta_m(S)$ relation may be showing an increasing departure from the Euclidean relation. High resolution observations of source samples at these flux levels are extremely desirable.

In an expanding universe, the form of the $\theta_m(S)$ relation would depend on the cosmological world model, the radio luminosity function, and on the distribution function of source sizes. These aspects of the $\theta_m(S)$ relation are investigated in the next chapter.

Chapter 5

ANGULAR SIZES AND COSMOLOGY

5.1 Introduction

It is widely believed that the flux density counts of extragalactic radio sources do not agree with the predictions of uniform world models and provide evidence of strong evolutionary effects in the mean properties of sources with epoch (Reviews by Longair 1971; Rees 1972). In Chapter 1 (Section 1.2) we have argued about the desirability of performing other independent cosmological tests in order to investigate the spatial distribution of extragalactic radio sources. In this Chapter we shall show how the statistics of angular sizes of radio sources observed over a range of apparent flux density can be used for such tests. We first summarize (Section 5.2) the results that have so far been obtained from cosmological tests with angular sizes of extragalactic objects. We shall apply two additional tests that have not hitherto been used; (a) the $\theta_m(S)$ relation which was discussed in the last Chapter and (b) the counts of angular sizes, i.e. the $N(\theta)$ relation. In Section 5.3 we outline the method of estimating the expected $N(\theta)$ and $\theta_m(S)$ relations for a uniform distribution of sources in space. The observed angular size counts for a complete sample of the 3CR sources are constructed in Section 5.4. A comparison of the predicted relations with observations (Section 5.5) provides independent support to the evolutionary interpretation of flux density counts of radio sources. It is difficult to explain the angular size data in the Steady State cosmology. In Section 5.6 the nature and magnitude of evolutionary effects are investigated for the Einstein-de Sitter cosmology. It is shown that evolution is required both in the space density (or luminosity) and in the linear sizes of radio sources with epoch.

5.2 Cosmological Tests Using Angular Sizes

5.2.1 The $\theta(z)$ test

It is well-known that the angular size θ, subtended by a class of extragalactic objects of constant physical size placed at different redshifts, depends on the world model. Observations of angular sizes can thus provide, in principle, a determination of q_o, the deceleration parameter (Hoyle 1959; Sandage 1961).

In the case of optical galaxies, the $\theta(z)$ test has had only limited application largely because the test refers to 'metric' diameters whereas one generally measures the 'isophotal' diameters of galaxies from their optical images (Sandage 1961, 1972). However, Baum (1972) has discussed a preliminary determination of q_o from measurements of metric sizes of elliptical cluster galaxies. The possibility of applying the $\theta(z)$ test to clusters of galaxies by using an empirically derived normalized cluster radius, has recently been reported by Austin and Peach (1974). In all the above applications of the $\theta(z)$ test, there are two additional problems in determining q_o.

(i) It is difficult to record and measure galaxy images at large redshifts ($z \gtrsim 0.5$) where differences in the predictions of various world models become important.

(ii) The necessary corrections that may be applicable to intrinsic sizes due to light travel times are not well understood.

The difficulties associated with using optical galaxies to determine q_o are largely overcome in the case of radio sources. Since most radio sources, at least in the low frequency surveys, have a double structure, the angular separation between the components which is used

as a measure of the angular extent is a metric size. Angular structures of many quasars at large redshifts have already been determined. Moreover, the effect of corrections due to light travel time are expected to be less important for radio sources since their typical life times (10^6 to 10^9 years) are appreciably smaller than the characteristic Hubble time, and the sources seen at large redshifts are, therefore, not likely to be individually younger. However, the test is made difficult by the fact that there is a large observed spread in angular sizes at any redshift, implying that radio sources do not have a fixed linear size. The inferred linear sizes can range from $<$ 1 kpc to over 1 Mpc.

Plots of the largest angular size θ (which refers to the angular separation of the two components for double sources, or to the largest angular scale associated with more complex source structures), against z for radio galaxies and QSOs have been investigated by Legg (1970) and Miley (1971). Wardle and Miley (1974) have recently extended the $\theta - z$ plot to include a total of 166 QSOs. The main conclusions from these studies may be summarized as follows.

(a) The upper envelope of the angular size data shows a clear correlation with z in the sense that sources at larger z have smaller θ. This correlation, together with the continuity in the points for radio galaxies and quasars, is a strong argument in favour of the cosmological origin of quasar redshifts. The scatter below the upper envelope of the $\theta - z$ plot is explained largely by the spread in the intrinsic sizes of radio sources and partly by the fact that the sources are seen in projection on the plane of the sky.

(b) At large redshifts ($z \sim 2$) the angular sizes of quasars fall well below the values expected in either the Steady State cosmology or in Friedman cosmologies. The angular size in fact decreases with z somewhat as z^{-1}, the relation expected in Euclidean geometry. The observed $\theta - z$ relation can, however, be explained by invoking evolution in the linear sizes of quasars with epoch. Although the exact form of evolution can not be determined from the data, a reasonable fit is obtained to the upper envelope of the data if the linear sizes vary as $(1 + z)^{-n}$, with n in the range of ~ 1 to 3. The data cannot be used to determine the value of q_o, since model differences are small compared to the evolutionary effects.

Reinhardt (1972) has pointed out that Miley's (1971) data for QSOs are consistent with a non evolving (with respect to size) population of QSOs in low density Friedmann universes (which predict a $\theta - z$ relation closer to the Euclidean relation). He has also suggested the possible existence of two classes of QSOs; those with intrinsic sizes < 0.23 Mpc and those with a strong concentration between about 0.33 and 0.43 Mpc (for $H = 50$ km sec^{-1} Mpc^{-1} and $\Omega = 0.1$, where $\Omega = 2q_o$ is the ratio of the actual and critical matter density in the universe). The discontinuity in the linear size distribution could, however, arise from observational selection effects (van der Kruit 1973). Jackson (1973) and Richter (1973) find that the upper envelope of the $\theta - z$ relation for QSOs can be explained reasonably well without the need for an evolution in source sizes, if it is assumed that the intrinsic luminosities of QSOs decrease with time (as e.g. in the model of Ryle and Longair 1967), for then the sources of high luminosities (i.e. large z) would be seen younger (therefore of smaller size). Such an explanation predicts an

anticorrelation between luminosity and source size, which is not evident in the data (this point is considered further in Section 5.3.1).

A study of the $\theta - z$ plot is limited to sources with known redshifts, and can therefore be affected by complex selection effects. Also, it does not tell us if the sizes of radio galaxies evolve as well, because large redshifts have not been measured for galaxies.

A test combining the $\theta - z$ relation and source counts has been applied in a limited sense by Longair and Pooley (1969), who compared the number of sources with $\theta > 70''$ arc observed in the 5C surveys down to flux limits of 0.03 Jy at 408 MHz, with the number expected in different cosmologies, as predicted from the properties of the stronger sources in the 3CR sample. The observed number was found to be larger than predicted in reasonable world models and could be explained by evolutionary effects in the space density of intermediate luminosity sources with epoch. A similar test covering a smaller range in flux density has been performed by Fanaroff and Longair (1972).

5.2.2 The $\theta(S)$ test

Since the variation of both angular size and flux density with z, depends on the world model, the $\theta - S$ relation can also be used as a statistical test of cosmology. Although such a relation introduces additional spread in the data due to the radio luminosity function, it has the advantage that complete or unbiased samples of sources can be used. We shall apply this test in this Chapter to the observed $\theta_m(S)$ relation discussed in Chapter 4.

5.2.3 Angular size counts

The smaller spread in the linear sizes of most radio sources compared to their luminosity, and the apparently rare occurrence of sizes larger than about 1 Mpc, suggest that it may be fruitful to study the angular size counts of radio sources, i.e., the log N-log θ relation, in which the number of sources N, in a given region of the sky, which have an angular size greater than a value θ, is plotted against θ, in a manner analogous to the log N-log S of radio source counts. The flux density information is implicit in such a study as we are considering angular size counts in a survey which is complete above a certain flux density, S. It is clear that such an $N(S,\theta)$ relation contains information on the cosmological world model as well as on any evolutionary effects in the properties of the source population with epoch.

As an ideal case, consider a survey of the sky in which the sensitivity limit is so low that every source is detected. If the sources are uniformly distributed in space and have a constant physical size, then in the case of Euclidean geometry, the number of sources varies with distance as r^3, and the angular size θ as r^{-1}, so that

$$N(>\theta) \propto \theta^{-3}$$

The above relation would be true for any distribution of linear sizes, provided the distribution is independent of epoch, since each range of linear sizes will give $N(>\theta) \propto \theta^{-3}$. In an actual survey that is complete above a flux density S, not all sources in the sky will contribute to the angular size counts at any θ, since some sources, though near enough to subtend an angle greater than θ, will not be luminous enough to have

a flux density greater than S and will not therefore be included in the catalogue. The slope of the log N-log θ relation would thus be flatter than -3; the actual slope would depend on the space density of sources of various luminosities i.e. the Radio Luminosity Function.

Since it is important in studying angular size counts that complete samples of sources be used, the 3CR sample of 199 sources appears to be the best available sample for this purpose. In Section 5.4 we have used the available angular size information to construct the counts for the 3CR sample, down to $\theta = 10''$ arc. The method of calculating the expected $N(S,\theta)$ and $\theta_m(S)$ relations from our knowledge about the radio source population is first outlined in Section 5.3.

We shall assume throughout that QSOs are at cosmological distances implied by their redshifts and treat them as indistinguishable from radio galaxies for the purposes of angular size counts. Since there seems to be little controversy about the cosmological nature of the redshifts of radio galaxies, we shall also consider slightly reduced samples of sources obtained by excluding the known QSOs from the complete samples. We shall come to very similar conclusions for the samples with and without QSOs.

5.3 Prediction of Angular Size Counts

In order to calculate the expected angular size counts, i.e. the $N(S,\theta)$ relation, we shall first assume that radio sources are uniformly distributed in space. We need to know the cosmological world model and the Luminosity Size Function, $\Phi(P,\ell)$, which can be defined such that the number of radio sources in a unit volume of space, which

have radio luminosities (at a fixed emitted frequency) in the range P to P + dP, and projected linear sizes in the range ℓ to $\ell + d\ell$, is given by

$$\Phi(P, \ell)\, dP\, d\ell$$

5.3.1 The luminosity-size function

We shall express the luminosity-size function as a product of the Luminosity function and the radio size function, ie.

$$\Phi(P, \ell) = \rho(P)\, \psi(\ell) \qquad \ldots (1)$$

where the radio size function $\psi(\ell)$, is normalized such that,

$$\int_0^\infty \psi(\ell)\, d\ell = 1$$

The factorization of eq. (1) appears to be justified as there is little evidence of a correlation between the size and luminosity of radio sources. An anticorrelation between P and ℓ might be expected if at large redshifts (therefore high luminosities) sources are seen to be individually younger (therefore of small size). But since the life times of most radio sources have generally been inferred to lie in the range of about 10^6 to 10^9 years, which is much smaller than the Hubble time, their age distribution should be practically independent of z. A plot of the projected size against luminosity P_{178} for the complete sample of 3CR sources appears to be more or less a scatter diagram, with only a slight tendency for

sources with small physical sizes to have high luminosities (Longair and Macdonald 1969). This tendency refers mainly to a few QSOs and does not necessarily imply a correlation of size with luminosity. It can arise in part from evolutionary effect in the sizes of sources at large redshifts that is indicated by the $\theta - z$ plots for QSOs. Furthermore, very compact angular sizes are generally associated with QSOs of flat or inverted radio spectra, but the fraction of such sources in low frequency catalogues is known to be quite small ($\lesssim 5\%$) even at the lower flux levels of the Ooty survey (Kapahi, Joshi and Kandaswamy 1972; see also Chapter 3, Section 3.4.1). In order to minimize the inclusion of possible evolutionary effects in source sizes in considering a possible $P - \ell$ correlation, one can look only at sources of small z. Mackay (1973) has made an ℓ -P plot for an approximately complete sub-set of 64 sources from the 3CR sample which are either known or estimated (from their optical magnitudes) to have $z < 0.3$. The plot is clearly a scatter diagram with a similar spread in the ℓ values at different luminosities, which range from about 5×10^{23} to 5×10^{26} W Hz^{-1} ster^{-1} (for a Hubble constant of H = 50 km sec^{-1} Mpc^{-1}) at 178 MHz. This sub-set consists almost entirely of radio galaxies. For sources of higher luminosity it becomes necessary to consider samples of QSOs of large z. From the $\theta - z$ data for QSOs, Strom (1973) and Wardle and Miley (1974) have noted that the effects of any possible anti-correlation between luminosity and size do not appear to exist in the data. It appears quite reasonable, therefore, to assume the radio size function to be independent of the luminosity function. We shall later consider the possible dependence of source sizes on z.

5.3.2 The radio luminosity function (RLF)

There is considerable uncertainty in the observationally determined form of the radio luminosity function (RLF), due largely to the difficulty of estimating the distances of radio sources. For instance, von Hoerner (1973) has plotted several existing determinations of the RLF and concluded that (a) there is an uncertainty of about a factor of 10 in the scale of the luminosity function and (b) if the luminosity function is expressed as a power law, $\rho(P) \propto P^{-\gamma}\, dP$, the exponent appears to have a value $\gamma = 2.5 \pm 0.5$ over the entire range of luminosities relevant to radio galaxies and QSOs.

For our purpose we shall, for simplicity, assume the radio luminosity function to be given by a truncated power law of the form,

$$\rho(P) = k\, P^{-\gamma}, \quad \text{for } P_L \leq P_{178} \leq P_u \qquad \ldots (2)$$

$$\text{and} = 0 \qquad \text{otherwise}$$

we shall take $P_L = 10^{23}$ W Hz^{-1} ster^{-1} and $P_u = 2 \times 10^{28}$ W Hz^{-1} ster^{-1} at 178 MHz, as indicated by the known luminosities of radio galaxies and QSOs. Our conclusions do not depend critically on these limits. We show in Section 5.5 that by comparing the predicted $N(S,\theta)$ relations for such a luminosity function with the observed counts for the 3CR sample, the value of the exponent γ can, in fact, be determined for $P_{178} \lesssim 10^{26}$ W Hz^{-1} ster^{-1}, and useful limits can be put on the value of γ for higher luminosities. Necessary modifications to the single power low form of eq. (2) at high luminosities are considered in Section 5.6.

5.3.3 Radio size function

The spread in the inferred sizes of radio sources is likely to be caused by a number of factors such as projection effects, distribution of source ages, the spread in initial conditions in the energetic events that give rise to the two radio components and the process of confinement of the source components. Since most of these factors are not well understood, the expected form of the size function is not known. We shall therefore use a purely empirical method to derive a simple form of the size function, that is consistent with observations.

Like the luminosity function, the size function can also be a function of epoch in the relativistic cosmologies. Since the relation between ℓ and θ depends on the world model, and since we do not know the exact form of the possible variation of ℓ with z, the local size function has to be derived from a complete sample of sources of small z, so that the geometrical effects of the world model and evolutionary effects in source sizes are not important. For the approximately complete sample of 64 3CR sources with $z < 0.3$ (Mackay 1973), a histogram of the distribution of projected linear sizes, calculated from the observed angular sizes in the Einstein-de Sitter model, is shown in Fig. 1(b). The histogram represents the distribution of projected sizes, $\psi(\ell)$, and we need to know what distribution of actual sizes $\psi_a(\ell_a)$, will give rise to the observed distribution. For this, we first work out how a distribution of true linear sizes is affected by random projection effects.

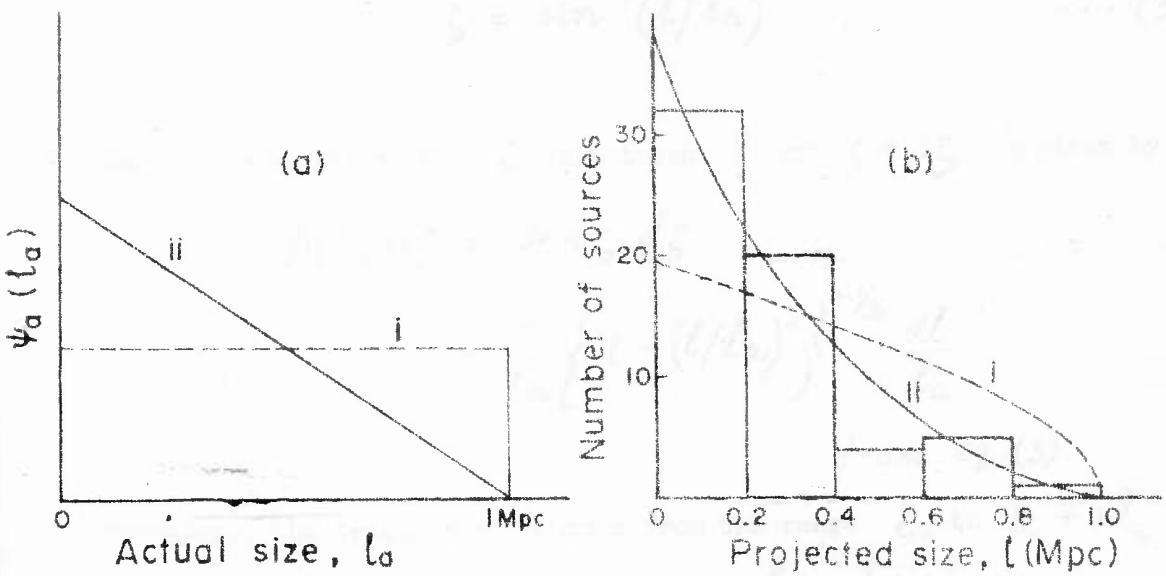

FIG. 5.1 Distribution functions of (a) actual source sizes and (b) projected source sizes, compared with the observed histogram for 64 3CR sources (Mackay 1973). Note that one source (3C 236) with l = 5.7 Mpc lies outside the range covered by the histogram.

If the major axis of a radio source makes an angle ζ ($0° < \zeta < 90°$) with the line of sight, the projected size $l = l_a \sin\zeta$. Consider the range of projected sizes l to $l + dl$. A source of true size between l_a and $l_a + dl_a$ will give a projected size in the above range if the angle ζ lies in the range ζ and $\zeta + d\zeta$, where

$$\zeta = \sin^{-1}(l/l_a) \qquad \ldots(3)$$

Now the probability that ζ is between ζ and $\zeta + d\zeta$ is given by

$$p(\zeta)\,d\zeta = \sin\zeta\, d\zeta$$

$$= \frac{l}{l_a}\left\{1 - (l/l_a)^2\right\}^{-1/2}\frac{dl}{l_a}$$

from eq.(3).

Therefore, the fraction of sources from the range l_a to $l_a + dl_a$ that gives a projected size in the range l to $l + dl$ is

$$\psi_a(l_a)(dl/l_a)(l_a^2 - l^2)^{-1/2} l\, dl_a,$$

and the fraction that have the projected size in the above range from the maximum possible range of actual sizes $l_a = l$ to $l_a = l_o$, where l_o is the maximum actual size, is given by

$$\psi(l)\,dl = l\,dl \int_l^{l_o} \frac{\psi_a(l_a)\,dl_a}{l_a\sqrt{l_a^2 - l^2}} \qquad \ldots(4)$$

(i) Let us first consider, following Legg (1970), a simple size distribution in which all true sizes from 0 to a maximum value l_o, are equally probable (see Fig. 3(a)i), i.e.

$$\psi_a(l_a)\, dl_a = dl_a / l_o \qquad \ldots (5)$$

By integrating equation (4) we get

$$\psi(l)\, dl = \frac{1}{l_o} \cos^{-1}(l/l_o)\, dl \qquad \ldots (6)$$

The above distribution, for the value of l_o = 1 Mpc is compared with the observed histogram in Fig. 3b. It is clear that the size function of eq. (6) predicts too many sources of large projected sizes as compared to the observed number.

(ii) We now try another analytically simple distribution of true sizes in which the probability of a size l_a reduces linearly with increasing l_a, (Fig. 3(a) ii), i.e.

$$\psi_a(l_a)\, dl_a = \frac{2}{l_o}\left(1 - \frac{l_a}{l_o}\right) dl_a \qquad \ldots (7)$$

From equation (4) we find for this distribution,

$$\psi(l)\, dl = \frac{2}{l_o}\left[\cos^{-1}(l/l_o) - (l/l_o) \ln\left\{\frac{l_o + \sqrt{l_o^2 - l^2}}{l}\right\}\right] dl \ldots (8)$$

The size function of eq. (8) gives a reasonable fit to the observations as shown in Fig. 3(b) and we shall use it for calculating the angular size counts and the $\theta_m(S)$ relation.

It should be noted that the recent discovery of two double radio galaxies of small z, having projected linear sizes of 2.0 and 5.7 Mpc (Willis, Strom and Wilson 1974) indicates that the local size function may have a weak tail extending to sizes larger than 1 Mpc. The exclusion of a few such large sources from the function of eq. (8) is, however, not likely to change our conclusions appreciably.

5.3.4 The N(S,θ) relation

Since evolutionary effects in source properties may be more important than the geometric differences in world models, we shall work out the expected $N(S,\theta)$ relations only in the Einstein-de Sitter model ($\Lambda = 0$, $q_0 = 0.5$) and in the Steady State model. For simplicity, we first illustrate the procedure in a static Euclidean universe and then include the necessary modifications in the two world models.

The basic relations to be used are

$$P = (c/H)^2 z^2 S \qquad \ldots(9)$$

and

$$\theta = \ell/(c/H)\, z \qquad \ldots(10)$$

where c is the velocity of light and H is the Hubble constant, which we take to be $H = 50$ km sec^{-1} Mpc^{-1}. For a given sensitivity limit S_0, the lower limit P_L to the RLF implies that all sources

nearer than a redshift z_* given by

$$z_* = (H/c)\ (P_L/S_o)^{1/2}$$

have a flux density $> S_o$. At the redshift z_*, a source of maximum linear size ℓ_o, subtends an angle θ_* given by

$$\theta_* = (H/c)\ (\ell_o/z_*)\ .$$

An observed angular size $\theta > \theta_*$ can thus arise only from the region $z < z_*$. In the angular size range of $\theta > \theta_*$ the counts do not depend on the luminosity function, and it is readily seen that

$$N(> S_o, > \theta) \propto \theta^{-3}$$

independent of the radio size function. Now for the 3CR sample we have $S_o = 9$ Jy, and for values of $P_L = 10^{23}$ W Hz^{-1} ster^{-1} and $\ell_o = 1$ Mpc, we get

$$z_* = 0.0057, \text{ and } \theta_* = 6100'' \text{ arc}$$

As the largest angular size of a source in the 3CR sample is only $\sim 3800''$ arc (for 3C 437.1), it is clear that the range $\theta > \theta_*$ is of little practical importance.

In the case of $\theta < \theta_*$, most of the contribution to the angular size count comes from the region of $z > z_*$. At any z greater than z_* only those sources that are sufficiently luminous to be seen above the survey limit can contribute to the angular size count, and since the fraction of such sources is controlled by the RLF, its form plays an important part in determining the counts. In order to see the importance of the RLF in determining the slope of the $N(\theta)$ relation, let us for simplicity assume for the moment, that the power law RLF of eq. (2) has no lower or upper cutoffs.

The number of sources per steradian from the shell z to $z + dz$, with luminosities P to $P + dP$ and sizes ℓ to $\ell + d\ell$ is

$$n(z,P,\ell)dz\, dP\, d\ell = (c/H)^3 z^2 dz\, k\, p^{-\gamma}\, dP\, \psi(\ell)d\ell$$

and the number that have a flux $S > S_o$ is given by

$$n(z, > S_o, \ell)dz\, d\ell = (c/H)^3 z^2 dz \int_{P = S_o(c/H)^2 z^2}^{\infty} k\, P^{-\gamma}\, dP\, \psi(\ell)d\ell$$

$$= \frac{k}{(\gamma-1)} (c/H)^{5-2\gamma}\, S_o^{1-\gamma}\, z^{4-2\gamma}\, dz\, \psi(\ell)d\ell$$

Changing the variable z to θ from eq. (10), we can write

$$n(>S_o,\theta,\ell)d\theta\, d\ell = \frac{k\, S_o^{1-\gamma}}{(\gamma-1)}\, \theta^{2\gamma-6}\, d\theta\, \ell^{5-2\gamma}\, \psi(\ell)d\ell$$

and the differential angular size count as

$$n(>S_o,\theta)d\theta = \frac{k\, S_o^{1-\gamma}}{(\gamma-1)}\, \theta^{2\gamma-6}\, d\theta \int_0^{l_o} l^{5-2\gamma}\, \psi(l)dl$$

The integral count is given by

$$N(>S_o, >\theta) = \int_\theta^\infty n(>S_o,\theta)d\theta$$

$$= \frac{k\, S_o^{1-\gamma}}{(\gamma-1)(5-2\gamma)}\, \theta^{2\gamma-5} \int_0^{l_o} l^{5-2\gamma}\, \psi(l)\, dl \quad \ldots(11)$$

for $1 < \gamma < 2.5$

As the integral with respect to l in eq. (11) does not depend on θ, the slope of the log N-log θ relation in a static Euclidean universe is <u>independent of the radio size function</u>. It is, however, very sensitive to the exponent γ of the RLF. If Γ is the slope of the log N-log θ relation, we have

$$\Gamma = 2\gamma - 5$$

For calculating the angular size counts for the assumed RLF of eq. (2), with lower and upper cutoffs in luminosity, we shall express the $N(S,\theta)$ relation as an integral with respect to z. In the range of interest, $\theta < \theta_*$, contribution to $N(S,\theta)$ comes from both the regions (i) $z < z_*$ and (ii) $z > z_*$, although for the 3CR sample, since the range of θ we are interested in is very much smaller than θ_*, the contribution from the first region should be quite small. Let us consider the two regions separately.

Region (i); $z < z_*$

We have,

$$n(>S_o, z, \ell)dz\, d\ell = \rho_o (c/H)^3 z^2\, dz\, \psi(\ell)d\ell$$

where $$\rho_o = \int_{P_L}^{P_u} \rho(P)dP = \frac{k}{(\gamma-1)}\left\{ P_L^{1-\gamma} - P_u^{1-\gamma} \right\}$$

If these sources have to subtend an angle $> \theta$, their projected sizes must be greater than $\ell = (c/H)z\theta$. Let $Q(z,\theta)$ be the fraction of sources in a shell at z that have a projected size $> \ell = (c/H)z\theta$. We have

$$Q(z,\theta) = \int_{\ell = (c/H)z\theta}^{\ell_o} \psi(\ell)d\ell$$

which on integration of the size function of eq. (8) gives

$$Q(z,\theta) = (1-\xi^2)^{1/2} + \xi^2 \ln\left\{ \frac{1+(1-\xi^2)^{1/2}}{\xi} \right\} - 2\cos^{-1}\xi \quad \ldots(12)$$

where $$\xi = (c/H)z\theta/\ell_o \quad \ldots(13)$$

We can now write,

$$n(>S_o, >\theta, z)dz = \rho_o (c/H)^3 z^2\, dz\, Q(z,\theta)$$

and $$N(>S_o, >\theta) = \rho_o (c/H)^3 \int_0^{z_*} z^2\, Q(z,\theta)dz \quad \ldots(14)$$

Region (ii); $z > z_*$

In this case,

$$n(>S_o, >\theta, z) = (c/H)^3 z^2 dz \int_{P=(c/H)^2 z^2 S_o}^{P_u} k P^{-\gamma} dP \; Q(z,\theta)$$

$$= \frac{(c/H)^3 k}{(\gamma-1)} \left\{ (c/H)^{2-2\gamma} z^{4-2\gamma} S_o^{1-\gamma} - z^2 P_u^{1-\gamma} \right\} Q(z,\theta)\, dz$$

and

$$N(>S_o, >\theta) = \frac{(c/H)^3 k}{(\gamma-1)} \left[\int_{z_*}^{z_u} \left\{ (c/H)^{2-2\gamma} S_o^{1-\gamma} z^{2-2\gamma} - P_u^{1-\gamma} \right\} z^2 Q(z,\theta)\, dz \right] \quad \ldots(15)$$

The upper limit of the integration, z_u, in the above equation is the smaller of $z_u(\theta) = \ell_o/(c/H)\theta$ and $z_u(P) = (H/c)\,(P_u/S_o)^{1/2}$. The total count for the case $\theta < \theta_*$ is the sum of eqns. (14) and (15), i.e.

$$N(>S_o, >\theta) = \frac{(c/H)^3 k}{(\gamma-1)} \left[\left(P_L^{1-\gamma} - P_u^{1-\gamma} \right) \int_0^{z_*} z^2 Q(z,\theta)\, dz \right.$$

$$\left. + \int_{z_*}^{z_u} \left\{ (c/H)^{2-2\gamma} S_o^{1-\gamma} z^{2-2\gamma} - P_u^{1-\gamma} \right\} z^2 Q(z,\theta)\, dz \right] \quad \ldots(16)$$

5.3.5 The $\theta_m(S)$ relation

In order to calculate the median value θ_m, of angular size as a function of flux density, we need to calculate the angular size counts for differential ranges of flux density, i.e. the $N(S, >\theta)dS$

relation. We have

$$n\,(P,z,>\theta)dz\,dP = k(c/H)^3\, z^2\, dz\, P^{-\gamma}\, dP\; Q(z,\theta)$$

Changing the variable P to S, from eq. (9), we get

$$n\,(S,z,>\theta)dS\,dz = k(c/H)^{5-2\gamma}\; z^{4-2\gamma}\; S^{-\gamma}\; dS\; Q(z,\theta)dz$$

and $$n\,(S,>\theta)dS = k(c/H)^{5-2\gamma}\; S^{-\gamma}\; dS \int_{z_L}^{z_u} z^{4-2\gamma}\, Q(z,\theta)dz \qquad \ldots (17)$$

where the lower limit of integration, $z_L = (H/c)\,(P_L/S)^{1/2}$, and the upper limit of integration z_u is decided, as in eq. (15), either by the maximum size ℓ_o, or by the maximum luminosity P_u. The values of θ_m can be estimated by plotting the $N(S,>\theta)dS$ relations for different values of S.

5.3.6 Calculations in Einstein-de Sitter cosmology

In cosmological models the expression for the element of proper volume, dV, in shell z to z + dz at the present epoch and the basic relations between P & S and between θ & ℓ get modified. The modified relations in the Einstein-de Sitter model are

$$\frac{dV}{4\pi} = 4(c/H)^3 \left\{1 - (1+z)^{-1/2}\right\}^2 (1+z)^{-3/2}\, dz \qquad \ldots (18)$$

$$P(\nu) = 4(c/H)^2\, S(\nu) \left\{1 - (1+z)^{-1/2}\right\}^2 (1+z)^{1+\alpha} \qquad \ldots (19)$$

and

$$\theta = \frac{\ell\,(1+z)}{2(c/H)\left\{1-(1+z)^{-1/2}\right\}} \qquad \ldots (20)$$

where the source is assumed to have a power law spectrum of the form $S(\nu) \propto \nu^{-\alpha}$. The spectral index distribution of radio sources at low frequencies is known to peak around $\alpha = 0.75$ with a relatively small dispersion. For simplicity we shall assume all sources to have a constant spectral index $\alpha = 0.75$.

It is clear from equations (19) and (20) that both the P-S and $\theta - \ell$ relations are not invertible, i.e. $z(P,S)$ and $z(\ell,\theta)$ cannot be got analytically, but have to be determined numerically. The most important feature of this model is that for a given size, θ does not decrease monotonically with z, but has a minimum at $z = 1.25$.

With the above modifications, the $N(S,\theta)$ relations can be worked out in a manner similar to that in the Euclidean case. It is easily shown that, for the case $\theta < \theta_*$

$$N(>S_o,>\theta) = \frac{4a^3k}{(\gamma-1)}\left[\left(P_L^{1-\gamma}-P_u^{1-\gamma}\right)\int_0^{z_*}\frac{X^2}{Y^{1.5}}\,Q(z,\theta)\,dz + \int_{z_*}^{z_u}\left\{4^{1-\gamma}a^{2-2\gamma}S_o^{1-\gamma}X^{2-2\gamma}Y^{1.75(1-\gamma)}-P_u^{1-\gamma}\right\}\frac{X^2}{Y^{1.5}}\,Q(z,\theta)\,dz\right] \qquad \ldots (21)$$

and

$$N(S,>\theta)\,dS = k4^{2-\gamma}a^{5-2\gamma}S^{-\gamma}\,dS\int_{z_L}^{z_u}\frac{X^{4-2\gamma}}{Y^{1.75\gamma-0.25}}\,Q(z,\theta)\,dz \qquad \ldots (22)$$

where

$$a = c/H$$

$$Y = (1 + z)$$

$$X = (1 - Y^{-1/2})$$

and $Q(z,\theta)$ is as given by eq. (12), but with the value of ξ (eq. 13) modified to

$$\xi_{E\text{-}dS} = (2a \; X \; \theta)/(\ell_o \; Y) \qquad \ldots (23)$$

Due to the minimum in the $z - \theta$ relation, the second integrand in eq. (21) and the integrand of eq. (22) are integrated in general over two ranges on either side of $z = 1.25$. Referring to Fig. 5.2, the first integration is from z_* to z_{u1} and the second from z_{u2} to z_u, where z_u is decided by the maximum luminosity i.e. $z(S_o,P_u)$. The lower limit of integration in eq. (22) is decided by P_L, i.e. $z_L(S,P_L)$.

5.3.7 Calculations in Steady State cosmology

Here $$\frac{dV}{4\pi} = \frac{(c/H)^3 \; z^2 \; dz}{(1 + z)^3}$$

$$P(\nu) = (c/H)^2 \; S(\nu) \; z^2 \; (1 + z)^{1+\alpha}$$

and $$\theta = \frac{\ell \; (1 + z)}{(c/H) z}$$

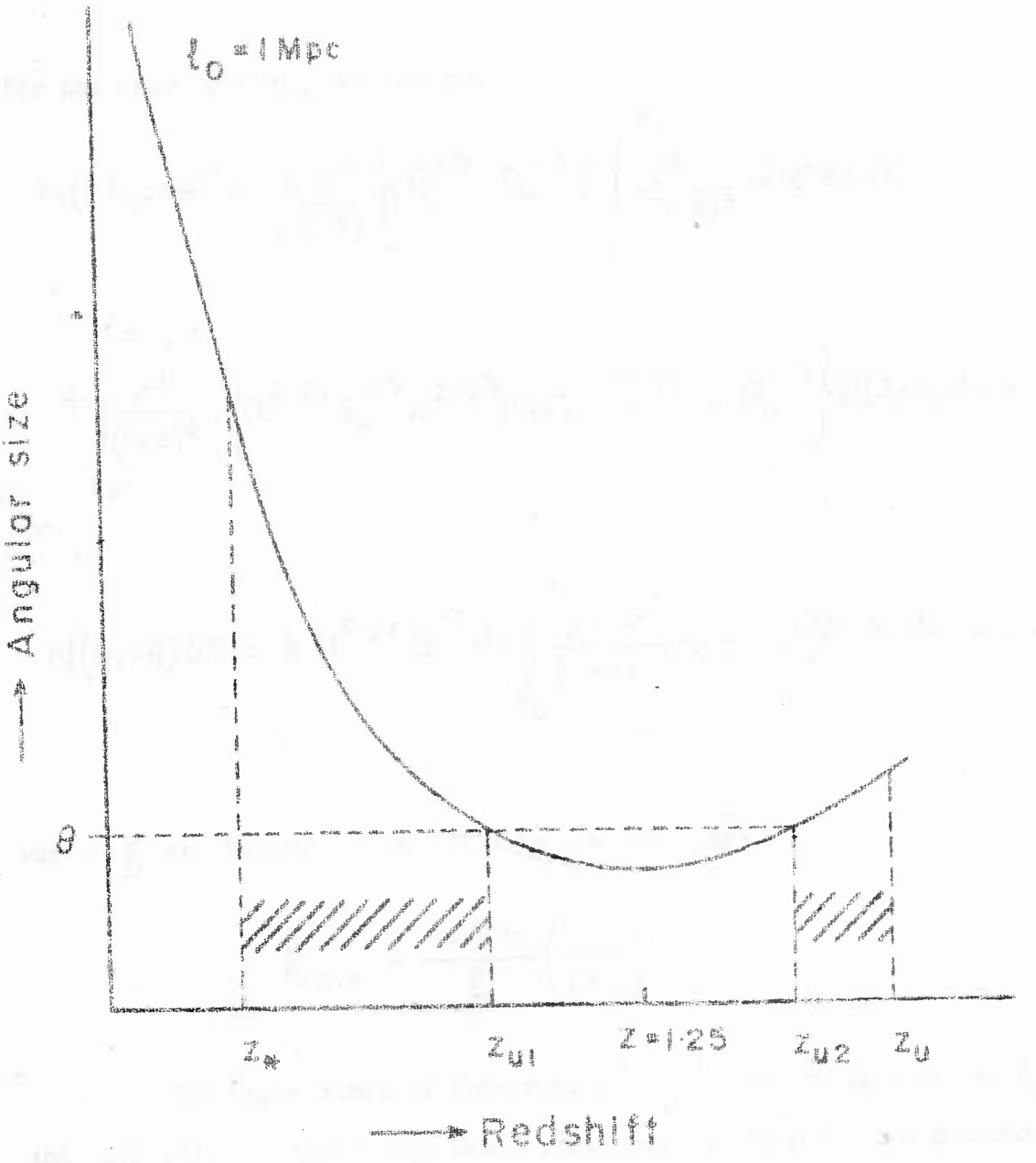

FIG. 5.2 The regions of integration with respect to z for calculating angular size counts $N(>\theta)$, in the Einstein-de Sitter cosmology.

For the case $\theta < \theta_*$, we now get,

$$N(>S_o, >\theta) = \frac{k a^3}{(\gamma-1)} \left[\left(P_L^{1-\gamma} - P_u^{1-\gamma} \right) \int_0^{z_*} \frac{z^2}{(1+z)^3} Q(z,\theta)\, dz \right.$$

$$\left. + \int_{z_*}^{z_u} \frac{z^2}{(1+z)^3} \left\{ a^{2-2\gamma} S_o^{1-\gamma} z^{2-2\gamma} (1+z)^{1.75(1-\gamma)} - P_u^{1-\gamma} \right\} Q(z,\theta)\, dz \right] \quad \ldots(24)$$

and

$$N(S, >\theta)\, dS = k a^{5-2\gamma} S^{-\gamma} dS \int_{z_L}^{z_u} \frac{z^{4-2\gamma}}{(1+z)^{1.75\gamma+1.25}} Q(z,\theta)\, dz \quad \ldots(25)$$

where ξ in $Q(z,\theta)$ of eq. (12) is now given by

$$\xi_{S.S} = \frac{(c/H)\theta}{\ell_o} \left(\frac{z}{1+z} \right)$$

The upper limit of integration z_u is the smaller of $z(\ell_o, \theta)$ and $z(P_u, S)$. In the Steady State universe, θ approaches a minimum value $\ell/(c/H)$ asymptotically as $z \to \infty$.

The calculations of $N(>S_o, >\theta)$ and $N(S, >\theta)dS$ relations were performed numerically in a computor.

5.4 The Observed Counts for the 3CR Sample

We have already used the complete sample of 199 sources from the 3CR catalogue in the last Chapter for studying the angular size-flux density relation. Remarks on some individual sources were also given there. We use the same values of θ as in the last chapter. For constructing the log N-log θ relation, it is required to go down to as low values of θ as possible. The Cambridge observations have been made with an angular resolution of 23" x 23" cosec δ arc. In order to minimize the effects of insufficient angular resolution at low declinations, and to avoid using angular size information obtained with different instruments at different observing frequencies, we have also considered a smaller subset of the 3CR sample defined by $\delta > 40^{\circ}$ and $|b| > 10^{\circ}$, covering 1.72 steradian of the sky. For larger angular sizes ($\theta > 60"$) we count the sources from the entire sample of 199 sources, but at smaller angular sizes ($10" < \theta < 60"$) we restrict the counts to the smaller sample and normalize them to the area of the complete sample. Since the upper limits to the angular sizes of unresolved sources in the complete sample and in the smaller sample are about 40" and 10" arc respectively, the counts so derived are unlikely to have been seriously affected by insufficient resolution. The angular resolutions of the existing observations do not permit a meaningful extension of the counts to $\theta < 10"$ arc at present. Due to the small fraction of QSOs ($\sim$22 per cent) in the 3CR sample, it does not also appear worthwhile to construct angular size counts for quasars separately.

TABLE 5.1

Angular Size Counts for the 3CR sample

θ (arc sec)	N (in 1.72 ster)	N(> θ) (in 1.72 ster)	N (in 4.25 ster)	N(> θ) (in 4.25 ster)
	1		3	
1000		1		3 ± 1.7
	1		3	
500		2		6 ± 2.4
	3		8	
250		5		14 ± 3.7
	7		18	
125		12		32 ± 5.6
	7		22	
62		19		54 ± 7.3
	16			
31		35 ± 5.9		86 ± 14.6
	7			
18		42 ± 6.5		104 ± 16
	14			
10		56 ± 7.5		138 ± 18.5

The counts are tabulated in Table 5.1, and shown plotted in Fig. 5.3a for the complete sample of 199 sources. Counts for the sample excluding QSOs (Fig. 5.3b) differ from those for the total sample only for values of $\theta < 65''$ arc, since this is the largest value of θ for a QSO (3C 323.1) in the sample. The errors shown are statistical errors. We have already considered possible observational or instrumental selection effects, in the last Chapter and found these unlikely to be serious. Counts for the total sample in the differential form are shown in Fig. 5.4. These show no evidence of an appreciable number of sources of large θ ($\gtrsim 5'$ arc) having been missed in the 3CR sample.

The observed log N-log θ relation appears to be linear in the range $\theta \gtrsim 125''$ arc and can be expressed as $N(>\theta) \propto \theta^{-\Gamma}$. The maximum likelyhood estimate of Γ from the ungrouped data (Crawford, Jauncey and Murdoch 1970) is found to be

$$\Gamma = 1.1 \pm 0.25$$

The slope of the log N-log θ relation flattens gradually for values of θ less than $\sim 100''$ arc.

5.5 Comparison of Predicted Counts with Observations

The angular size counts for the 3CR sample calculated for different exponents of the RLF, as outlined in Section 5.3, are compared with the observed counts in Figures 5.4 and 5.5. The value of the constant k of the RLF for each γ has been chosen to fit the observed counts at

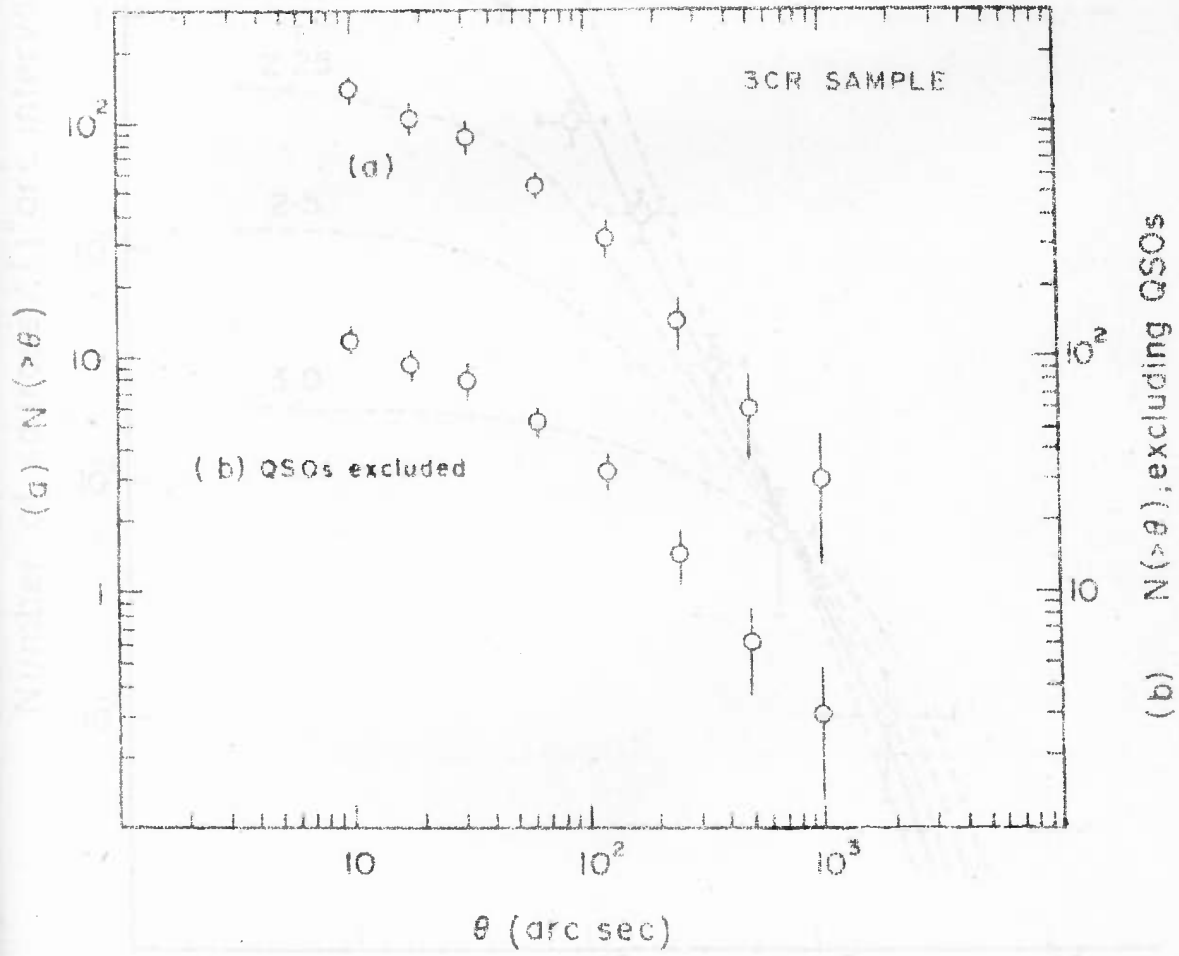

FIG. 5.3 The observed log N-log θ relation for the 3CR sample; (a) total sample and (b) sample without QSOs.

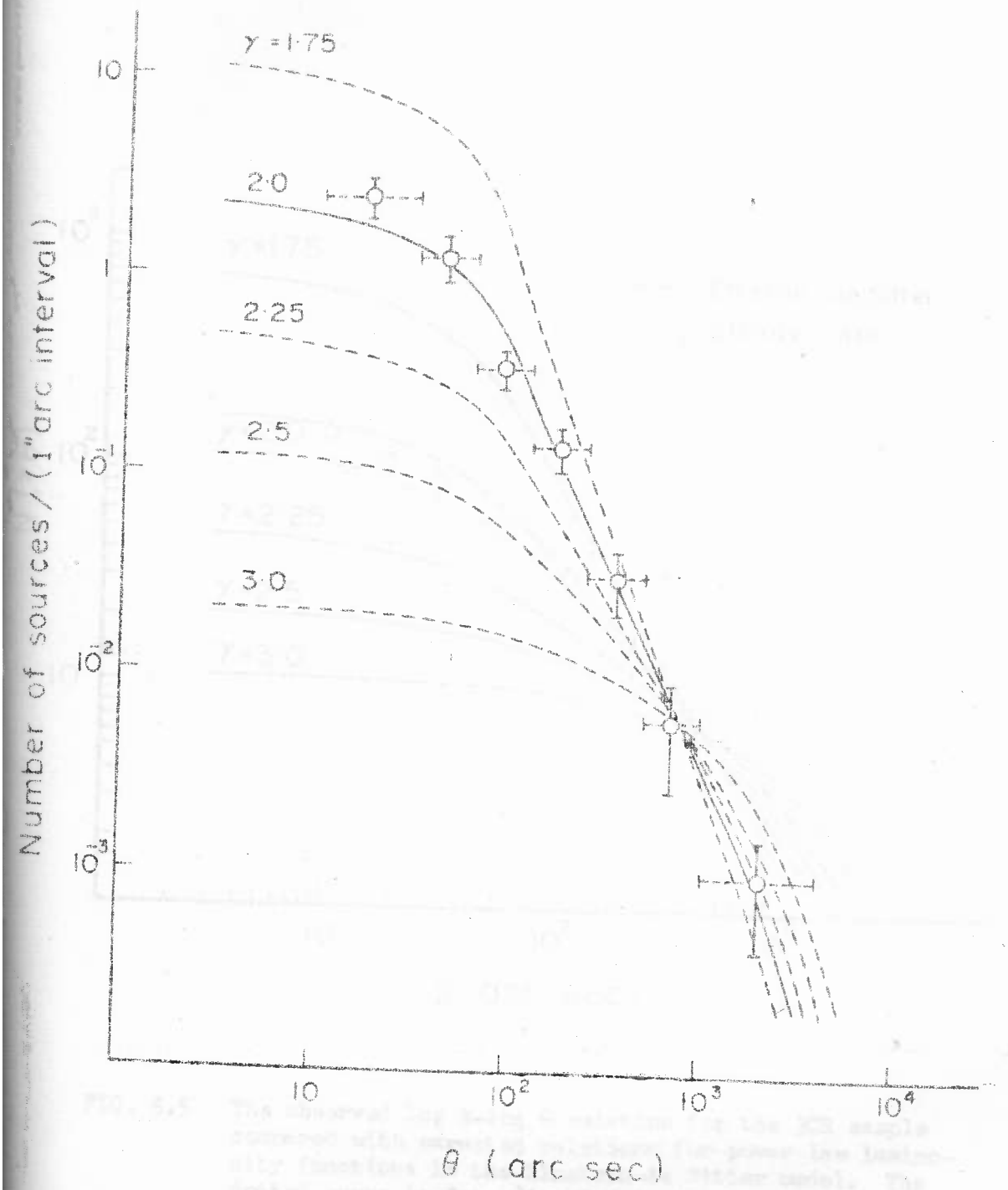

FIG. 5.4 Differential angular size counts for the 3CR sample. The curves show the predicted $N(\theta)$ relations for different exponents of the radio luminosity function, in the Einstein-de Sitter world model.

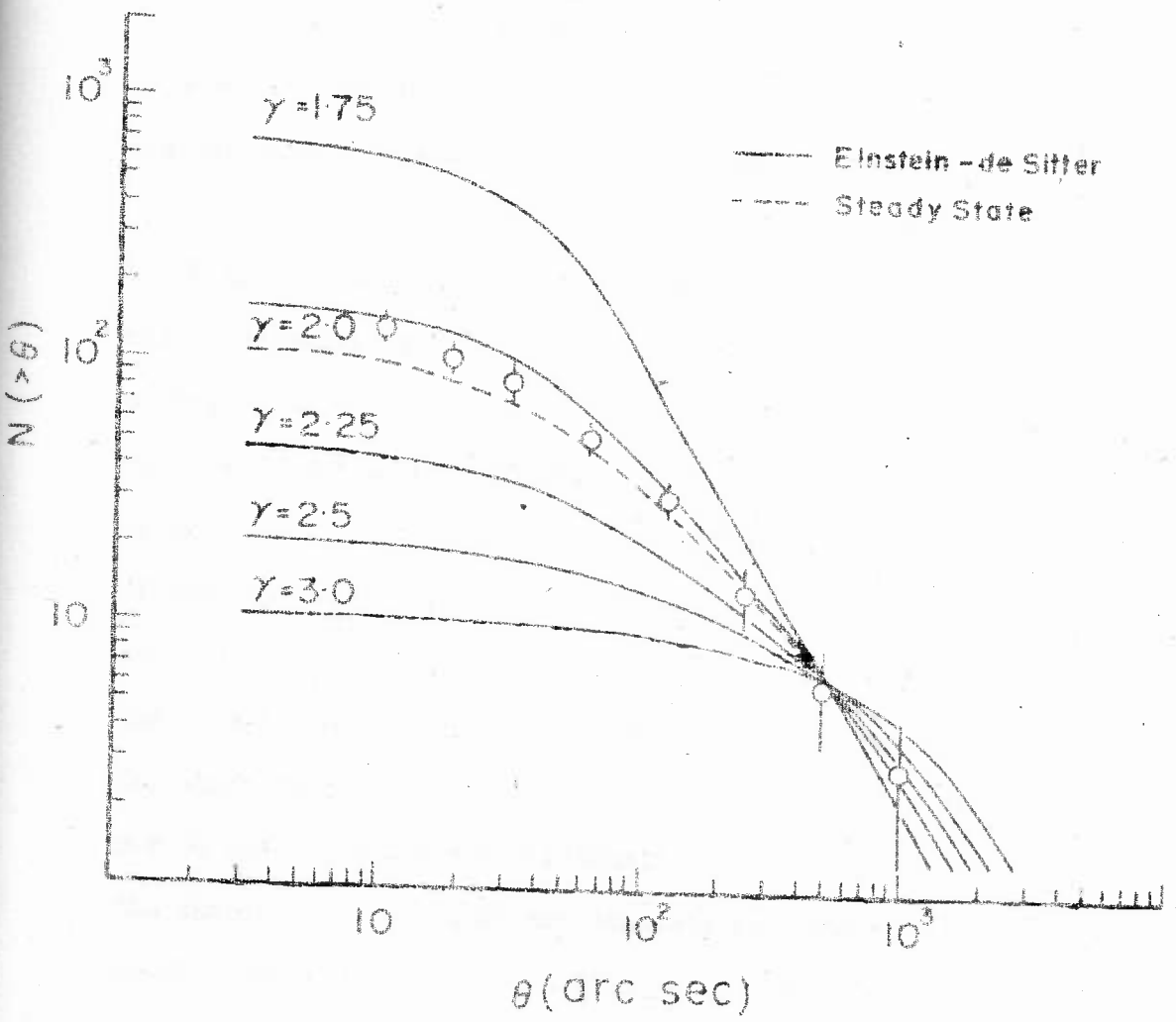

FIG. 5.5 The observed log N-log θ relation for the 3CR sample compared with expected relations for power law luminosity functions in the Einstein-de Sitter model. The dotted curve is for $\gamma = 2.0$ in the Steady State model.

the large θ end. The value of the constant k depends on the lower limit P_L of the RLF and on the exact form of the radio size function, $\psi(\ell)$. We shall be interested mainly in the exponent γ of the RLF. The strong dependence of the counts on γ is quite apparent in Fig. 5.5. In interpreting the angular size counts, let us first consider the large angular size part (say $\theta > 125"$) of the observed counts.

It is clear from the radio size function, $\psi(\ell)$ of eq. (8) and Fig. 5.1 (b) that a vast majority of the sources that have $\theta > 125"$ arc must have small z. In the Einstein-de Sitter model about 90% of the sources with $\theta > 125"$ arc should have $z < 0.25$. There are 32 sources with $\theta > 125"$ in the 3CR sample and 28 of these are identified with galaxies. Of the remaining 4, one (3C 33.1) lies in an obscured region of the sky and two (3C 437.1 with $\theta \sim 3800"$ and 3C 435.1 with $\theta \sim 3348"$ arc) have the largest angular sizes in the sample, which possibly explains the lack of unambiguous identifications for them. Most of the 26 galaxies for which redshifts are known have $z < 0.1$, the largest value being $z = 0.239$ for 3C 284 (Burbidge and Strittmatter 1972). It is clear, therefore, that the sample with $\theta > 125"$ arc consists essentially of radio galaxies of small redshifts with luminosities in the range of about $10^{23} < P_{178} < 10^{26}$ W Hz^{-1} ster^{-1}. Due to the small values of z involved, the slope of the log N-log θ relation for these sources depends mainly on the form of the radio luminosity function and is practically independent of the cosmological model and the radio size function. Any evolutionary effects in the space density or sizes of radio sources with epoch should also be relatively unimportant because of small z.

5.5.1 The luminosity function for radio galaxies

The best fit to the observed log N-log θ relation in the range $\theta > 125''$ is provided by a value of $\gamma = 2.05$ in the Einstein-de Sitter model and $\gamma = 2.0$ in the Steady State model. Considering that the inclusion of a few radio sources of large angular size ($\theta \gtrsim 500''$ arc), that may have been missed in the 3CR catalogue, would tend to flatten the observed log N-log θ relation slightly, we shall take the local luminosity function of radio galaxies in the range of about $10^{23} < P_{178} < 10^{26}$ W Hz^{-1} ster^{-1} to be given by

$$\rho(P) \propto P^{-2.1 \pm 0.15} dP$$

How does the value of $\gamma = 2.1 \pm 0.15$, determined from angular size counts for the 3CR sample compare with other determinations of the luminosity function? Merkelijn (1971) has determined the luminosity function at 400 MHz from the optical magnitudes of radio galaxy identifications in selected regions of the Parkes catalogue. In the range of about $4.10^{23} < P_{400} < 4.10^{26}$ W Hz^{-1} ster^{-1}, she finds that the RLF can be expressed as a power law with $\gamma = 2.06$ (no error is given on this value, but from her tabulated values we estimate the error to be comparable to that obtained from angular size counts). Sholomitskii (1968) has determined the RLF for normal galaxies and radio galaxies by noting the increase in the number of sources stronger than a limiting flux density with redshift. He estimated $\gamma = 2.18$ for the entire range of about $10^{21} < P_{178} < 6.10^{26}$ W Hz^{-1} ster^{-1}, covering both normal and radio galaxies, (no error was estimated. Also,

the value of γ could have been affected somewhat by incompleteness of data with regard to z). More recently, Mackay (1973) has determined the RLF from sources in the 3CR sample for which the redshift is either known to be, or estimated (from optical identifications) to be < 0.3. He estimates $\gamma = 2.16 \pm 0.15$ in the range of about $10^{22} < P_{178} < 5.10^{26}$ W Hz^{-1} $ster^{-1}$.

The value of γ determined independently from the $N(\theta)$ relation, without the explicit use of redshift data, is thus in good agreement with other determinations based on measured redshifts or on the optical magnitudes of identified galaxies.

It is also clear from Fig. 5.5, that power law luminosity functions for radio galaxies with $\gamma \gtrsim 2.5$ in the range $P_{178} \lesssim 10^{26}$ W Hz^{-1} $ster^{-1}$ are quite inconsistent with the observations. An RLF of the form $\rho(P) \propto P^{-2.5}\, dP$ has been suggested by Hoyle & Burbidge (1970) on the basis of the redshift distribution of only those radio galaxies in the 3CR catalogue whose redshifts have been measured. Such a sample, as we have already pointed out in the last Chapter, suffers from serious optical selection effects. Values of $\gamma \gtrsim 2.5$ are, in fact, incompatible with observations even if evolutionary effects are taken into consideration. Although evolutionary schemes can be worked out for the $\gamma = 2.5$ function to fit the log N-log S observations (as shown by von Hoerner 1973), it is difficult to fit the log N-log θ relation at the high θ end, where sources have small redshifts. For instance, if one considers simple density evolution of the form $(1 + z)^{\beta}$, values of $\beta > 10$ are required for sources of $P_{178} \lesssim 10^{26}$ W Hz^{-1} $ster^{-1}$ to fit the observed slope at high θ. Such an evolutionary scheme predicts a large fraction of the fainter sources

to be of low luminosity and small z, and cannot explain the observed $\theta_m(S)$ relation at small S (Section 5.5.2). We conclude, therefore, that steep luminosity functions ($\gamma \geq 2.5$) in the range of about 10^{23} to 10^{26} W Hz^{-1} ster^{-1} can be ruled out on the basis of the observed angular size data.

In order to obtain information about the form of the RLF for $P_{178} \gtrsim 10^{26}$ W Hz^{-1} ster^{-1}, we have to consider also the small angular size part of the observed $N(\theta)$ relation for the 3CR sample. Since smaller values of θ can arise from sources at large redshifts, the counts would depend significantly on the cosmological model and on any evolutionary effects in the properties of radio sources with epoch. The $N(\theta)$ relation cannot therefore be used to determined the RLF at high luminosities unambiguously. Before considering the possible form of the RLF at high luminosities, we shall first examine if the angular size data can be explained in uniform world models without evolutionary effects.

5.5.2 No evolution

It is seen from Fig. 5.5 that a value of $\gamma = 2$ in the entire range of luminosities gives a reasonable fit to the observed $N(\theta)$ relation down to the lowest values of θ. The fit could however be fortuitous. To check this we must now look at the θ_m-S relation.

The $\theta_m(S)$ relation

We calculate the $N(S, > \theta)dS$ relations for different values of flux density S, as outlined in Section 5.3 and estimate the value of θ_m as a function of S. In Fig. 5.6 the predicted $\theta_m(S)$ relations for various luminosity functions are compared with the observed relation

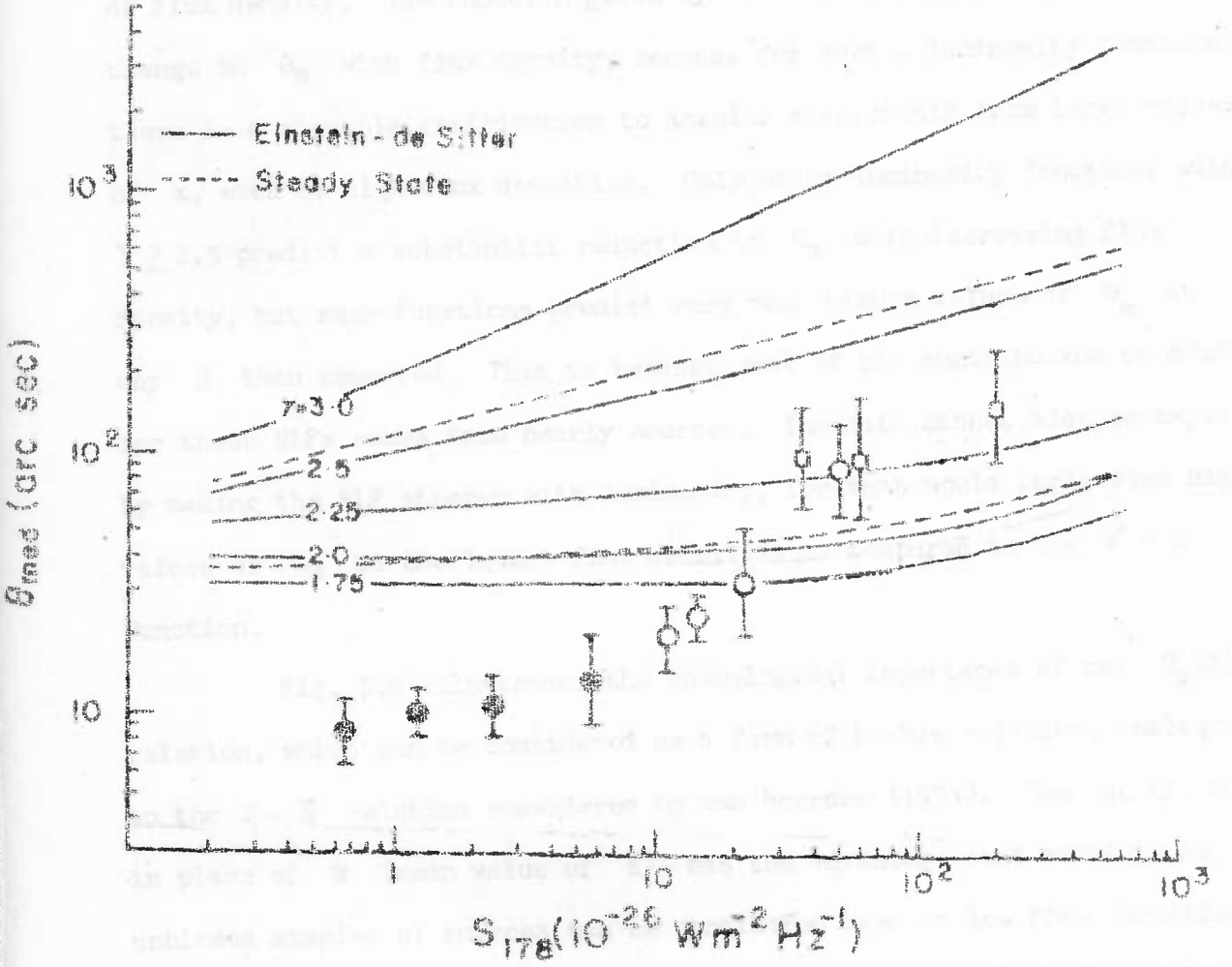

FIG. 5.6 The observed $\theta_m(S)$ relation of Chapter 4, compared with the expected relations for different exponents of the radio luminosity function. The dotted curves in Steady State universes are for $\gamma = 2$ and 2.5.

derived in Chapter 4. It is clear from Fig. 5.6 that no power law luminosity function can fit the θ_m-S relation over the entire range of flux density. The function given by $\gamma = 2$ predicts very little change in θ_m with flux density, because for such a luminosity function there is a sizeable contribution to angular size counts from large values of z, even at high flux densities. Only steep luminosity functions with $\gamma \gtrsim 2.5$ predict a substantial reduction in θ_m with decreasing flux density, but such functions predict very much higher values of θ_m at any S than observed. This is because most of the contribution to counts for these RLFs comes from nearly sources. The data cannot also be explained by making the RLF steepen with luminosity, for that would imply even higher values of θ_m at the lowest flux densities as compared to the $\gamma = 2$ function.

Fig. 5.6 illustrates the cosmological importance of the $\theta_m(S)$ relation, which can be considered as a form of Hubble relation, analogous to the $S - \bar{z}$ relation considered by van Hoerner (1973). The use of θ_m in place of $\bar{z}$ (mean value of z) has the advantage that complete or unbiased samples of sources can be considered even at low flux densities, whereas redshifts are not known for all sources even at high flux densities.

We note also from Figs. 5.5 and 5.6 that the differences in the predictions of the two world models considered are much smaller than the discrepancy with observations. It appears thus that the angular size data are incompatible with the predictions of simple cosmological models in which the co-moving density or physical sizes of radio sources do not change with epoch and in particular with the predictions of the simple Steady State cosmology.

5.5.3 Steady State cosmology and the deficit of strong sources

The differential flux density counts of radio sources indicate (Kellermann 1972; Mills, Davies and Robertson 1973) that in the range of about S_{408} = 10 to 1 Jy, the slope of the N-S relation does not differ significantly from that expected in a static Euclidean universe and that the steep slope of the log N-log S is confined to sources with $S_{408} \gtrsim 10$ Jy. In a uniformly filled expanding universe the Euclidean slope can result only if the redshifts of the sources in the corresponding flux range are extremely small. Since the measured redshifts of many radio galaxies in the above flux range are $\lesssim 0.1$, it is often pointed out that the evolutionary interpretation of source counts rests only on the acceptance of quasar redshifts being cosmological. In the Euclidean region of the 408 MHz counts we note that the value of θ_m decreases continuously with decreasing flux density, which, as was argued in Chapter 4, is likely to be due to a distance effect. Moreover, by comparing the values of θ_m for radio galaxies of known z in the 3CR sample, with those for galaxies of unknown z and for the unidentified sources in the 3CR and Ooty samples, it was estimated in Chapter 4 that the median value of z for sources other than QSOs, in the flux range of S_{408} = 10 to 1 Jy was likely to be considerably greater than 0.1. At such redshifts the observed slope of the N-S relation should be appreciably flatter than the Euclidean value (see e.g. Longair & Rees 1972), and cannot be explained in the simple Steady State theory, unless the redshifts of radio galaxies have a non-cosmological origin.

It has also been suggested that the steep observed slope of the log N-log S relation at high flux densities can be interpreted as a local deficiency of strong sources rather than as an excess of weak sources (e.g. Hoyle 1968). The difficulties with such an interpretation with regard to the size of the local 'hole' and the observed isotropy in the distribution of radio sources are well-known (e.g. Ryle 1968; Longair and Rees 1972). Kellermann (1972) has estimated that an addition of only 30 to 50 strong sources over the whole sky would bring the slope of the N-S relation to the Euclidean value for the stronger sources as well. From the 408 MHz differential counts tabulated by Mills et al. (1973), which for the stronger sources are based on the All-sky catalogue, we estimate the deficiency of sources with $S_{408} > 10$ Jy to be 6 to 7 sources ster^{-1}. It must be stressed, however, that the above estimates of the deficiency are with respect to the expected number in a static Euclidean universe. The deficiency would be much larger with respect to the predictions of cosmological models because the effect of redshift should reduce the slope of the log N-log S curve continuously with decreasing flux density. For instance, von Hoerner (1973) has pointed out that for Steady State cosmology, the luminosity function ($Y = 2$) that fits the differential counts reasonably well at the lowest flux values implies a large deficiency of sources with $S_{408} > 1$ or 2 Jy, which we estimate to be atleast 200 sources ster^{-1}.

Apart from the question of the number of 'missing sources' it is interesting to enquire about the angular sizes of such sources. If the angular size distribution of the 'missing' sources is similar to that for the observed sources, as would be expected if the deficiency

were to be caused by a statistical fluctuation, the observed $\theta_m(S)$ relation should not be affected by the addition of the 'missing' sources. The observed data would, therefore, still be incompatible with the Steady State cosmology.

A second possibility is to consider the 'missing' sources to have large angular sizes. In fact it is conceivable that some of the deficiency arises from the difficulty of recognizing sources of large angular extent ($\theta \gtrsim 500$" arc) in radio surveys. The effect of adding such 'missing' sources would be to flatten the observed log N-log θ relation (Fig. 5.5) and consequently to steepen the local RLF ($\gamma > 2$). It is clear from Fig. 5.6, however, that a steeper RLF would only increase the discrepancy between the observed values of θ_m at the lowest flux densities, where presumably there are no missing sources, and those predicted by the Steady State theory.

The most favourable case for the Steady State theory appears to be to assume the missing sources to have small angular sizes for the RLF of $\gamma \sim 2$. At the lowest flux values of Fig. 5.6, the $\gamma = 2$ RLF predicts θ_m values about 4 times larger than those observed. To fit the observations at the smallest S, the missing sources (of large S) are required to alter the distribution of linear sizes in local space so as to reduce the observed median value of ℓ of ~ 200 kpc (Fig. 5.1b) to only about 50 kpc. Such a modified size function would, however, imply θ_m of only ~ 15" arc at high flux densities. To reduce the observed θ_m, the missing sources must therefore have angular sizes $\lesssim 15$" arc. If the size of the local hole is to be less than say 100 Mpc (Hoyle 1968), the missing sources should have linear sizes less than ~ 8 kpc. It is hard to see how such sources could have been missed.

It seems then, that the angular size data cannot be explained in the Steady State cosmology even if the known QSOs are excluded from the source samples and a local deficiency of strong sources is postulated. Evolutionary effects with epoch in the radio luminosity function and/or in the radio size function must be postulated in order to explain the angular size data; these effects are investigated in the next section.

5.6 Evolutionary Effects

It is evident from Fig. 5.6, that in order to fit the observed $\theta_m(S)$ relation at low flux densities we require that at lower flux levels, either (a) there should be a greater contribution from sources at larger redshifts (to get more sources of smaller θ), ie. 'density evolution' or 'luminosity evolution', or (b) that the intrinsic sizes of radio sources must decrease with redshift, ie. 'size evolution'. It is also possible that both (a) and (b) are necessary. Let us first consider the case of size evolution.

5.6.1 Size evolution

It is easily seen that evolution in source sizes alone can not explain the observations. If the mean linear size of a source is taken to vary as $(1 + z)^{-n}$ with epoch, such evolution reduces the number of sources $N(>\theta)$ at any θ, since a smaller range of z now contributes to the counts at θ. But at large and very small values of θ, size evolution has little effect on $N(>\theta)$. This is because large θ values arise from small z where evolution is unimportant, and in the limit

$\theta \to 0$, all the sources luminous enough to be seen above the survey limit must still contribute to $N(>\theta)$ so that the total is not affected. Size evolution would therefore effect the log N-log θ relation only at intermediate values of θ.

In order to incorporate the effects of size evolution in the Einstein-de Sitter cosmology, we replace the $\ell - \theta$ relation of eq. (20) by

$$\theta = \frac{(1+z)^{1-n}\,\ell}{2(c/H)\left\{1-(1+z)^{-1/2}\right\}}$$

where ℓ is now the source size at $z = o$. We assume the distribution of actual sizes at any z to be of the same mathematical form as eq. (7), but with the maximum linear size ℓ_o decreasing with z as $(1+z)^{-n}$; i.e.

$$\psi_a(\ell_a, z) = \frac{2}{\ell_o (1+z)^{-n}}\left\{1 - \frac{\ell_a}{\ell_o (1+z)^{-n}}\right\} d\ell_a$$

and

$$\int_0^{\ell_o(1+z)^{-n}} \psi_a(\ell_a, z)\, d\ell_a = 1$$

In the corresponding expression for $Q(z,\theta)$ of eq. (12), the value of ξ is now given by

$$\xi_{\text{E-dS}} = (2a \times \theta)/(\ell_o\, Y^{1-n}),$$

instead of by eq. (23). With the above modifications we calculate the $N(>S_o, >\theta)$ and $\theta_m(S)$ relations in the Einstein-de Sitter cosmology as before. It should be noted that size evolution can remove the occurrence of a minimum in the $z - \theta$ relation. For $n > 1$, the value of θ corresponding to a size ℓ at $z = 0$ becomes a monotonically decreasing function of z.

The predicted log N-log θ relation for the 3CR sample, and the $\theta_m - S$ relation for $\gamma = 2.0$ and 2.5 are shown in Figs. 5.7 and 5.8 respectively, for values of $n = 1.0$ and 3.0. While the log N-log θ relation for $\gamma = 2$ is still in fair agreement with observations, the $\theta_m - S$ relation is not. Size evolution only reduces the value of θ_m at all flux densities (Fig. 5.8).

It is thus clear from Fig. 5.8 that the observed $\theta_m(S)$ relation cannot be explained by a uniform distribution of radio sources in space, even if possible size evolution is taken into account. An increase with z, in either the co-moving space density of radio sources or in the mean luminosities of radio sources, as has been inferred from the log N-log S work, is therefore needed. There has been much discussion in the literature on whether 'density evolution' or 'luminosity evolution' gives a better fit to the observed source counts. It seems clear, however, that it is not possible from source counts to distinguish between the two possibilities; both appear to be equivalent (Longair and Scheuer 1970). In the case of angular size counts, since we have no clear evidence that the maximum linear size of a source is related to its luminosity, it would not also seem possible to distinguish between density and luminosity evolution. We shall therefore consider only the simple case of density evolution and work out the amount of evolution necessary to explain the angular size data.

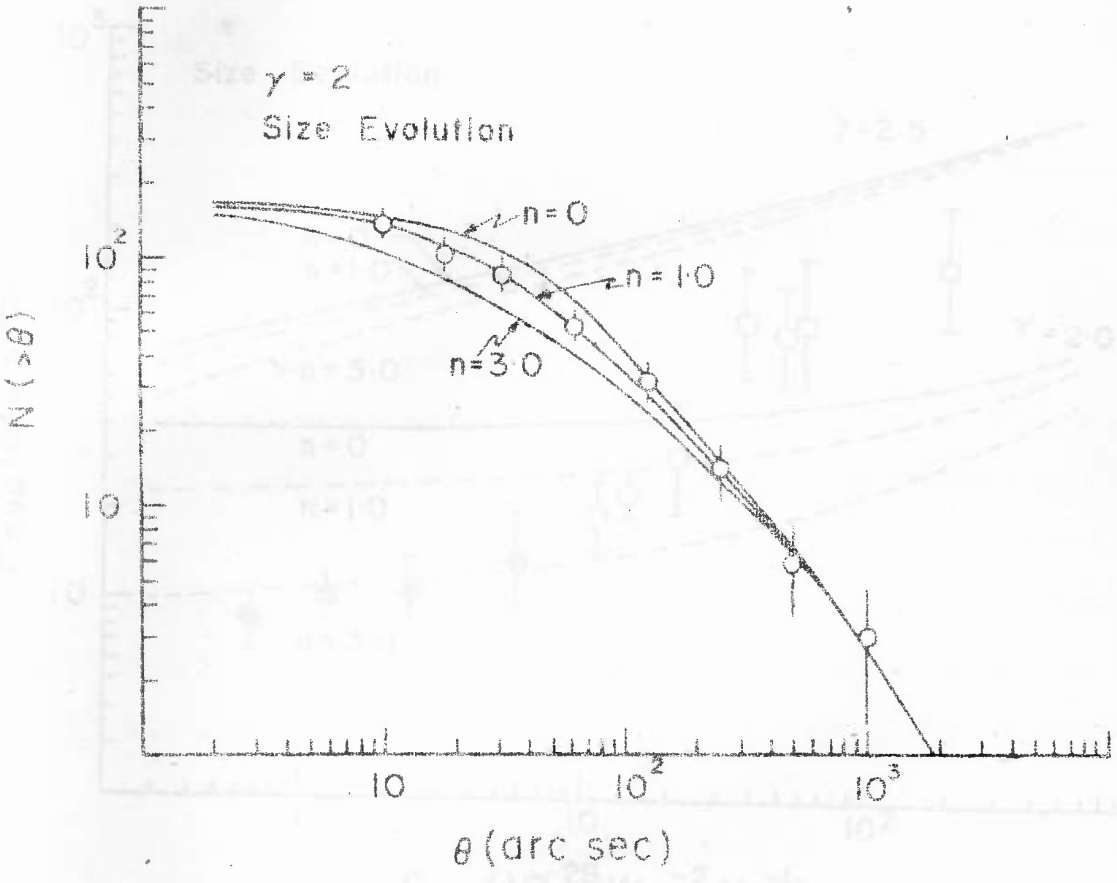

FIG. 5.7 The observed log N–log θ relation for the 3CR sample compared with the expected relations for different amounts of size evolution. Einstein-de Sitter model with γ = 2.0.

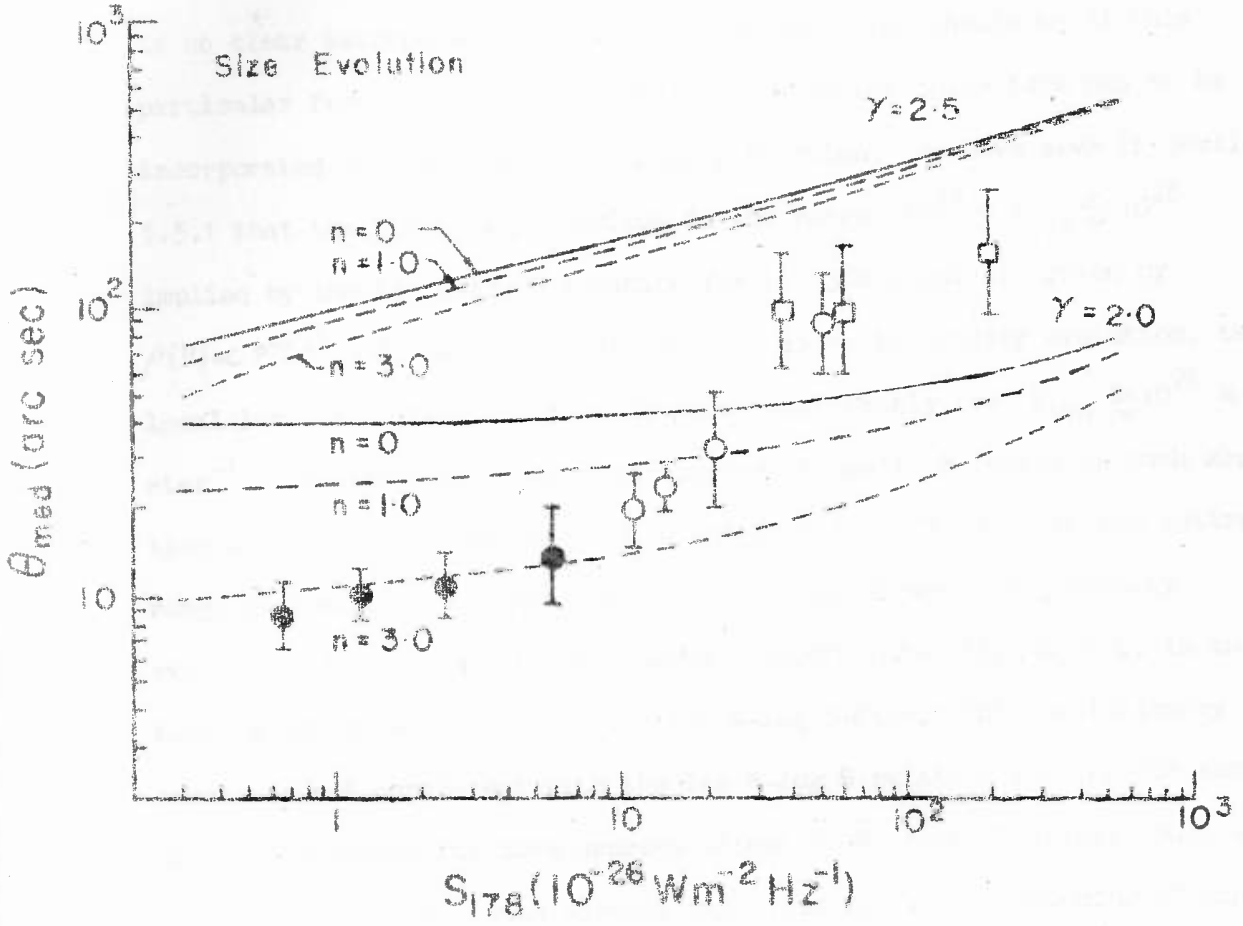

FIG. 5.8 The observed $\theta_m(S)$ relation compared with models for size evolution.

5.6.2 Density evolution

The simplest mathematical form of density evolution that has most commonly been considered is $\rho(z) \propto (1+z)^{\beta}$. We shall also consider this form of evolution although it must be remembered that there is no clear astrophysical reason why the evolution should be of this particular form (see eg. Rees 1972). This evolutionary term has to be incorporated into the radio luminosity function. We have seen in Section 5.5.1 that the luminosity function in the range $10^{23} \lesssim P_{178} \lesssim 10^{26}$ implied by the log N-log θ relation for the 3CR sample is given by $\rho(P) \propto P^{-2.1}$. It is clear that if there is to be density evolution, the local luminosity function must steepen considerably for $P_{178} \gtrsim 10^{26}$ W Hz^{-1} ster^{-1}; otherwise the number of sources at small θ would be much more than observed. (It may be pointed out that for $\gamma = 2$ in the entire range of luminosities, van Hoerner (1973) has shown that a density evolution of the form $(1+z)^4$ upto a cutoff redshift, $z_c = 4$, is in fair agreement with the observed log N-log S data. This evolutionary scheme is not consistent with the log N-log θ relation for the 3CR sample since it predicts far more sources at small θ than observed. Such an RLF in fact fits the data without any evolution). A steepening of the RLF at high luminosities is required also to fit the observed $\theta_m(S)$ relation at high flux densities. For mathematical simplicity we shall assume the local luminosity function to be given by a power law with two slopes, of the form

$$\rho(P, z=o) = k\, P^{-\gamma_1}\, dP \quad , \quad P_L \leq P \leq P_m$$

$$\text{and} \qquad = k'\, P^{-\gamma_2}\, dP \quad , \quad P_m < P \leq P_u \qquad \ldots (26)$$

where for continuity at $P = P_m$, we must have $k' = k P_m^{\gamma_2 - \gamma_1}$. It was argued in Section 5.5.1 that evolution for sources of $P \lesssim 10^{26}$ W Hz^{-1} ster^{-1} is relatively unimportant because of small z. We therefore consider density evolution only for the high luminosity sources, so that we take $\rho(P, z = o)$ for $P \leq P_m$ to be independent of z and write

$$\rho(P,z) = k' \; P^{-\gamma_2} \; (1 + z)^{\beta} \; dP$$

$$\text{for} \quad P_m < P \leq P_u$$

We take $\gamma_1 = 2.1$, $P_m = 10^{26}$ W Hz^{-1} ster^{-1} and determine the unknown parameters in the following sequence.

(i) Since sources of the largest S have small z, the value of θ_m at high S should be practically independent of evolutionary effects, depending principally on the RLF. We therefore calculate the $\theta_m(S)$ relation for different values of γ_2 ($\gamma_2 > \gamma_1$), ignoring evolutionary effects and determine γ_2 by requiring a fit with observations at high S.

(ii) With the local RLF thus determined, we estimate the log N-log θ relation for the 3CR sample for different amounts of density evolution and determine the value of β that best fits the observed relation at the smallest values of θ, where size evolution has little effect on the results, as was argued in Section 5.6.1, and is clear from Fig. 5.7.

(iii) A comparison of the calculated $\theta_m(S)$ relation, including the amount of density evolution determined as above, with observations now shows that in order to fit the data at low flux densities size evolution is also necessary (see Fig. 5.10). We therefore repeat the calculations after including size evolution for sources of all luminosities as outlined in Section 5.6.1, for different values of n and determine the value of n that best fits the observed $\theta_m(S)$ relation.

As a result of the above procedure we find that reasonable fits to the log N-log θ and the $\theta_m(S)$ data can be obtained for values of P_m in the range of $\sim 10^{26}$ to 5.10^{26} W Hz^{-1} ster^{-1}; γ_2 in the range of ~ 2.7 to 2.9; β in the range of ~ 5 to 6; and n in the range of ~ 1 to 1.5. One set of parameters that gives a good fit to the data is listed in Table 5.2, and the fits are shown in Figures 5.9 and 5.10.

In computing the $N(\theta)$ relation for the 3CR sample, the upper limit of integration ($z_u = 2.3$) is determined by the high luminosity cutoff in the radio luminosity function. In the $\theta_m(S)$ relation at lower flux densities where the limit of integration is higher, we have assumed a cutoff in the source density beyond $z_c = 3$. The cutoff is however not very critical at the lowest flux values of the data and values of $z_c = 5$ or 6 can still provide a reasonable fit to the data.

The log N-log θ and the $\theta_m(S)$ relations for source samples obtained by excluding the known QSOs can be explained reasonably well by the same set of parameters as in Table 5.2, but with the upper cutoff to the RLF reduced to $P_u = 5.10^{27}$ W Hz^{-1} ster^{-1}. A lowering of P_u is required to prevent the possibility of high flux density radio galaxies from having large redshifts. The fits with the data are shown in Figures 5.9(b) and 5.11.

TABLE 5.2

Parameters of a Satisfactory Evolutionary Model

1. Local Luminosity Function
(178 MHz)

$\gamma_2 = 2.8$

$\rho(P) \propto P^{-2.1}\, dP \quad , \quad P_L \leq P \leq P_m \qquad P_L = 10^{23}$ W Hz^{-1} ster^{-1}

$\rho(P) \propto P^{-\gamma_2}\, dP \quad , \quad P_m < P \leq P_u \qquad P_m = 10^{26}$ W Hz^{-1} ster^{-1}

$P_u = 2.10^{28}$ W Hz^{-1} ster^{-1}

2. Density Evolution

$\rho(P,z) = \rho(P,z = o) \quad , \quad P_L \leq P \leq P_m$

$\rho(P,z) = \rho(P,z = o)\ (1 + z)^{\beta} \qquad \beta = 5.5$

for $P_m < P \leq P_u$

3. Size Evolution

$\ell(z) = \ell(z = o)\ (1 + z)^{-n} \qquad n = 1.0\ ,\ 1.5$

4. Cutoff redshift

$\rho(P,z) = 0 \quad , \quad z > z_c \qquad z_c = 3.0$

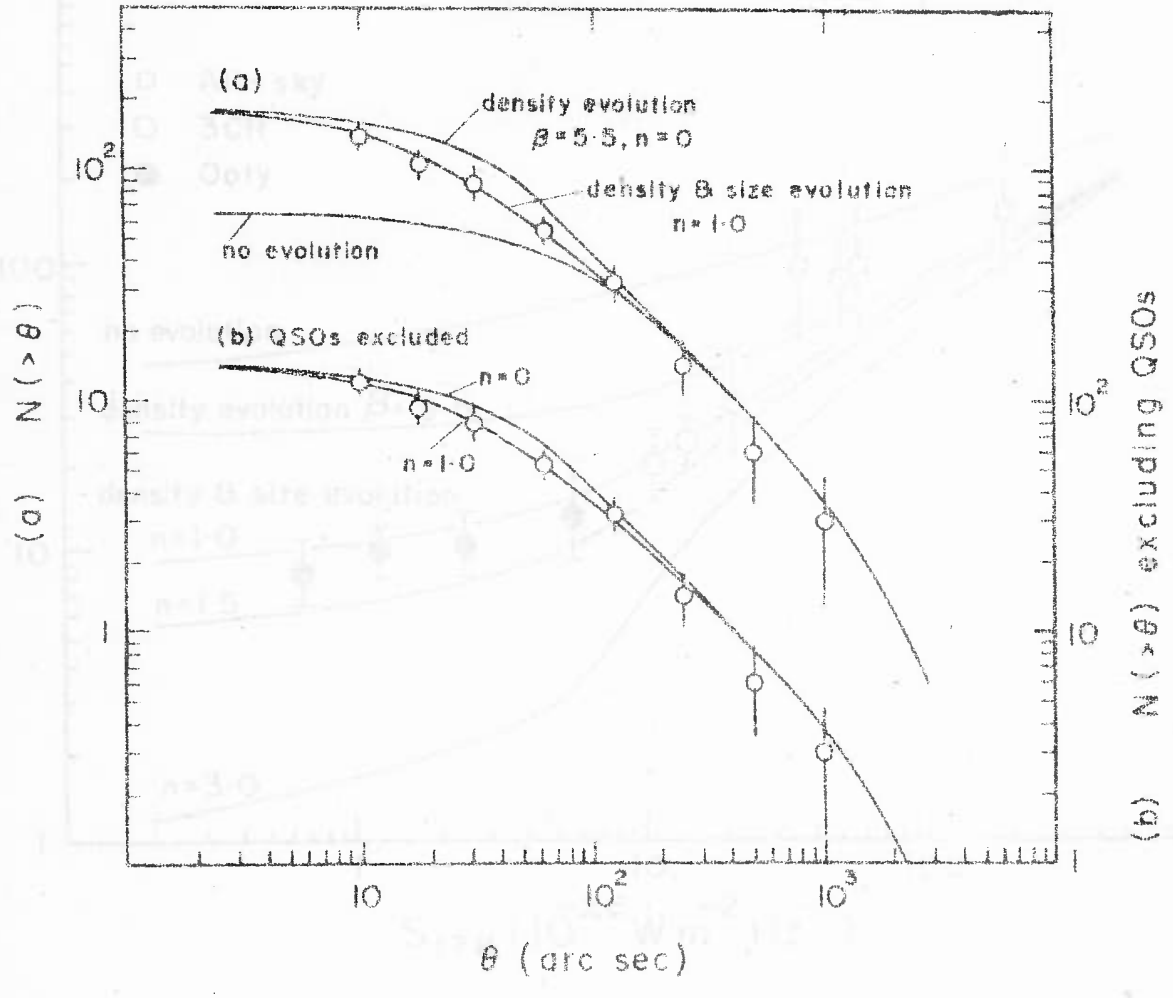

FIG. 5.9 The observed log N-log θ relations for the 3CR sample with and without QSOs, compared with the predicted relations for the parameters of the satisfactory evolutionary model of Table 5.2. (a) $P_u = 2.10^{28}$ W Hz^{-1} ster^{-1} and (b) $P_u = 5.10^{27}$ W Hz^{-1} ster^{-1}.

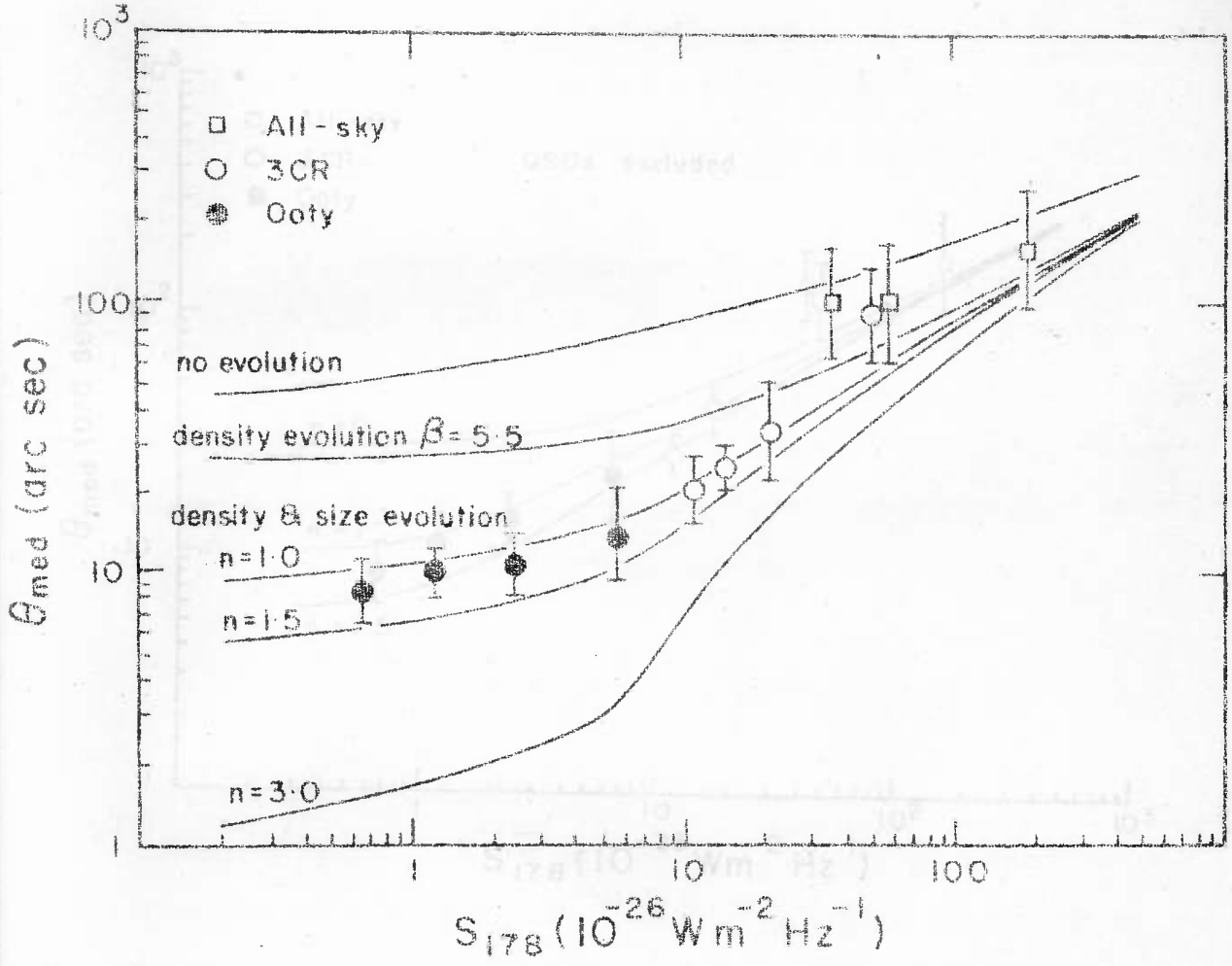

FIG. 5.10 The observed $\theta_m(S)$ relation compared with the predicted relation for the model of Table 5.2, for different amounts of size evolution; $P_u = 2.10^{28}$ W Hz^{-1} ster^{-1}.

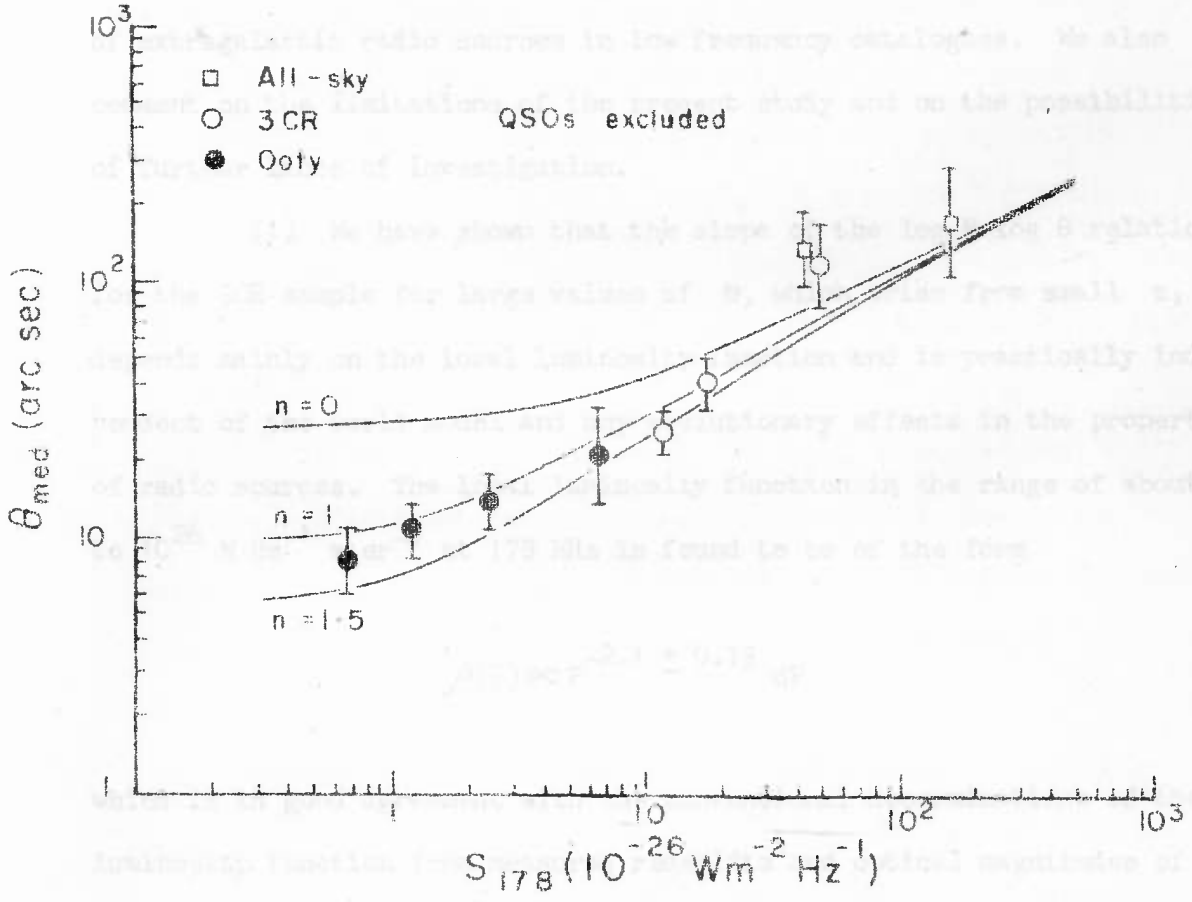

FIG. 5.11 The $\theta_m(S)$ relation for samples without QSOs compared with predicted relations for the model of Table 5.2; $P_u = 5.10^{27}$ W Hz^{-1} $ster^{-1}$.

Chapter 6

SUMMARY AND COMMENTS

In this Chapter we summarize the principal results from our analysis of the cosmological implications of the observed angular sizes of extragalactic radio sources in low frequency catalogues. We also comment on the limitations of the present study and on the possibilities of further lines of investigation.

(1) We have shown that the slope of the log N-log θ relation for the 3CR sample for large values of θ, which arise from small z, depends mainly on the local luminosity function and is practically independent of the world model and any evolutionary effects in the properties of radio sources. The local luminosity function in the range of about 10^{23} to 10^{26} W Hz^{-1} $ster^{-1}$ at 178 MHz is found to be of the form

$$\rho(P) \propto P^{-2.1 \pm 0.15}\, dP$$

which is in good agreement with the conventional determinations of the luminosity function from measured redshifts and optical magnitudes of identified radio galaxies. In the log N-log θ relation the redshift information for radio sources has been used only to derive the radio size function which, in any case, is not very important in determining the slope of the log N-log θ relation at large θ. The knowledge of the range of redshifts involved, however, is important in order to determine the range of luminosities to which the RLF refers.

The above derivation of the luminosity function is based essentially on the 32 sources in the 3CR sample in a region of 4.25 ster of the sky, that have an angular size greater than 125" arc. It should be possible to reduce the uncertainty in the exponent of the luminosity function by using the angular sizes of sources over a larger area of the sky or by using surveys to lower limiting flux densities. Such large samples of data are not available at present. It is interesting to note that the above form of the RLF is consistent with the log N-log θ relation for the All-sky sample of $S_{408} \geq 16.5$ Jy as shown in Fig. 6.1. However, this sample has only 29 sources with $\theta > 125$" arc, of which 11 are common to the 3CR sample.

(2) We find that the observed $\theta_m(S)$ relation over a flux density range of about 300 to 1 does not agree with the predictions of reasonable world models for any local luminosity function. The data provide independent evidence of strong evolutionary effects in the mean properties of the source population with epoch. Moreover, evolutionary effects appear to be more important than the geometric differences in world models.

The data cannot, in particular, be explained in the Steady State theory of the universe, even if the QSOs are excluded from the analysis and a local deficiency of strong sources is postulated, as has been proposed to explain the flux density counts of radio sources. Apart from the known result that the number of such 'missing' sources has to be rather large the angular size data indicate that the 'missing' sources must be mainly of small angular size ($\lesssim 15$" arc). It is difficult to understand such a deficiency of compact sources as a statistical fluctuation or as arising from observational difficulties.

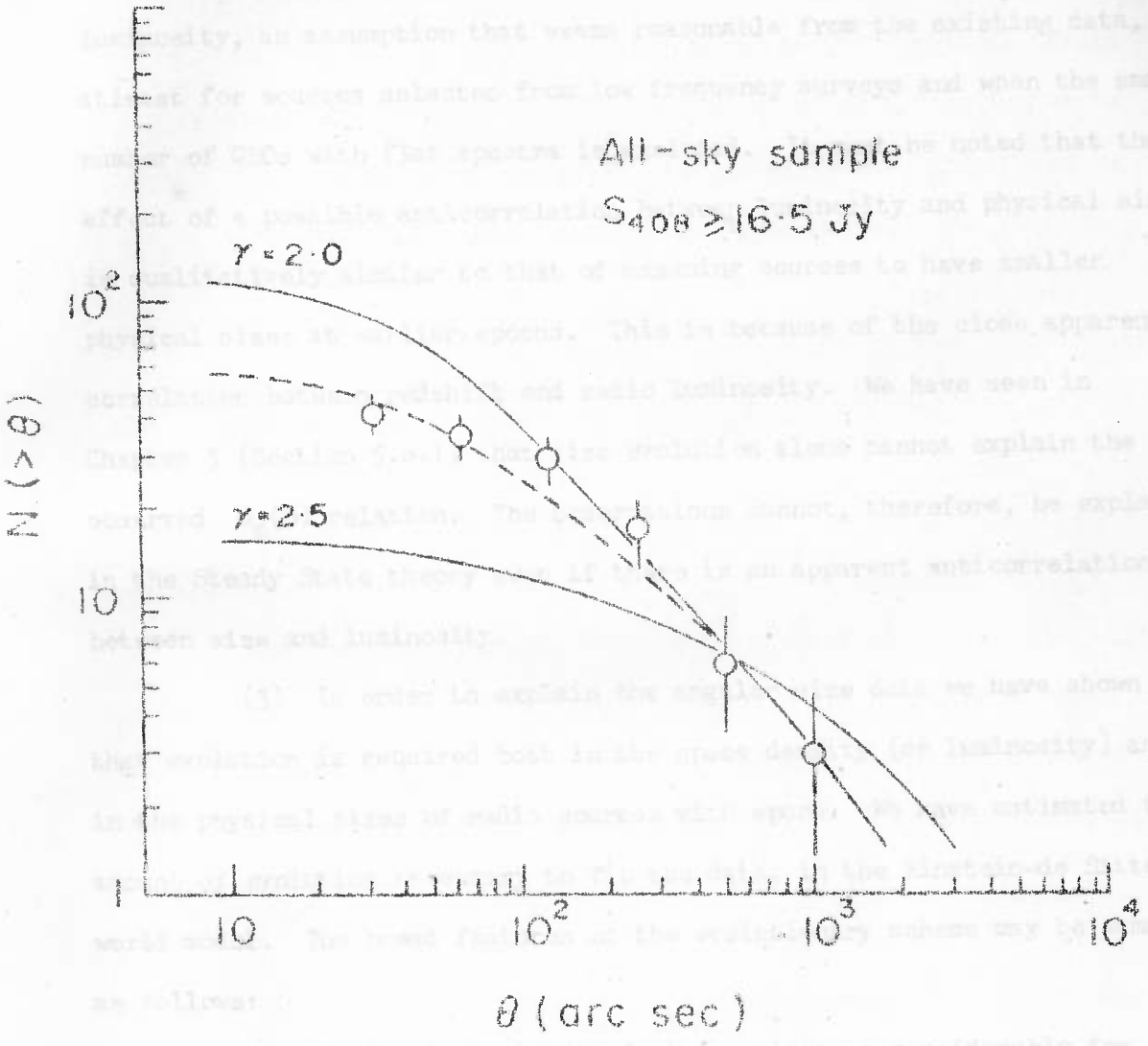

FIG. 6.1 The observed log N-log θ relation for the All-sky sample with $S_{408} \geq 16.5$ Jy, and the predicted relations for power law luminosity functions with $\gamma = 2.0$ and 2.5, in the Einstein-de Sitter cosmology. The broken line is for the evolutionary scheme of Table 5.2, with $\beta = 5.5$ and $n = 1.0$.

In calculating the expected angular size counts we have taken the distribution of physical sizes of radio sources to be independent of luminosity, an assumption that seems reasonable from the existing data, atleast for sources selected from low frequency surveys and when the small number of QSOs with flat spectra is excluded. It must be noted that the effect of a possible anticorrelation between luminosity and physical size is qualitatively similar to that of assuming sources to have smaller physical sizes at earlier epochs. This is because of the close apparent correlation between redshift and radio luminosity. We have seen in Chapter 5 (Section 5.6.1) that size evolution alone cannot explain the observed $\theta_m(S)$ relation. The observations cannot, therefore, be explained in the Steady State theory even if there is an apparent anticorrelation between size and luminosity.

(3) In order to explain the angular size data we have shown that evolution is required both in the space density (or luminosity) and in the physical sizes of radio sources with epoch. We have estimated the amount of evolution necessary to fit the data, in the Einstein-de Sitter world model. The broad features of the evolutionary scheme may be summarized as follows:

i) The local luminosity function steepens considerably for luminosities $P_{178} \gtrsim 10^{26}$ W Hz^{-1} ster^{-1}.

ii) The comoving density of high luminosity sources ($\gtrsim 10^{26}$ W Hz^{-1} ster^{-1}) changes with epoch approximately as $(1 + z)^{5.5}$.

iii) The physical sizes of radio sources evolve approximately as $(1 + z)^{-1}$.

The form of the local RLF indicated by the angular size data is similar to that inferred from the log N-log S work (e.g. Longair 1971). The local RLF derived by Longair (1971) from the known optical identifications and a model fitting technique to fit the observed flux density counts, steepens continuously with increasing luminosity for $P_{178} \gtrsim 10^{24}$ W Hz^{-1} ster^{-1}. The simplified power law RLF with two slopes, i.e.

$$\rho(P) \propto P^{-2.1}\, dP \quad \text{for} \quad 10^{23} \lesssim P_{178} \lesssim 10^{26} \text{ W Hz}^{-1} \text{ ster}^{-1}$$

and $$\rho(P) \propto P^{-2.8}\, dP \quad \text{for} \quad 10^{26} \lesssim P_{178} \lesssim 2.10^{28} \text{ W Hz}^{-1} \text{ ster}^{-1}$$

derived by us from the angular size data appears to be a reasonable approximation to Longair's model RLF.

The amount of density evolution required to explain the angular size data is also found to be of the same order as required to explain log N-log S data (e.g. Longair 1966; Doroshkevich, Longair and Zeldovich 1970) or as inferred from the Volume-Luminosity (V/V_m) tests for quasars (e.g. Schmidt 1968).

It should be noted that the form of the RLF and the amount of evolution implied by our work are largely independent of flux density counts, for we have made no use of the available log N-log S data, except to require the total number of sources with $S_{178} > 9$ Jy in the 3CR catalogue to agree with the observed number.

The type of size evolution indicated by the observed $\theta_m(S)$ relation is also similar to what has been inferred from the observed $\theta - z$ relation for QSOs. In Friedman cosmologies an epoch dependance of source sizes is readily explained by models that require an intergalactic

medium to decelerate and confine the radio source components (DeYoung and Axford 1967), because the intergalactic density should increase as $(1 + z)^3$. For instance DeYoung (1971) has estimated from detailed numerical calculations that the ram pressure of an intergalactic medium should limit the extent of double radio sources approximately as $(1 + z)^{-0.8}$. This is in fair agreement with the size evolution required to explain the $\theta_m(S)$ relation.

Evolution in source sizes can arise also from the 'snuffing out' of source components at high redshifts before they have reached their maximum extent (e.g. Rees and Setti 1968; Christiansen 1969). The 'snuffing out' can be produced by inverse compton losses against the universal background radiation whose energy density should increase as $(1 + z)^4$. In single burst models of double radio sources the maximum life times of electrons due to synchrotron and inverse compton losses (van der Laan and Perola 1969) imply that the maximum source extents should vary even faster than $(1 + z)^{-3.5}$ (Wardle and Miley 1974). Such rapid evolution in source sizes is not supported by the angular size data (see Fig. 5.10) even allowing for the possible uncertainty in the local size function. Other difficulties with such models have been considered by van der Laan and Perola (1969) and by Wardle and Miley (1974).

Our simple evolutionary schemes for density and size evolution have been chosen for ease of computation and are admittedly oversimplified in several respects. For instance we have considered only the case of power low density evolution that starts abruptly above a luminosity P_m ($\sim 10^{26}$ W Hz^{-1} $ster^{-1}$). One can of course consider other functional forms of

evolution, such as exponential, $\rho(P,z) \propto \rho(P, z = 0)e^{-kt}$ (e.g. Rowan-Robinson 1968), where t is the cosmic time. One may have other types of evolution such as 'luminosity scale', 'luminosity slope' or 'luminosity range' evolution (van Hoerner 1973). The amount of evolution could also be a function of luminosity (e.g. Schmidt 1972a). It is doubtful, however, if more detailed computations are warranted by the data in view of the uncertainties in the world model, the luminosity function and the radio size function.

(4) We have also seen that the exclusion of known QSOs from the source samples has little effect on the amount of evolution required to explain the angular size data. This is because of (a) the relatively small number of sources identified with QSOs ($\sim$ 22% of the 3CR sample and $\sim$13% of the Ooty sample) and (b) because of the general continuity in the physical parameters of radio galaxies and quasars, particularly so far sources of normal radio spectra. If most of the unidentified radio sources in the low frequency catalogues are indeed distant radio galaxies, as is suggested by several arguments, then the angular size data show that similar evolutionary effects in the radio luminosity function and in source sizes exist both for QSOs as well as radio galaxies.

(5) High resolution angular size data is not yet available below the flux levels of the Ooty occultation survey. The Ooty data together with the limited angular size information in a recent deep survey with the Westorbork synthesis telescope at 1415 MHz (Katgert and Spinrad 1974) suggest that the median value of θ may be approaching a constant value in the region of about 5" to 8" arc at flux levels of

$S_{408} \sim 0.1$ Jy. This is in broad agreement with the predictions of the evolutionary scheme that we have reported in this thesis to explain the $\theta_m(S)$ relation down to flux levels of the Ooty sample. High resolution observations of weaker radio sources should provide valuable information concerning the evolutionary behaviour of radio sources of intermediate and low luminosities.

(6) We have attempted to investigate the evolutionary behaviour of radio sources independently of the vast amount of available data on the number-flux density relation for radio sources. By combining the N(S) data with the angular size data it should be possible to further our understanding of the evolution of radio sources.

REFERENCES

Austin, T.B. and Peach, J.V., 1974, Mon. Not. Roy. Astron. Soc., 167, 437.

Baade, W. and Minkowski, R., 1954, Astrophys. J., 119, 206.

Baum, W.A., 1972, in External Galaxies and Quasi Stellar Objects, p. 393, ed. D.S. Evans, D. Reidel, Dordrecht.

Bennett, A.S., 1962, Mem. Roy. Astron. Soc., 68, 163.

Bhandari, S.M., Ananthakrishnan, S. and Rao, A. Pramesh, 1974, Aust. J. Phys., 27, 121.

Blum, E.J., 1959, Ann. d'Astrophys., 22, 140.

Bolton, J.G., 1969, Astron. J., 74, 131.

Branson, N.J.B.A., Elsmore, B., Pooley, G.G. and Ryle, M., 1972, Mon. Not. Roy. Astron. Soc., 156, 377.

Braude, S. Ya, Megn, A.V., Ryabov, B.P. and Zhouck, I.N., 1970, Astrophys. Sp. Sc., 8, 275.

Brecher, K., Burbidge, G.R. and Strittmatter, P.A., 1971, Comm. Astrophys. Sp. Phys., 3, 99.

Bridle, A.H., Davis, M.M., Famalont, E.B. and Lequeux, J., 1972, Astron. J., 77, 405.

Burbidge, E.M. and Strittmatter, P.A., 1972, Astrophys. J., 172, L37.

Burbidge, G.R., 1970, Ann. Rev. Astron. Astrophys., 8, 369.

Burbidge, G.R., 1973, Nature Phys. Sci., 246, 17.

Christiansen, W., 1969, Mon. Not. Roy. Astron. Soc., 145, 327.

Cohen, M.H., 1969, Ann. Rev. Astron. Astrophys., 7, 619.

Colla, G., Fanti, C., Fanti, R., Ficarra, A., Formiggini, L., Gandolfi, E., Lari, C., Marano, B., Padrielli, L. and Tomasi, P., 1972, Astron. Astrophys. Suppl., 7, 1.

Conway, R.G., Kellermann, K.I. and Long, R.J., 1963, Mon. Not. Roy, Astron. Soc., 125, 261.

Conway, R.G. and Munro, R.E.B., 1972, Mon. Not. Roy. Astron. Soc., 159, 21P.

Cooper, B.F.C., Price, R.M. and Cole, D.J., 1965, Aust. J. Phys. 18, 589.

Crawford, D.F., Jauncey, D.L. and Murdoch, H.S., 1970, Astrophys. J, 162, 405.

Critchley, J., Palmer, H.P. and Rowson, B., 1972,
Mon. Not. Roy. Astron. Soc., 160, 271.

DeYoung, D.S. and Axford, W.I., 1967, Nature, 216, 129.

DeYoung, D.S., 1971, Astrophys. J., 167, 541.

DeYoung, D.S. and Burbidge, G.R., 1973, Comm. Astrophys. Sp. Phys., 5, 29.

Dixon, R.S., 1970, Astrophys. J. Supp. Ser., 20, 1.

Doroshkevich, A.G., Longair, M.S. and Zeldovich, Ya, B., 1970,
Mon. Not. Roy. Astron. Soc., 147, 139.

Ehman, J.R., Dixon, R.S. and Kraus, J.D., 1970, Astron. J., 75, 351.

Ekers, R.D., 1969, Aust. J. Phys., Astrophys. Suppl. No.6.

Elsmore, B. and Mackay, C.D., 1969, Mon. Not. Roy. Astron. Soc., 146, 361.

Fanaroff, B.L. and Longair, M.S., 1972, Mon. Not. Roy. Astron. Soc. 159, 119.

Fomalont, E.B., 1968, Astrophys. J. Supp. Ser., 15, 203.

Fomalont, E.B., 1969, Astrophys. J., 157, 1027.

Fomalont, E.B. and Moffet, A.T., 1971, Astron. J., 76, 5.

Gopal-Krishna and Subrahmanya, C.R. 1975, in preparation.

Gopal-Krishna, Joshi, M.N. and Ananthakrishnan, S., 1975, in preparation.

Hargrave, P.J. and Ryle, M., 1974, Mon. Not. Roy. Astron. Soc., 166, 305.

Harris, D.E. and Hardebeck, E.G., 1969, Astrophys. J. Supp. Ser., 19, 115.

Hazard, C., 1961, Nature, 191, 58.

Hazard, C., 1962, Mon. Not. Roy. Astron. Soc., 124, 343.

Hazard, C., Mackey, M.B. and Shimmins, A.J., 1963, Nature, 197, 1037.

Hoerner, S. von, 1964, Astrophys. J., 140, 65.

Hoerner, S. von, 1973, Astrophys. J., 186, 741.

Hoyle, F., 1959, Paris Symp. on Radio Astron., p 529, ed. R.N. Bracewell, Stanford Univ. Press.

Hoyle, F., 1968, Proc. Roy. Soc. London, A 308, 1.

Hoyle, F. and Burbidge, G.R., 1970, Nature, 227, 359.

Jackson, J.C., 1973, Mon. Not. Roy. Astron. Soc., 162, 11P.

Jennison, R.C. and Das Gupta, M.K., 1953, Nature, 172, 996.

Joshi, M.N., Kapahi, V.K., Gopal-Krishna, Sarma, N.V.G. and Swarup, G., 1973, Astron. J., 78, 1023.

Joshi, M.N., 1975, in preparation.

Kapahi, V.K., 1971, Nature Phys. Sci., 234, 42

Kapahi, V.K., Joshi, M.N. and Gopal-Krishna, 1972, Astrophys. Lett., 11, 155.

Kapahi, V.K., Joshi, M.N. and Kandaswamy, J., 1973, Astrophys. Lett., 14, 31.

Kapahi, V.K., Joshi, M.N., Subrahmanya, C.R. and Gopal-Krishna, 1973, Astron. J., 78, 673.

Kapahi, V.K., Gopal-Krishna and Joshi, M.N., 1974, Mon. Not. Roy. Astron. Soc., 167, 299.

Kapahi, V.K., Joshi, M.N. and Sarma, N.V.G., 1974, Astron. J., 79, 515.

Kapahi, V.K., Damle, S.H., Balasubramanian, V. and Swarup, G., 1975, J. Inst. Electron. & Telecom. Engrs., (in press).

Katgert, J.K. and Spinrad, H., 1974, Astron. Astrophys., 35, 393.

Kellermann, K.I., Pauliny-Toth, I.I.K. and Williams, P.J.S., 1969, Astrophys. J., 157, 1.

Kellermann, K.I., Davis, M.M. and Pauliny-Toth, I.I.K., 1971, Astrophys. J., 170, L1.

Kellermann, K.I., 1972, Astron. J., 77, 531.

Kristian, J., Sandage, A. and Katem, B., 1974, Astrophys. J., 191, 43.

Kruit, P.C. van der, 1973, Astrophys. Lett., 15, 27.

Laan, H. van der and Perola, G.C., 1969, Astron. Astrophys., 3, 468.

Legg, T.H., 1970, Nature, 226, 65.

Longair, M.S., 1966, Mon. Not. Roy. Astron. Soc., 133, 421.

Longair, M.S. and Scheuer, P.A.G., 1967, Nature, 215, 919.

Longair, M.S. and Pooley, G.G., 1969, Mon. Not. Roy. Astron. Soc., 145, 121.

Longair, M.S. and Macdonald, G.H., 1969, Mon. Not. Roy. Astron. Soc., 145, 309.

Longair, M.S. and Scheuer, P.A.G., 1970, Mon. Not. Roy. Astron. Soc., 151, 45.

Longair, M.S., 1971, Rep. Prog. Phys., 34, 1125.

Longair, M.S. and Rees, M.J., 1972, Comm. Astrophys. Sp. Phys., 4, 79.

Longair, M.S., Ryle, M. and Scheuer, P.A.G., 1973,
Mon. Not. Roy. Astron. Soc., 164, 243.

Longair, M.S. and Gunn. J.E., 1975, Mon. Not. Roy. Astron. Soc., 170, 121.

Lynds, R., 1971, Astrophys. J., 168, L87.

Macdonald, G.H., Kenderdine, S. and Neville, A.C., 1968,
Mon. Not. Roy. Astron. Soc., 138, 259.

Mackay, C.D., 1969, Mon. Not. Roy. Astron. Soc., 145, 31.

Mackay, C.D., 1971, Mon. Not. Roy. Astron. Soc., 154, 209.

Mackay, C.D., 1973, Mon. Not. Roy. Astron. Soc., 162, 1.

Merkelijn, J.K., 1971, Astron. Astrophys.. 15, 11.

Miley, G.K., 1971, Mon. Not. Roy. Astron. Soc., 152, 477.

Miley, G.K., Perola, G.C., Kruit, P.C. van der and Laan, H. van der, 1972,
Nature, 237, 269.

Mills, B.Y., Davies, I.M. and Robertson, J.G., 1973, Aust. J. Phys., 26, 417.

Minkowski, R., 1960, Astrophys. J., 132, 908

Parkes, A.G. and Penston, M.V., 1973, Mon. Not. Roy. Astron. Soc., 162, 117.

Pooley, G.G. and Ryle, M., 1968, Mon. Not. Roy. Astron. Soc., 139, 515.

Readhead, A.C.S. and Hewish, A., 1974, Mem. Roy. Astron. Soc., 78, 1.

Rees, M.J. and Setti, G., 1968, Nature, 219, 127.

Rees, M.J., 1971, Nature, 229, 312.

Rees, M.J., 1972, in External Galaxies and Quasi Stellar Objects, p 407 ed. D.S. Evans, D. Reide Dordrecht.

Reinhardt, M., 1972, Astrophys. Lett., 12, 135.

Richter, G.M., 1973, Astrophys. Lett., 13, 63.

Robertson, J.G., 1973, Aust. J. Phys. 26, 403.

Roger, R.S., Bridle, A.H. and Costain, C.H., 1973, Astron. J., 78, 1030.

Rowan-Robinson, M., 1968, Mon. Not. Roy. Astron. Soc., 138, 445.

Ryle, M., 1952, Proc. Roy. Soc. London, A 211, 351.

Ryle, M. and Longair, M.S., 1967, Mon. Not. Roy. Astron. Soc., 136, 123.

Ryle, M., 1968, Ann. Rev. Astron. Astrophys., 6, 249.

Ryle, M. and Windram, M.D., 1968, Mon. Not. Roy. Astron. Soc., 138, 1.

Sandage, A., 1961, Astrophys. J., 133, 355.

Sandage, A., 1972, Astrophys. J., 173, 485.

Sarma, N.V.G., Joshi, M.N., Bagri, D.S. and Ananthakrishnan, S., 1975, J. Inst. Electron. & Telecom. Engrs., (in press).

Scheuer, P.A.G., 1962, Aust. J. Phys., 15, 333.

Schmidt, M., 1963, Nature, 197, 1040.

Schmidt, M., 1968, Astrophys. J., 151, 393.

Schmidt, M., 1972, Nature, 240, 399.

Schmidt, M., 1972a, Astrophys. J., 176, 303.

Schwarz, U.J., Cole, D.J. and Morris, D., 1973, Aust. J. Phys., 26, 661.

Sholomitskii, G.B., 1968, Sov. Astron. AJ, 11, 756.

Spinrad, H. and Smith, H.E., 1973, Astrophys. J. 179. L71.

Strom, R.G., 1973, Nature Phys. Sci., 244, 2.

Subrahmanya, C.R., 1975, Bull. Astron. Soc. India, 3, 13.

Sutton, J., 1966, Ph.D. Thesis, University of Sydney.

Swarup, G., Sarma, N.V.G., Joshi, M.N., Kapahi, V.K., Bagri, D.S., Damle, S.H., Ananthakrishnan, S., Balasubramanian, V., Bhave, S.S. and Sinha, R.P., 1971a, Nature Phys. Sci., 230, 185.

Swarup, G., Kapahi, V.K., Sarma, N.V.G., Gopal-Krishna, Joshi, M.N. and Rao, A.P., 1971b, Astrophys. Lett., 9, 53.

Swarup, G., 1975, Mon. Not. Roy. Astron. Soc. (in press).

Swarup, G. and Sutton, J., 1975, in preparation.

Tritton, K.P., 1972, Mon. Not. Roy. Astron. Soc., 158, 277.

Veron, M.P. and Veron, P., 1974, Astron. Astrophys. Suppl., 18, 309.

Wall, J.V., Shimmins, A.J. and Merkelijn, J.K., 1971, Aust. J. Phys. Astrophys. Suppl. 19.

Wall, J.V. and Cole, D.J., 1973, Aust. J. Phys. 26, 881.

Wampler, E.J., Robinson, L.B., Baldwin, J.A. and Burbidge, E.M., 1973, Nature, 243, 336.

Wardle, J.F.C. and Miley, G.K., 1974, Astron. Astrophys., 30, 305.

Watts, C.B., 1963, The Marginal Zone of the Moon (Naut. Alman. Office, U.S. Naval Obs.)

Wilkinson, P.N., Richards, P.J. and Bowden, T.N., 1974, Mon. Not. Roy. Astron. Soc., 168, 515.

Willis, A.G., Strom, R.G. and Wilson, A.S., 1974, Nature, 250, 625.

Wills, B.J. and Wills, D., 1974, Astrophys. J., 190, L97.

Wyllie, D.V., 1969, Mon. Not. Roy. Astron. Soc., 142, 229.

Yule, U.G. and Kendall, M.G., 1950, An Introduction to the Theory of Statistics, p. 425, Charles Griffin, London.